

33 IGC excursion No 35*



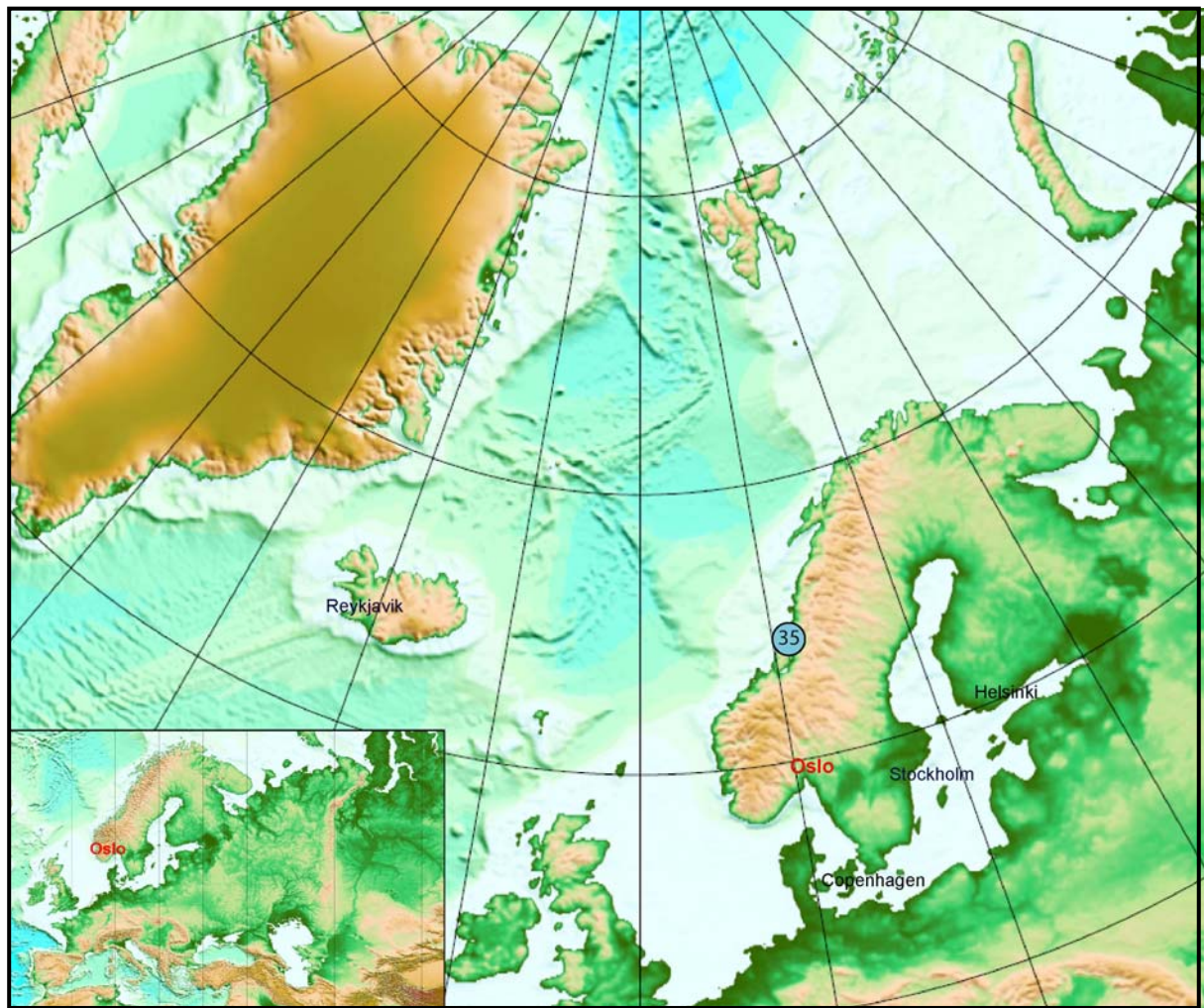
33 IGC, The Nordic Countries



Pre-Scandian tectonic and magmatic evolution of the Helgeland Nappe Complex, Uppermost Allochthon

Organizers:

Ø. Nordgulen, C.G. Barnes, A.S. Yoshinobu, C. Frost, T. Prestvik, H. Austrheim, H.S. Anderson, W.T. Marko, and K. McArthur



StatoilHydro

* not running due to insufficient participation




United Nations
Educational, Scientific and
Cultural Organization
Under the Patronage of UNESCO

TABLE OF CONTENTS

<i>Abstract</i>	5
<i>Authors</i>	5
<i>Logistics</i>	6
Dates and location	6
Travel arrangements	6
Accommodation	6
Field logistics	6
<i>General Introduction</i>	6
<i>Regional Geology</i>	7
The Uppermost Allochthon	9
The Leka ophiolite and Skei Group (Day 4)	12
Nappes with ophiolitic basement rocks (Days 2 & 5)	12
Nappes characterized by migmatite (Day 2)	14
Bindal Batholith (Days 1 & 3)	15
Structural and Tectonic Context of the Helgeland Nappe Complex	19
<i>Excursion Route And Road Log</i>	19
<i>Excursion Stops</i>	20
Day 1. Vega	20
Introduction	20
Stop No. 1-1: Kjul outcrops (Langhalsan)	22
Location	22
Introduction	23
Description	23
Stop No. 1-2: Outcrops along the east side of Vikasjøen (Trollrevheian).	23
Location	23
Introduction	23
Description	23
Stop No. 1-3: Levika area.	25
Location	25
Introduction	25
Description	26
Stop No. 1-4: Tangvika quay.	27
Location	27
Introduction	27
Description	27
Stop No. 1-5: Sørneset coastline.	29
Location	29
Introduction	29
Description	29
Stop No. 1-6: Gullsvågsjøen area.	29
Location	29
Introduction	29
Description	29
Day 2	31
Introduction. Nappes of the Helgeland Nappe Complex	31
Stop No. 2-1: Route 76 road cuts near Lande.	32
Location	32

Introduction	32
Description	32
Stop No. 2-2: Aunlia road cuts.	34
Location	34
Introduction	34
Description	34
Stop No. 2-3: Nordfjellmark road	35
Location	35
Introduction	35
Description	36
Stop No. 2-4: Skogmoen	36
Location	36
Introduction	36
Description	36
Stop No. 2-5: Sjøvatnet.	38
Location	38
Introduction	38
Description	38
Stop No. 2-6: Gåslia.	38
Location	38
Introduction	38
Description	39
Day 3	39
Introduction. Middle and Late Ordovician plutons of the Bindal Batholith	39
Stop No. 3-1: Shoreline between Lislvågen and Storvågen.	39
Location	39
Introduction	39
Description	39
Stop No. 3-2: Hundkjerka marble mine (optional)	41
Location	41
Introduction	41
Description	41
Stop No. 3-3: Svarthopen quarry.	42
Location	42
Introduction	42
Description	42
Stop No. 3-4: Andalsvågen ferry quay	44
Location	44
Introduction	44
Description	44
Stop No. 3-5A: Vollvika East.	47
Location	47
Introduction	47
Description	47
Stop No. 3-5B: Vollvika West.	49
Location	49
Introduction	49
Description	49
Stop No. 3-6: Vistnesodden road cuts.	51
Location	51
Introduction	51
Description	51
Stop No. 3-7: Forvik quarry	52
Location	52
Introduction	52
Description	52
Day 4	52
Introduction. The Leka ophiolite and Skei Group	52
Stop No. 4-1: Lauvhatten	54
Location	54

Introduction	54
Description	54
Stop No. 4-2: Skråa block.	55
Location	55
Introduction	55
Description	55
Stop No. 4-3: South of Kvaløya farms	56
Location	56
Introduction	56
Description	56
Stop No. 4-4: North of Aunekollen	56
Location	56
Introduction	56
Description	56
Stop No. 4-5: Leka geology trail in Våttvika–Stortjørna area.	59
Location	59
Introduction	59
Description	59
Stop No. 4-6: Quarry at the Skei ferry terminus.	61
Location	61
Introduction	61
Description	61
Day 5	62
Introduction. Middle Nappe structures and Scandian extension in the Helgeland Nappe Complex.	62
Stop No. 5-1: Road cuts along Simlestraumen	63
Location	63
Introduction	63
Description	63
Stop No. 5-2: Quarry and road cuts north of Sandvikfjellet	64
Location	64
Introduction	64
Description	64
Stop No. 5-3: Road cuts near Saltbunesodden, NE of Breivika (optional)	67
Location	67
Introduction	67
Description	67
Stop No 5-4: Åbogen	67
Location	67
Introduction	67
Description	67
<i>Discussion</i>	68
Sediment provenance and paleogeographic considerations	68
Timing of nappe imbrication and metamorphism	69
Bindal Batholith magmatism	70
<i>Acknowledgements</i>	72
<i>References</i>	72

Abstract

This excursion will present an overview of the development of the Helgeland Nappe Complex (HNC), which is the structurally highest nappe complex of the Uppermost Allochthon in the Norwegian Caledonides. The HNC consists of at least five nappes separated by east-dipping shear zones. The nappes are characterized by variable proportions of pelitic and semipelitic rocks, marble and calc-silicate gneiss, monomict and polymict metaconglomerates, and metasandstone. They can be distinguished on the basis of metamorphic grade and the presence or absence of ophiolitic depositional basement. Ages of deposition, as inferred from detrital zircons and Sr isotope chronostratigraphy of marble, range from Neoproterozoic to Early Ordovician, with ophiolite development in Late Cambrian time. Peak metamorphic conditions were evidently reached from 482–475 Ma, soon after the end of deposition. Magmas that formed the Bindal Batholith were emplaced from 478–424 Ma; magmatism began during or immediately after amalgamation of the nappe sequence. The magmas ranged from older strongly peraluminous (“S-type”) through a range of calc-alkalic to alkalic ones. Many of the magmas emplaced after 469 Ma display supra-subduction zone signatures.

The HNC is interpreted to have Laurentian affinities on the basis of the vergence of nappe-bounding structures, long-lived arc-like magmatism, the similarity of detrital zircon populations with those from Dalradian rocks in Scotland, and sedimentologic data from the Fauske Marble (north of the study area; Roberts et al., 2002). The ages of ophiolite formation, basin formation and closure, and the initiation of Early Ordovician magmatism all point to an origin of the HNC by Taconian-style tectonic activity, presumably near modern East Greenland. The HNC escaped Scandian-age deep burial and eclogite-grade metamorphism as Baltica collided with Laurentia; however, magmatism and deformation continued episodically until <435 Ma. End-Scandian exhumation along a regional detachment system resulted in NE-directed transport of the HNC and emplacement on peri-Baltican basement rocks.

Authors

Øystein Nordgulen (oystein.nordgulen@ngu.no)

Geological Survey of Norway, N-7491 Trondheim, Norway

Calvin G. Barnes (cal.barnes@ttu.edu)

Aaron S. Yoshinobu (aaron.yoshinobu@ttu.edu)

Department of Geosciences, Texas Tech University, Lubbock, TX 79409-1053, USA

Carol Frost (frost@uwyo.edu)

Department of Geology and Geophysics, University of Wyoming, Laramie, WY 82071, USA

Tore Prestvik (tore.prestvik@ntnu.no)

Department of Geology and Mineral Resources Engineering, Norwegian university of Science and Technology, N-7491 Trondheim, Norway

H. Austrheim (h.o.austrheim@geo.uio.no)

Department of Geosciences, University of Oslo, N-0371 Oslo, Norway

Heather S. Anderson (hs.anderson@ttu.edu)

Wayne T. Marko (wayne.t.marko@ttu.edu)

Department of Geosciences, Texas Tech University, Lubbock, TX 79409-1053, USA

Kelsey McArthur (kmcarthu@uwyo.edu)

Department of Geology and Geophysics, University of Wyoming, Laramie, WY 82071, USA.

Logistics

Dates and location

Timing: From 1 August – to 5 August
Start location: Trondheim: 0900 on 31 July OR
Brønnøysund 1800 on 31 July.
End location: Trondheim or Værnes airport, 2000 on 5 August.

Travel arrangements

The excursion vans will travel from Trondheim to Brønnøysund on July 31. Brønnøysund may also be reached by air from Oslo and Trondheim, via the Hurtigruten (coastal express) from Trondheim or Bergen, and via a combination of rail to Trofors and bus to Brønnøysund. On return to Trondheim, participants may be dropped off at Værnes (Trondheim) airport late Tuesday evening or they may make arrangements to stay in Trondheim. Flights out of Trondheim should not be booked earlier than 2100. It is also possible to take a night train from Trondheim to Oslo, but it is popular and expensive, so booking well in advance is necessary. The organizers advise staying in Trondheim on the night of Day 5; early hotel booking is highly recommended.

Accommodation

Accommodation on the nights of 31 July – 3 August will be at hotels in Brønnøysund. The night of 4 August will be spent at Leka Motel & Camping on the island of Leka. Those wishing to arrive early to Brønnøysund may make hotel reservations via the Kystriksveien Travel Guide: www.rv17.no.

Field logistics

Excursion stops will vary from road cuts to short walks (no more than 1.5 km round-trip). Coastal exposures are accessible but may be slippery depending on weather and tide conditions. None of the stops require strenuous hiking or climbing. Participants should be prepared for wet weather and wet conditions underfoot.

General Introduction

The purpose of this excursion is to present the geologic development of the Helgeland Nappe Complex, or HNC, which is the highest nappe complex in the Norwegian Caledonides. Because the HNC did not undergo ultra-high-pressure (UHP) metamorphism before or during the Scandian event, its component nappes retain a pre-Scandian history that is much easier to read than in rocks that underwent UHP metamorphism. During the past few years, a consensus has emerged that the HNC nappes represent tectonostratigraphic terranes that formed on the western side of the Iapetus Ocean basin. Therefore, a better understanding of the deposition, tectonic history, metamorphism, and magmatic activity of the nappes will improve our understanding of geologic evolution of the western side of Iapetus.

The goals of the excursion are to (1) introduce the nappe structure of the HNC, the nature of known basement rocks, the provenance of (meta)sedimentary deposits, and the timing of metamorphism, (2) study examples of pre-Scandian magmatic activity (Bindal Batholith; Leka ophiolite), (3) study the history and timing of deformation of the HNC, (4) study the evidence for post-Scandian exhumation of the HNC, and (5) place all of this information into a broad tectonic context.

Regional Geology

The Scandinavian Caledonides, extending ca. 2000 km along strike, form part of a large system of Early Paleozoic orogenic belts in the North Atlantic region. During the Silurian-Devonian closure of the Iapetus Ocean, major allochthons were thrust eastwards onto the Baltoscandian margin (Fig. 1; Gee 1975, Roberts & Gee, 1985; Grenne et al., 1999; Roberts, 2003; Tucker et al., 2004, and references therein). The Precambrian rocks of the foreland

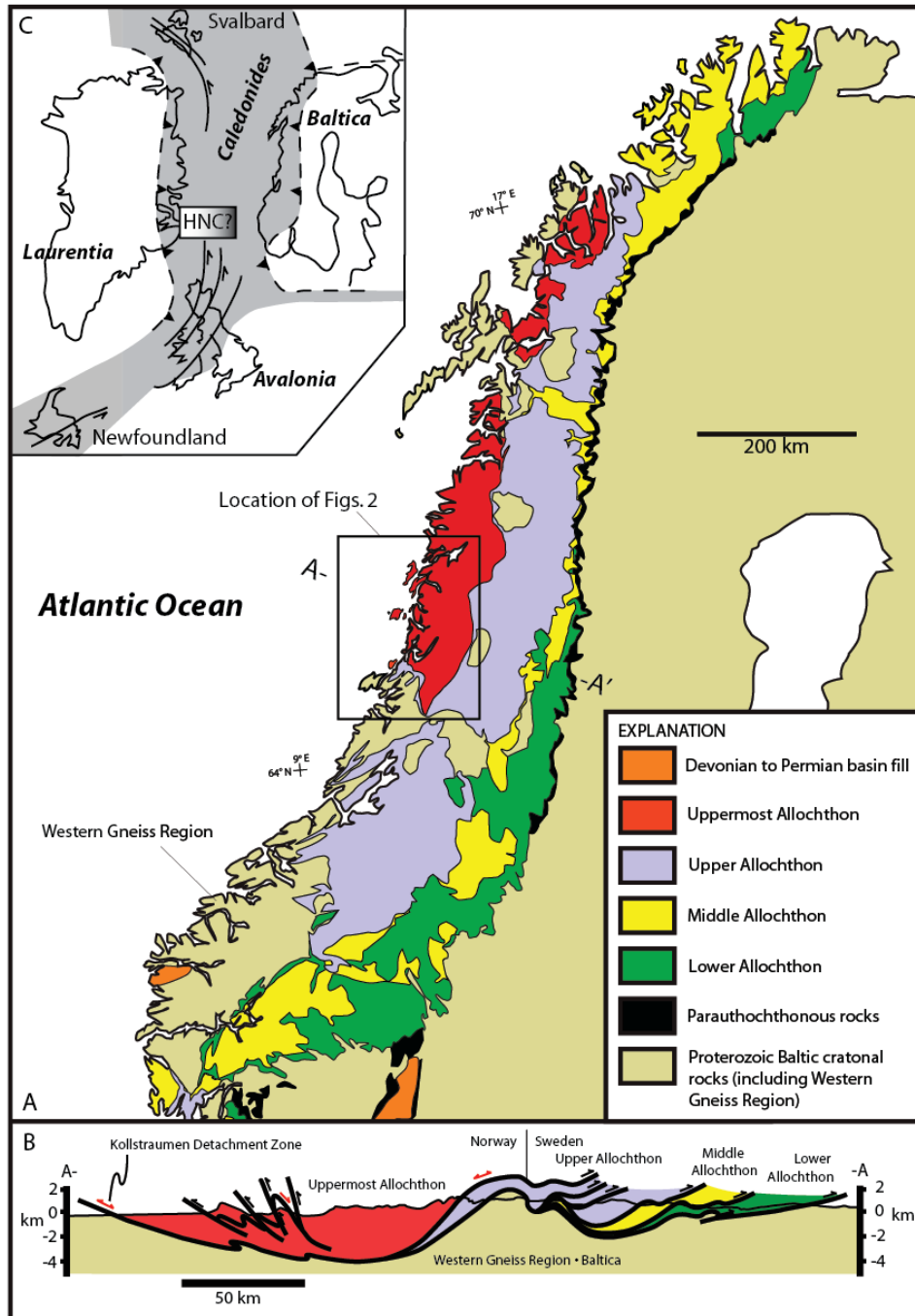


Figure 1. (A) Tectonostratigraphic map displaying the major units within the Scandinavian Caledonides (after Gee and Sturt, 1985). (B) Simplified geologic cross section across the Caledonides at the latitude of this study depicting the general structural style contained within the Uppermost Allochthon. (C) Speculative Ordovician-Silurian reconstruction of the Caledonide orogen and possible location of rocks within the Helgeland Nappe Complex (HNC). After Greiling and Garfunkel (2007).

belong to the Fennoscandian Shield and range in age from Archean in the north to Mesoproterozoic in the south. Along the eastern mountain/thrust front, a thin unit of autochthonous to parautochthonous Vendian–Cambrian sedimentary rocks are present. These sediments were deposited unconformably on the deeply eroded and peneplained crystalline basement of the Fennoscandian Shield.

The Caledonides of Scandinavia are divided into a series of allochthonous complexes, each comprising numerous thrust sheets or nappes that were juxtaposed during multiple events culminating with the Laurentia-Baltica (*Scandian*) oblique collision in the Late Silurian to Early to Mid-Devonian (Stephens et al., 1985, 1989; Roberts, 2003). The Scandian thrust sheets contain rocks that are derived both from the Baltoscandian margin and from a variety of terranes that originated outboard of Baltica.

The Lower and Middle Allochthons are indigenous to Baltica and composed of sedimentary rocks that were deposited along the Baltoscandian margin in Neoproterozoic to Early Cambrian time. Very low-grade, platformal sedimentary successions characterize the Lower Allochthon, whereas the Middle Allochthon mainly consists of arenaceous rocks from a continental rise setting. The Upper Allochthon formed outboard of these thrust complexes and consists of two different types of rock associations. The lower thrust sheets (Seve Nappes) consist of medium- to high-grade metasedimentary rocks and probably derived from a continent-to-ocean transition zone. They are overlain by mainly oceanic terranes (Köli Nappes) containing low-grade fragmented ophiolites, island-arc magmatic rocks, and back-arc or marginal-basin successions that are exotic to the Baltoscandian margin (Stephens & Gee, 1985; Stephens et al., 1989; Roberts, 2003). Faunal evidence shows either North American or Baltic, or even mixed provincial characteristics. Finally, the highest thrust sheets constitute the Uppermost Allochthon – the topic of this excursion.

Granitoids of Early Ordovician to Early Silurian age occupy a substantial part of the Upper and Uppermost Allochthons. The rocks are present as isolated intrusions or as major batholiths with a broad range in composition. The West-Karmøy Igneous Complex in southwesternmost Norway is Early Ordovician in age and consists of a number of quartz-dioritic to granitic rocks that were derived by melting of fertile upper crustal rocks. They appear to have formed in response to accretion of ophiolites and island-arcs with continental crust with many similarities to the rocks of Vega (Day 1).

The Sunnhordland Batholith (Andersen & Jansen, 1987) in western Norway consists of gabbroic to granitic rocks that have intruded a variety of lithologies including Lower Ordovician ophiolite and island-arc sequences. The oldest gabbro-diorite unit (Vardefjellet Gabbro) has a U-Pb age of 472 ± 2 Ma. Younger, calc-alkaline granodiorite and granite plutons have yielded Early Silurian dates. Early Silurian gabbro and granite are also present further to the north along the coast of western Norway (Skjerlie 1992, Skjerlie et al. 2000, Hansen 2002, Hacker et al. 2003).

The Smøla-Hitra Batholith is located in the coastal districts west of Trondheim in central Norway. Some calcic low-K gabbro to granodiorite occurs; however, the batholith is dominated by and calc-alkaline to alkali-calcic, high-K monzodiorite to quartz-monzonite to granite forming compositionally distinct plutons. A number of dates from the batholith have given ages between 460 and 428 Ma (Gautneb & Roberts 1989, Nordgulen et al. 1995, 2002, Tucker et al. 2004). Strongly deformed Caledonian-age intrusive rocks have also been

recognized in the nappes present in the southwest part of the Central Norway Basement Window (see Tucker et al. 2004 for a detailed treatment).

To the north of the Bindal Batholith, similar granitoid intrusions occur in the Beiarn Nappe of the Uppermost Allochthon. Granitoids are also present in a stack of nappes in the Ofotfjorden area (Gustavson 1969, Steltenpohl et al. 2003). In the northernmost part of the Caledonides, mainly Silurian granitoids are present (Kirkland et al. 2005, 2006, Corfu et al. 2006; for an overview; see Roberts et al. 2007)

The Scandian Orogeny (ca. 430-390 Ma) culminated with the collision between Baltica and Laurentia. During the late stages of continent-continent collision, ultra-high-pressure metamorphism took place in continental crust subducted to mantle depths at ca. 410-400 Ma (e.g., Terry & Robinson, 2004; Hacker and Gans, 2005). Late- to post-orogenic extension of the Caledonian (Scandian) nappe-stack in Scandinavia probably started in Early Devonian times and continued into the Early Carboniferous. Significant movement along extensional detachment zones led to exhumation of high-pressure rocks and the formation of post-orogenic extensional basins (Norton 1986; Seranne & Seguret 1987; Andersen & Jamtveit 1990; Fossen 1992; Fossen & Dunlap 1998; Osmundsen et al. 1998; Osmundsen & Andersen 2001, Eide et al. 2005). The extensional shearing and faulting affected the regional geometry of the nappe pile and also influenced the geometry of the gneiss-cored culminations in North-Central Norway (Braathen et al. 2000, 2002; Eide et al. 2002, Nordgulen et al. 2002, Osmundsen et al. 2003).

The Uppermost Allochthon

In north-central Norway, the Uppermost Allochthon consists of at least two nappe complexes (Fig. 2; Roberts et al., 2007), the structurally lower Rödingsfjället Nappe Complex and the structurally higher Helgeland Nappe Complex (HNC). This excursion focuses almost entirely on the HNC. There are five named nappes in the HNC (Figs. 2, 3) and others are likely to exist. The nappe nomenclature was developed in southern and central Helgeland, particularly by Nordgulen et al. (1989), Thorsnes & Løseth (1991), and Yoshinobu et al. (2002). In structurally descending order, the nappes are the Upper, Middle, Lower, Sauren-Torghatten, and Horta nappes (Barnes et al., 2007). Figure 3 illustrates the structural sequence of the nappes and shows some of their characteristic features. Although all of the nappes share similar rock assemblages, they can be distinguished on the basis of their metamorphic grade, the nature of depositional basement rocks (if exposed), and the presence or absence of conglomeratic sequences. The nappes are bounded by east-dipping shear zones. Some of these shear zones have reverse displacement (e.g., Thorsnes & Løseth, 1991) but others place lower grade over higher grade rocks and have normal displacement (Figs. 2, 3; Yoshinobu et al., 2002).

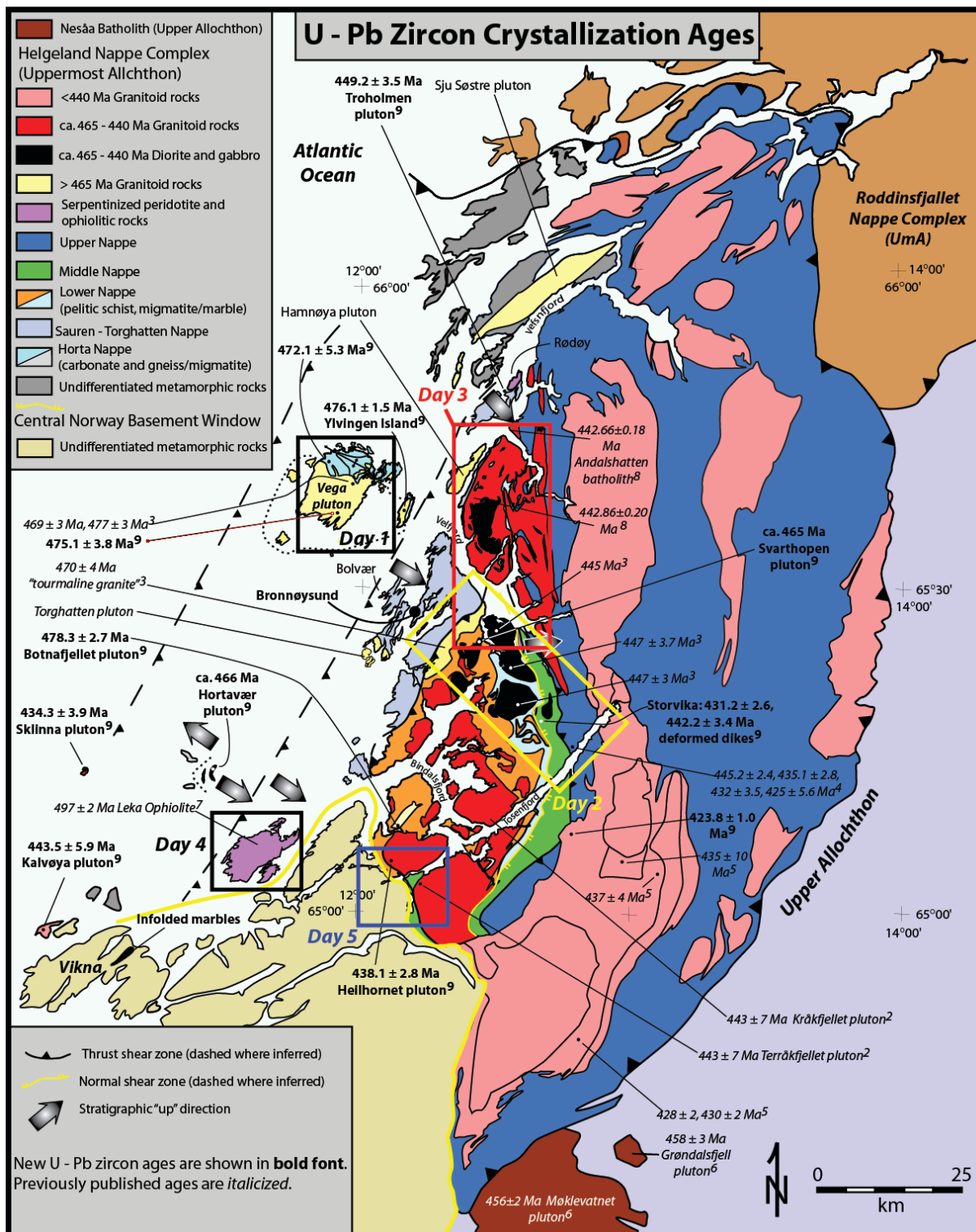


Figure 2. Regional geologic map showing the position of the Helgeland Nappe Complex in north-central Norway and the location and U/Pb ages of dated plutonic rocks. Ages reported in bold print are from Barnes et al. (2007). Sources for previously published data: T. Heldal, written communication, ²Nordgulen et al. (1993), ³Yoshinobu et al., (2002), ⁴Yoshinobu et al. (2005), ⁵Nissen et al. (2006), ⁶Meyer et al., (2003), ⁷Pedersen and Furnes (1991), ⁸Anderson et al. (2007), and Barnes et al. (2007).

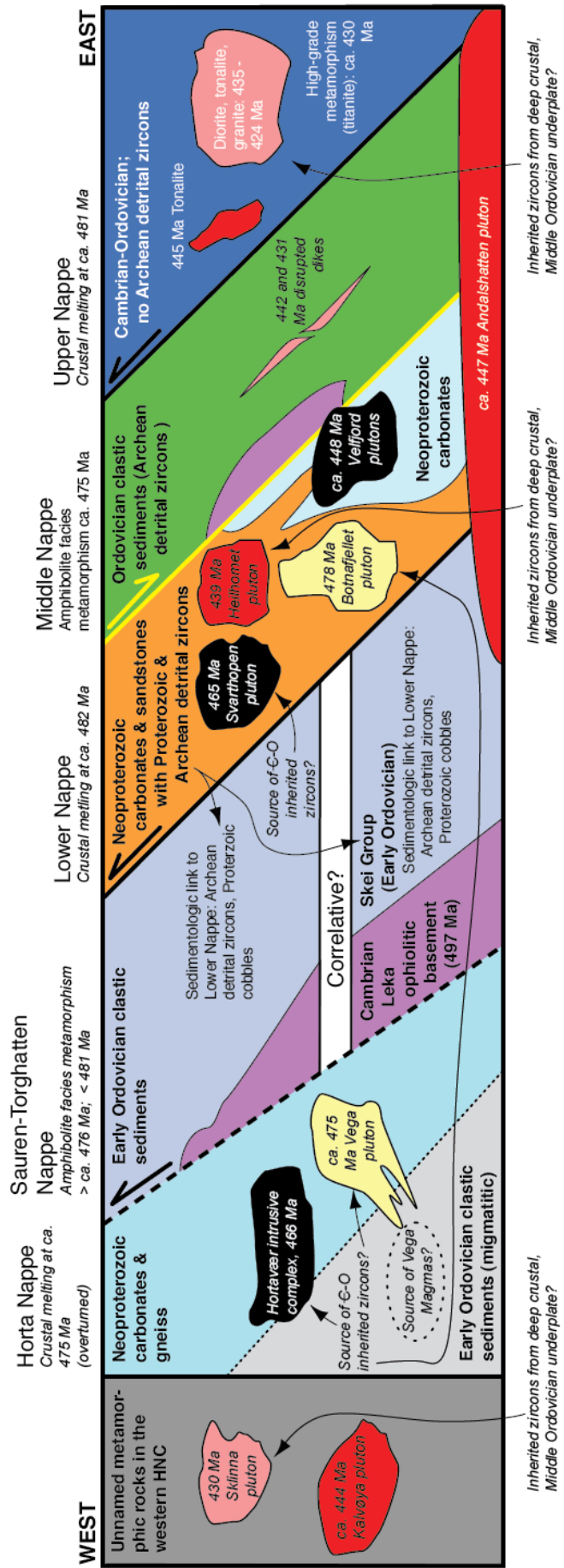


Figure 3. Schematic cross section of the Helgeland Nappe Complex nappes and plutons at the beginning of Scandian thrusting (c. 430 Ma; from Barnes et al., 2007). Colors correspond to lithologies illustrated in Figure 2. The nature of the contact between the unnamed metamorphic rocks to the west and the Helgeland Nappe Complex is unknown. The thrust that juxtaposes the Horta Nappe against the Sauren-Torghatten Nappe is inferred. Possible sedimentologic and magmatic links between nappes and plutons (magma sources or contaminants) are shown with arrows.

The Leka ophiolite and Skei Group (Day 4)

For reasons discussed below and during the excursion, we consider the Leka ophiolite (Fig. 2) and its cover sequence, the Skei Group, to be part of the HNC. The ophiolite contains a complete ophiolitic sequence (e.g., Prestvik, 1980; Furnes et al., 1988) and high-level plagiogranites were dated at 497 ± 2 Ma (i.e., Cambrian; Dunning and Pedersen, 1988). The Skei Group unconformably overlies the ophiolite and consists of a lower unit of interbedded conglomerate, conglomeratic sandstones, and sandstones, and an upper unit of wackes, marble, and metapelitic rocks (Sturt et al., 1985). Detrital zircon data indicate that the Skei Group is Ordovician in age (McArthur, 2007).

Mineral assemblages in the metagabbro and the Skei Group are consistent with upper greenschist facies regional metamorphism (Prestvik, 1972; Sturt et al., 1985). The presence of rodingites within the ophiolite and the pattern of serpentinization in the ultramafic rocks both suggest an earlier sea-floor metamorphism.

Nappes with ophiolitic basement rocks (Days 2 & 5)

The Sauren-Torghatten and Middle Nappes are sequences of metamorphosed clastic and carbonate rocks. The metasedimentary sequences in both nappes lie unconformably over discontinuously-exposed, tectonically fragmented basement rocks of ophiolitic affinity. These basement rocks include peridotite (mostly serpentinized), metapyroxenite, metagabbro and mafic metavolcanic rocks (Thorsnes and Løseth, 1991; Haldal, 2001). None of these ophiolitic slivers has been successfully dated. An interesting distinction between these two units is that whereas ophiolitic rocks are known to crop out only at the base of the Middle Nappe, serpentinized ultramafic rocks occur within the sedimentary section of the Sauren-Torghatten Nappe.

The overlying metasedimentary rocks include metawackes, metapelites, calc-silicate rocks, and marble, with interbedded conglomerates. Conglomeratic strata vary from monomict amphibolitic and calcareous units to polymict beds (Thorsnes and Løseth, 1991; Nordgulen et al., 1992; Haldal, 2001). The metamorphic grade in these nappes is typically amphibolite facies. Haldal (2001) reported kyanite-zone assemblages from metapelitic rocks that overlie the ophiolitic basement of the Sauren-Torghatten Nappe. In contrast, kyanite has not been found in the Middle Nappe, where sillimanite-zone assemblages are typical.

Detrital zircons from pelitic rocks of the Middle Nappe and metasandstone from the Sauren-Torghatten Nappe (Fig. 4) indicate that deposition ended at or just prior to ~ 480 Ma (Barnes et al., 2007). The age of metamorphism has been more difficult to determine; however, metamorphic titanite from a conglomerate clast from the Middle Nappe yielded a U-Pb age of 475 Ma (Barnes et al., 2007), which we interpret to place a younger limit on peak metamorphism.

The stratigraphic relationships, ages of deposition, and rock types present in the basement–cover sequence of the Sauren-Torghatten Nappe are very similar to the Leka ophiolite basement and Skei Group cover sequence on Leka (McArthur, 2007). On this basis, McArthur (2007) concluded that the units are correlative, as indicated in Figure 3.

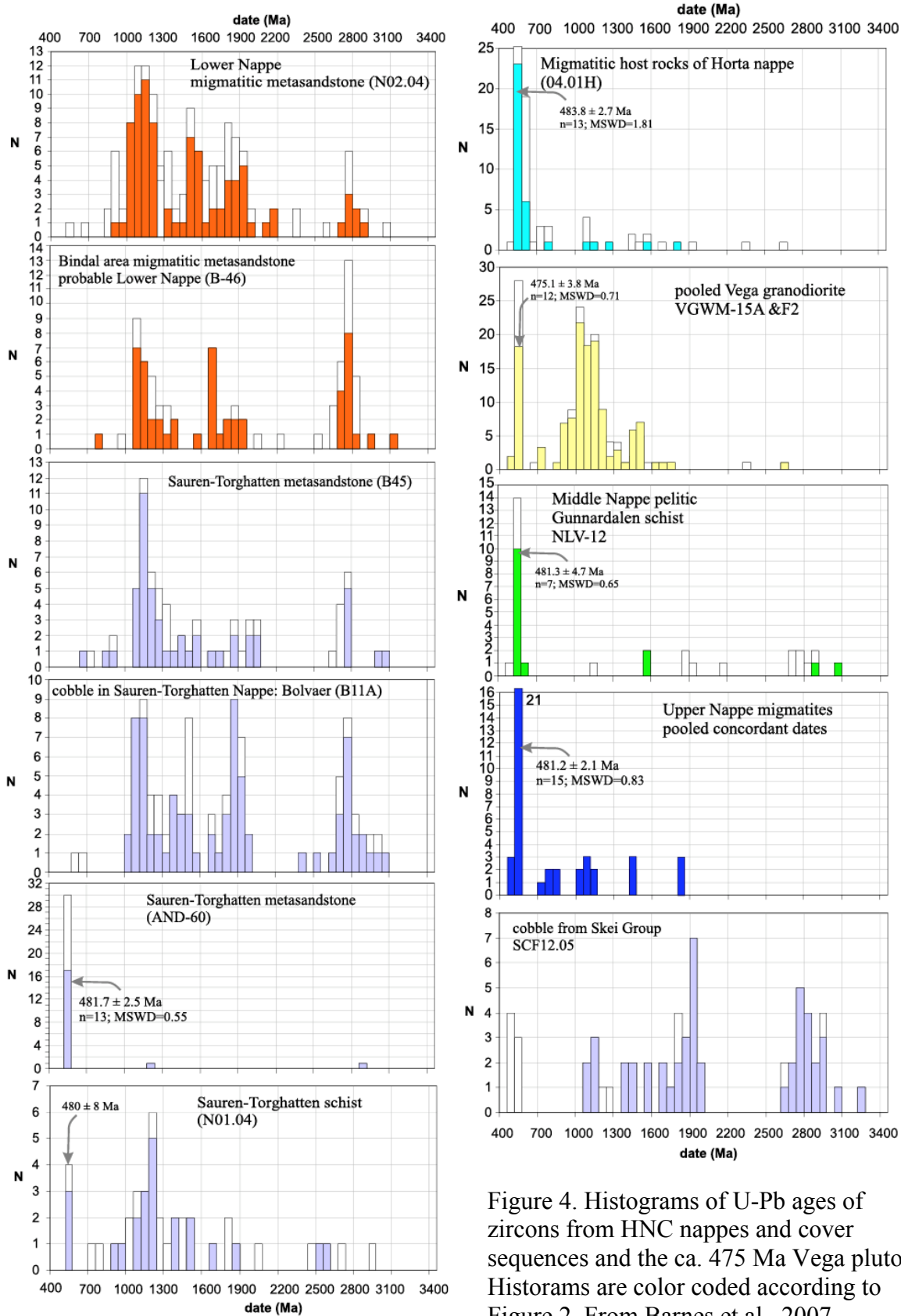


Figure 4. Histograms of U-Pb ages of zircons from HNC nappes and cover sequences and the ca. 475 Ma Vega pluton. Histograms are color coded according to Figure 2. From Barnes et al., 2007.

Nappes characterized by migmatite (Day 2)

The Upper and Lower Nappes, as defined by Thorsnes and Løseth (1991), and the Horta Nappe (Barnes et al., 2007) consist almost entirely of metasedimentary rocks. All three nappe sequences lack crystalline basement. The principal rock types are migmatitic quartzofeldspathic and semi-pelitic gneiss, calc-silicate gneiss, and marble. The presence of migmatite indicates that regional metamorphism was above the solidus in upper amphibolite to lower granulite facies conditions (e.g., Barnes and Prestvik, 2000; Reid, 2004; Yoshinobu et al., 2005).

Because fossils are lacking in these nappes, age determinations have relied on U-Pb dating of zircon and titanite plus chemostratigraphic studies of calcite marble. The chemostratigraphic approach (e.g., Melezik et al., 2001, 2005) is based on the concept that pure calcite limestone protoliths behaved as closed systems during burial and metamorphism, thus preserving their original carbon and strontium isotopic signatures. With the exception of a detailed study in the Hommelstø area (Sandøy, 2003), this approach has been used sparingly in parts of the HNC visited during the excursion.

Migmatization of the Upper Nappe was dated at ~480 Ma (Fig. 4; Yoshinobu et al., 2005). Detrital zircons in these samples were interpreted to indicate deposition of Upper Nappe sediments during Ordovician time. In contrast, the age of migmatization in the Lower Nappe has yet to be directly dated. Yoshinobu et al. (2002) inferred an Early Ordovician (~480 Ma) age for migmatization on the basis of inheritance in younger anatectic granites.

Chemostratigraphic data indicate that much of the marble in the Lower Nappe is Neoproterozoic (Sandøy, 2003; Fig. 5). However, at least one marble unit that has been interpreted as part of the Lower Nappe yielded an Ordovician age (Day 3). If this marble unit is truly part of the Lower Nappe, then the Lower Nappe consists of a Neoproterozoic sedimentary sequence unconformably overlain by an Ordovician sequence.

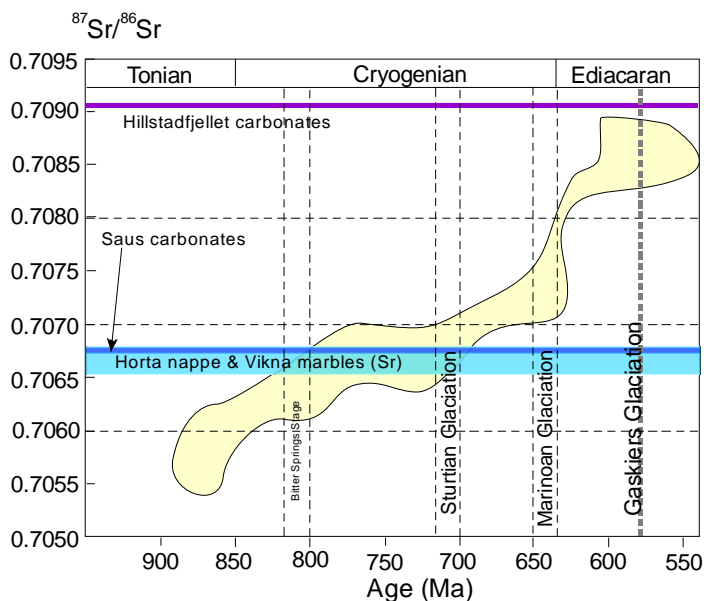


Figure 5. Variation in $^{87}\text{Sr}/^{86}\text{Sr}$ (yellow) of pure Neoproterozoic limestones (Halverson et al., 2007). The range of $^{87}\text{Sr}/^{86}\text{Sr}$ in pure marbles from the Horta nappe and in-folded Caledonian rocks on Vikna is shown by the pale blue band and the range of the Saus carbonates of the Lower Nappe by the dark blue band. The $^{87}\text{Sr}/^{86}\text{Sr}$ values of marble screens in the Hillstadjellet pluton (Day 3) are shown by the purple band. The Horta, Vikna, and Saus carbonates have $^{87}\text{Sr}/^{86}\text{Sr}$ ratios that indicate a depositional age from 700–800 Ma, whereas the Hillstadjellet carbonates are clearly post-Neoproterozoic, in this case Ordovician (Sandøy, 2003). The Tonian–Cryogenian boundary is from Ogg (2004).

The Horta Nappe crops out in the Horta archipelago and is host to the Hortavær igneous complex (Fig. 2; Gustavson and Prestvik, 1979; Barnes et al., 2003). Barnes et al. (2007) interpreted the Horta Nappe to consist of two parts: migmatitic quartzofeldspathic gneiss with minor quartzite and marble, and a section of predominantly marble, calc-silicate gneiss, and calc-silicate stretched-pebble conglomerate, with minor quartzofeldspathic gneiss. Small prismatic zircons from leucosomes in the migmatitic unit have been dated at ~480 Ma (Fig. 4), which Barnes et al. (2007) interpreted to indicate the age of migmatization. Detrital zircons in the same rocks are as young as Ordovician, which indicates that deposition was closely followed by high-grade metamorphism. In contrast, marbles from the Horta Nappe have Sr and carbon isotope ratios consistent with deposition during Neoproterozoic time (Fig. 5; Barnes et al., 2007). Thus, the Horta Nappe and Lower Nappe may both contain an unconformity that separates Neoproterozoic from Ordovician sedimentary sections.

Bindal Batholith (Days 1 & 3)

The HNC is host to the largest Caledonian (s.l.) batholith in Norway, the Bindal Batholith (Nordgulen, 1993). The batholith consists of plutons whose emplacement ages range from 478 to 424 Ma (Nordgulen et al., 1993; Yoshinobu et al., 2002; Nissen et al., 2006; Barnes et al., 2007). Plutons range in size from km-scale to > 100 km², so that some could be described as distinct batholiths. Plutons of the Bindal Batholith were generally emplaced in the middle crust, at pressures as high as ~800 MPa (Barnes & Prestvik, 2000; Marko et al., 2006). Moreover, at least some of the magmatic activity occurred while the host rocks were undergoing regional metamorphism, or were still hot following such metamorphism. Thus, the Batholith is an excellent locality to study middle crustal emplacement and differentiation processes.

The Bindal Batholith is remarkable in terms of its compositional diversity (Fig. 6). Some plutons are peraluminous to strongly peraluminous, and at least two of these could be classified as “classic” S-type (White & Chappell, 1977). In the classification of Frost et al. (2001) the largest volume of plutonic rocks is magnesian (Fig. 6A) and calc-alkalic to alkali-calcic (Fig. 6B). The few samples that plot in the ferroan field are primarily from the 466 Ma Hortavær complex and the 447 Ma Hillstadfjellet pluton (Fig. 6A). These same samples plot on compositional trends in Figure 6B that extend into the alkalic field, even though parental magma compositions were magnesian and calcic. In the case of the Hortavær complex, Barnes et al. (2005b) explained this compositional trend as the result of assimilation of carbonate-rich host rocks. With the exception of mafic rocks, very few samples of the Batholith are calcic in nature (Fig. 6B), which is in contrast to the abundance of calcic plutonic rocks in Cordilleran-style batholiths.

As the number of radiometric ages of Bindal plutons has increased, attempts have been made to discern time-dependent compositional variation. These attempts have met with only moderate success. At present, the following generalizations can be made, with more detailed information presented during the excursion. (1) The oldest activity in the Batholith (478–470 Ma) was dominated by peraluminous to strongly peraluminous magmas (Fig. 6C). The resulting plutons include the >25-km diameter S-type Vega pluton (Day 1) and a number of tourmaline-bearing two-mica granites, for example the 470 Ma pluton west of Velfjord (Day 3). The compositions of three mafic rocks from the Vega pluton are plotted in Figure 6; these are disrupted mafic dikes and mafic magmatic enclaves. (2) Two plutons make up the next younger subset, from 469–460 Ma, and they are petrogenetically quite distinct. The Hortavær complex is nearly entirely metaluminous (Fig. 6C) and ranges from olivine gabbro through

syenite to alkali-feldspar granite. It is the only pluton in the Batholith known to contain nepheline. Its unusual evolutionary path is thought to result from assimilation of carbonate-rich metasedimentary rocks. The Svarthopen pluton is predominantly calc-alkalic and is characterized by unusual garnet-bearing intermediate rocks (see Day 3). (3) The 450–440 Ma age range contains the greatest diversity of rock types and compositions (Fig. 6). Two of these plutons (Hillstadjellet and Andalshatten) will be visited on Day 3. (4) Among the group of

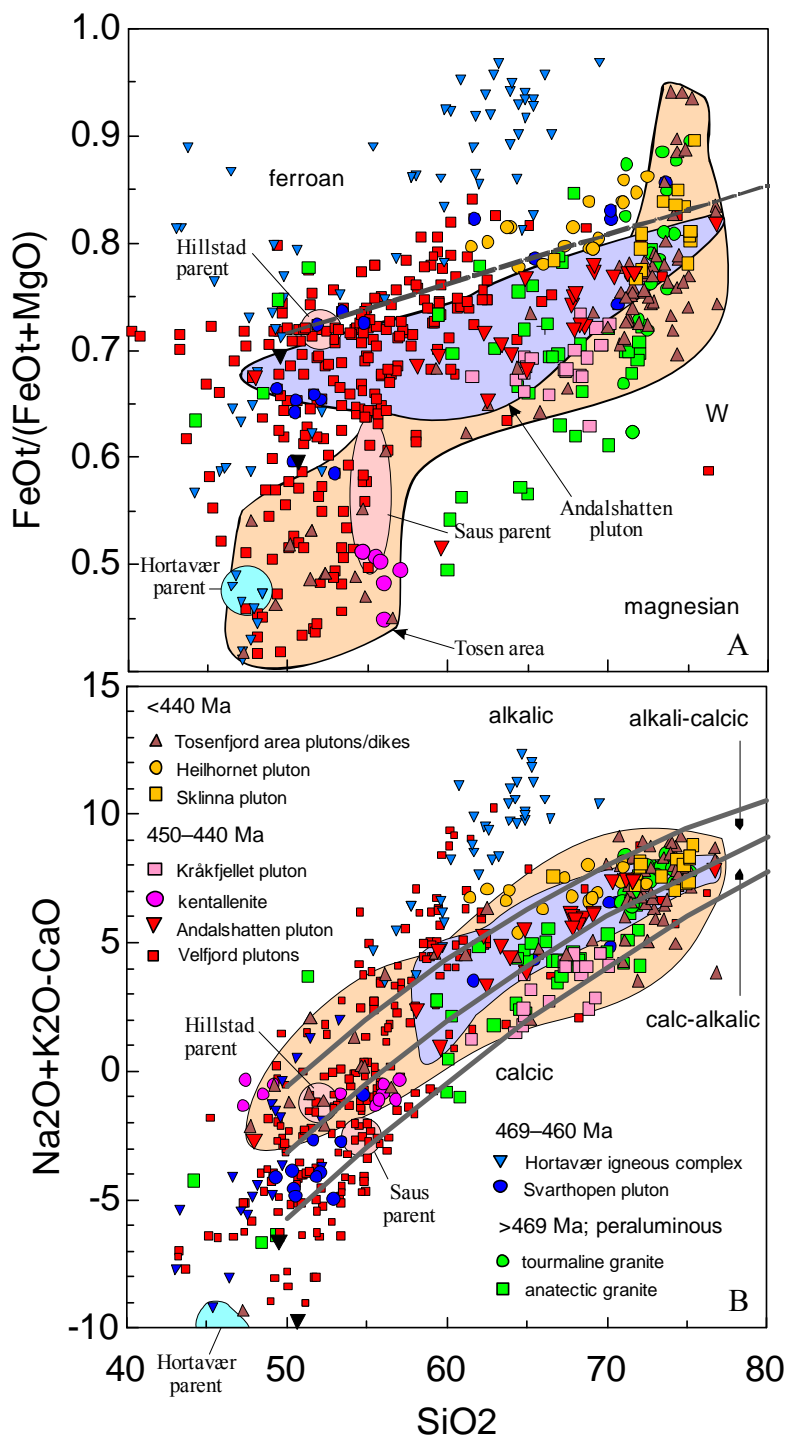


Figure 6. Geochemical variation of Bindal Batholith (see text for references). Symbols are color-coded according to age. The pale brown shaded field encloses compositions of plutonic rocks in the Tosenfjord area (Day 2) and the pale lavender field encloses compositions of the Andalshatten pluton (Day 3). The small shaded fields indicate compositions of parental magmas inferred for the ~447 Ma Hillstadjellet and Sausfjellet plutons and the 466 Ma Hortavær igneous complex. A. Ferroan versus magnesian classification of Frost et al. (2001). B. Modified alkali-lime index classification of Frost et al. (2001).

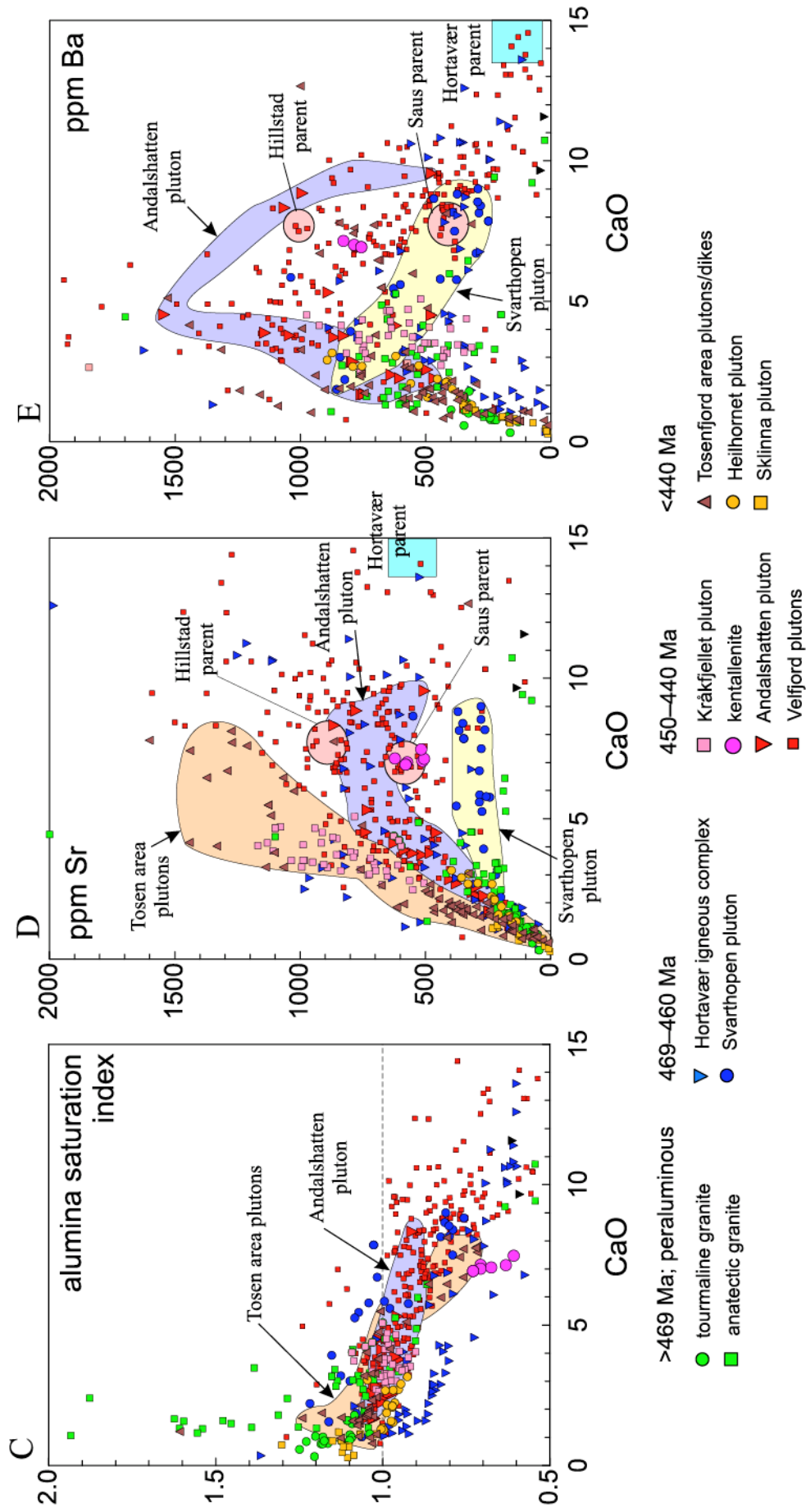


Figure 6, continued. C. Alumina saturation index plotted versus CaO concentrations (wt %). D. Sr versus CaO. E. Ba versus CaO. young plutons (<440 Ma), the Heilhornet pluton (Nordgulen & Schouenber, 1990) is distinct because of its ferroan and alkalic nature (Figs. 6A, B). In addition, a suite of plutons and dikes in the Tosenfjord region are distinct because of their comparatively high Sr contents (Fig. 6D).

Isotopic data for the Batholith were presented by Nordgulen and Sundvoll (1992), Birkeland et al. (1993), and Barnes et al. (2002, 2004, 2005b). These data along with unpublished results (C. Frost, W. Marko, K. Reid, and Y. Li) are plotted in Figure 7. The peraluminous granites of the oldest stage of the Batholith have characteristically high initial $^{87}\text{Sr}/^{86}\text{Sr}$ and ϵ_{Nd} between -7 and -9.5; these ϵ_{Nd} values are similar to ones found for Upper Nappe migmatites (Fig. 7) and semipelitic rocks of the Lower Nappe (Barnes et al., 2002). In contrast, anatectic granites associated with the 465 Ma Svarthopen pluton and ca. 447 Ma Velfjord plutons have ϵ_{Nd} between about -5 and -6. The isotopic compositions of samples from the Hortavær complex are characterized by low ϵ_{Nd} and relatively low initial $^{87}\text{Sr}/^{86}\text{Sr}$ compared to other plutons in the Batholith. These distinctive isotopic values are consistent with an origin involving assimilation of carbonate-rich crustal rocks (Barnes et al., 2005b). Nearly all samples of the two youngest groups of plutons have ϵ_{Nd} between +1 and -5 and initial $^{87}\text{Sr}/^{86}\text{Sr}$ less than 0.710. This data cluster also encompasses a few of the most primitive samples from the Hortavær complex and most samples from the Svarthopen pluton.

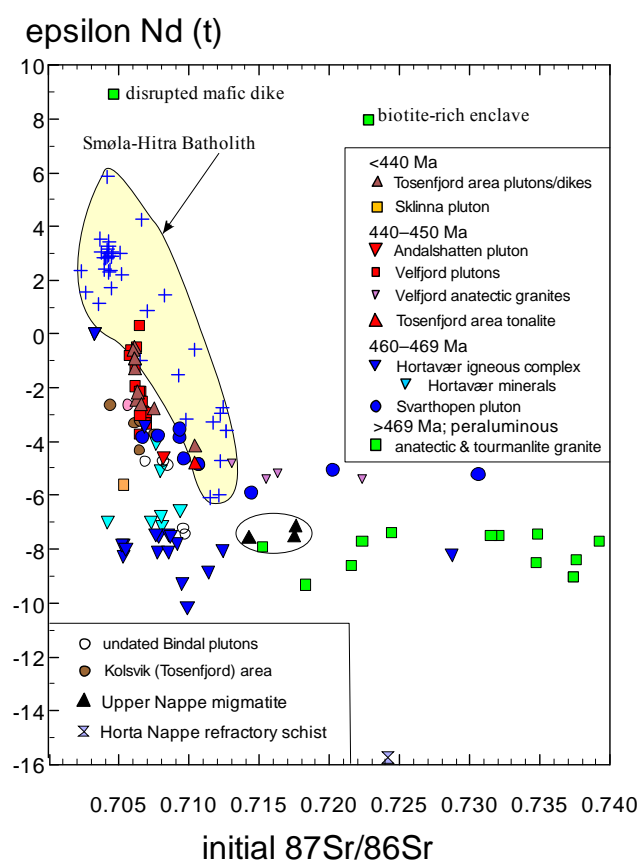


Figure 7. Nd and Sr isotopic compositions for the Bindal Batholith (see text for references). Symbol shapes and colors follow those used in Figure 6, with additional symbols for enclaves in the Vega (anatectic) pluton, mineral compositions from the Hortavær complex, and metamorphic rocks from the Upper and Horta Nappes. The field of compositions of the ca. 448–435 Smøla-Hitra Batholith, which crops out west of Trondheim, is also shown.

Structural and Tectonic Context of the Helgeland Nappe Complex

The first major synthesis of the tectonic evolution of the Uppermost Allochthon recognized structural and lithologic similarities with Laurentia, rather than Baltica, and that the Allochthon underwent a tectonic history that predated the Scandian (i.e., 430-390 Ma) period of the Caledonide orogeny (Gee and Sturt, 1985). Since then, a number of regional and detailed studies have elucidated the structural and tectonic evolution of the HNC and composite nappes and plutons (e.g., Thorsnes and Løseth, 1991; Nordgulen et al., 1989; 1992; 1993; Yoshinobu et al., 2002; Dumond et al., 2005; Barnes et al., 2007). Roberts et al. (2002) and Yoshinobu et al. (2002) noted the west vergence of structures throughout the HNC and suggested that such deformation may be attributed to west-directed thrusting during ‘Taconic’-style collisional orogenesis near the Laurentian margin.

Earlier workers documented at least four distinct stages of deformation within the HNC based on cross-cutting relations and porphyroblast-matrix relationships (e.g., Thorsnes and Løseth, 1991). We have focused our efforts on unravelling the structural evolution where absolute ages of deformation can be accurately constrained using geochronology. U-Pb zircon age data (Yoshinobu et al., 2002; Barnes et al., 2007) and structural relations (Dumond et al., 2005; Anderson et al., 2005; 2007) delineate at least two distinctive regional structural events. The first event resulted in regional tight to isoclinal folds of at least two generations that formed during thrusting and nappe emplacement contemporaneous with 481-475 Ma crustal melting (e.g., the Vega pluton). These structures will be seen throughout the trip on Days 1, 2, and 3. The second structural event occurred during a surge of mafic magmatism between 448 and 442 Ma and resulted in regional extension and exhumation of the Lower Nappe. While many workers noted contractional deformation that was probably Ordovician – and thus pre-Scandian in age – recent work has demonstrated the importance of extensional exhumation of some of the crystalline nappes within the HNC prior to Scandian time (Barnes and Prestvik, 2000; Yoshinobu et al., 2002). On Day 3 we will visit selected outcrops that exhibit Ordovician extension.

Lastly, a fundamental emphasis of our on-going research is understanding the structural history of pluton-host rock systems (e.g., Barnes et al., 2004; Dumond et al., 2005; Anderson et al., 2005; 2007). To that end, Days 2 and 3 will emphasize the structural complexities associated with magma emplacement in the middle crust.

Excursion Route and Road Log

Regions that will be visited on each day are shown in boxes in Figure 2. Road maps for each of the Days may be found in Figures 9, 16, 22, and 27. The first three days of the excursion will use Brønnøysund as a base. Day 1 (Friday, 1 August) will be spent investigating Early Ordovician anatectic magmatic events, S-type granites, their relationship to tectonism, and the constraints these relationships provide for our understanding of Taconian-aged deformation.

Day 2 (Saturday, 2 August) will be a transect through nappes of the Helgeland Nappe Complex along Route 76, with a focus on the structural and thermal history of the nappes.

Day 3 (Sunday, 3 August) has a focus on Middle–Late Ordovician (465-440 Ma) magmatism of the Bindal Batholith. In the morning, we take route 76 to Hommelstø, to study interactions of mafic magmas of the Bindal Batholith with their aureoles. The afternoon will focus on

emplacement of the Andalshatten pluton. Dinner will be at Handelsstedet Forvik, with items from the “Arctic Menu”.

Day 4 (Monday, 4 August) will involve a drive on Route 17 along the Helgeland coast and a visit to the Leka ophiolite and its cover sequence, the Skei Group. Dinner will be in the Leka Motel and Camping Steinsentret, with displays of local and regional rocks and minerals. We will use this venue for a general discussion.

Day 5 (Tuesday, 5 August) will investigate internal structures and deformation of the Middle Nappe and end-Scandian extension on the Kollstrømen detachment zone. We will follow Routes 17 and E6 for a late return to Trondheim.



Figure 8. Route from Trondheim to Brønnøysund shown in blue.

Excursion Stops

Day 1. Vega

Introduction

The focus of this part of the excursion is the earliest plutonic activity in the Bindal Batholith. We presently view this early stage of magmatic activity to range from about 478 to 470 Ma. It is characterized by three types of pluton: tourmaline two-mica granite, biotite granite (generally gneissic), and so-called “anatectic granite”, more familiarly “S-type” granite. We will be looking at the largest example of early Bindal activity, the S-type Vega plutonic complex (Fig. 9). Because of ferry schedules, it is imperative that we take the first (0730, weekdays) ferry. This means that we must be on the road by 0700.

The Vega plutonic complex underlies the southern two-thirds of Vega, the western two-thirds of Ylvingen, the island of Søla, and many smaller islands south and southwest of Vega (Fig. 10). The bulk of the plutonic complex consists of enclave-bearing garnet-biotite \pm sillimanite \pm cordierite granite and granodiorite. Diatexitic rocks are exposed in a discontinuous band along the northern contact on Vega and on northern Ylvingen (Fig. 10). Biotite granite is the main plutonic rock type exposed on Ylvingen and also occurs in northeastern Vega. Small

Pods (<1 km²) of quartz diorite are exposed along the northern contact and also as meter-scale dikes in the host rocks.

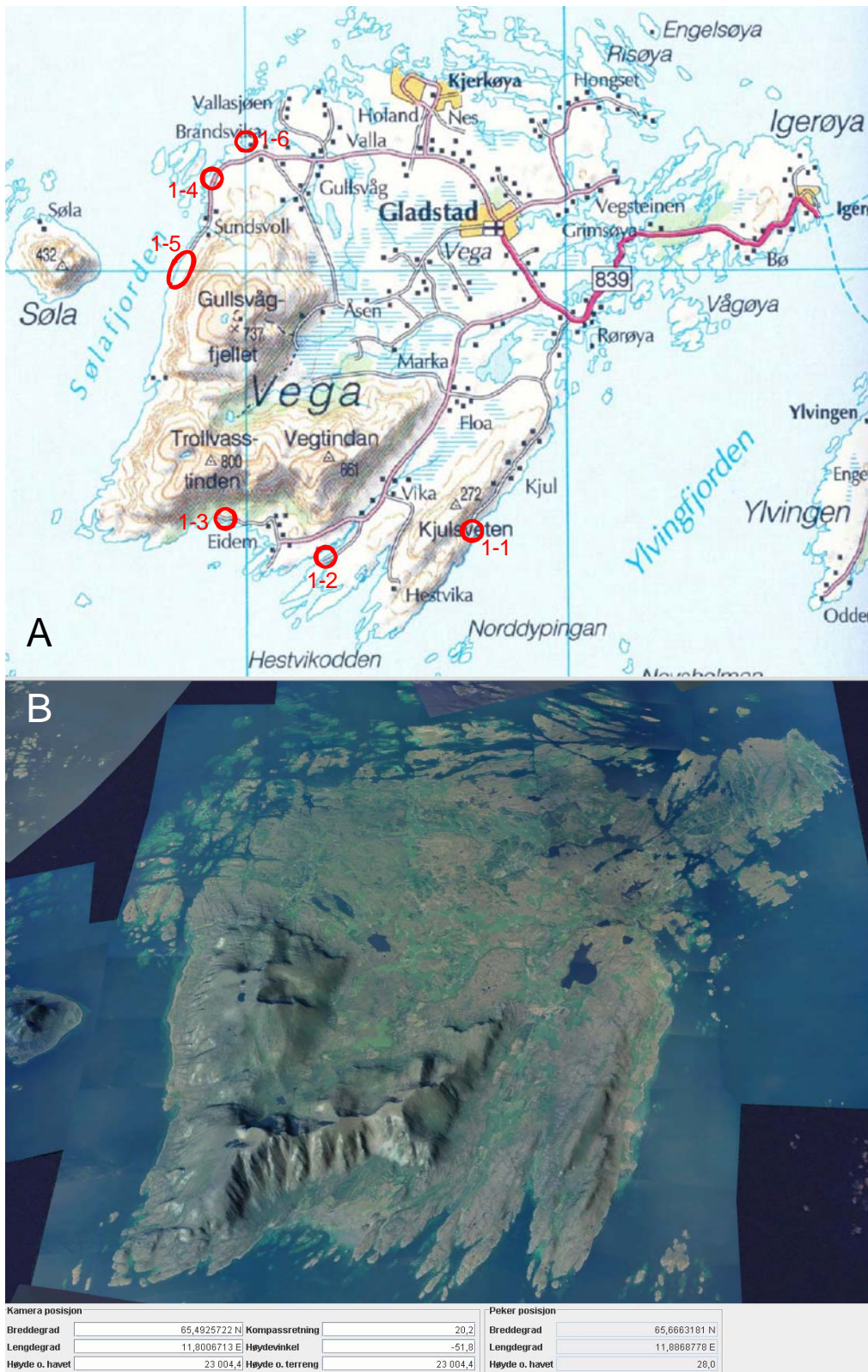


Figure 9. (A) Road map of Vega with field trip stops. (B) Satellite view of Vega (<http://www.norgei3d.no/>).

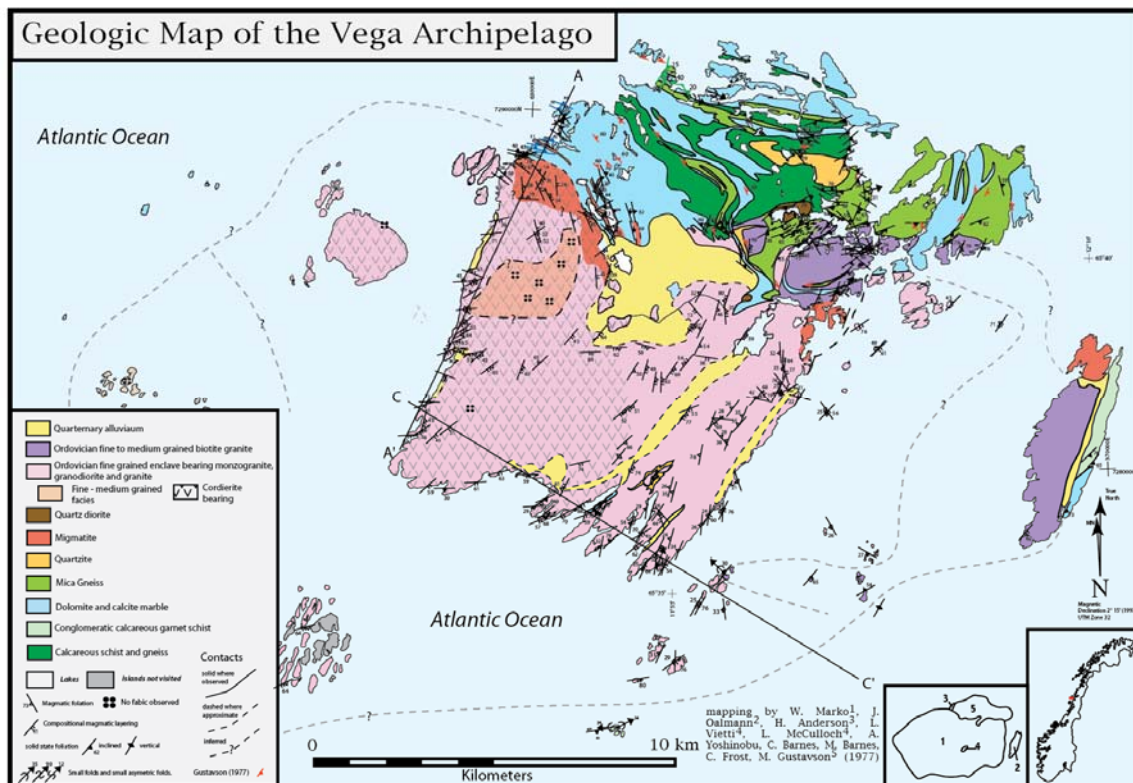


Figure 10. Geologic map of Vega and adjacent islands (after Gustavson, 1975, 1977; W.T. Marko, in preparation).

Conditions of emplacement are constrained by assemblages in diatexites at Bø and northern Ylvingen and by the presence and distribution of cordierite in the main pluton. In the diatexites, the peak metamorphic mineral assemblage (quartz-plagioclase-biotite-kyanite-staurolite-garnet-muscovite-melt) and GASP calculations suggest partial melting at $P > 650$ MPa and $T < 700^\circ$ C. Cordierite is stable in western exposures of granite and granodiorite but is absent in eastern Vega and Ylvingen. This contrast between the higher pressure assemblages in the east and lower pressure assemblages in the west suggests that the Vega complex is tilted toward the west or southwest.

Vega granitic rocks are characteristically peraluminous to strongly peraluminous (Fig. 6C), although leucogranites exposed along the NW contact range from peraluminous to metaluminous. Initial $^{87}\text{Sr}/^{86}\text{Sr}$ values in the granitic rocks range from 0.7096 to 0.7432, and initial ϵ_{Nd} values range from -7.5 to -10.8 (Fig. 7). The mafic pod, dikes, and enclaves define a distinct $\text{MgO} + \text{FeO}_t$ -rich, metaluminous compositional group and two of these mafic rocks have distinctly high ϵ_{Nd} values (Fig. 7).

Stop No. 1-1: Kjul outcrops (Langhalsan)

Location

Drive south from Rørøy toward Kjul (Fig. 9). Park at UTM 32W 0635811, 7280000, where a narrow track departs to the left, toward the sea. Follow this track to a sandy beach, then walk along the beach (Langhalsan) to the southeast toward the nearest outcrops. The stop begins at the northern end of these outcrops: UTM 32W 0636094, 7279802.

Introduction

With the exception of some leucogranitic granites, enclaves are ubiquitous in granitic parts of the Vega plutonic complex. The enclaves include diatexite, high-grade, compositionally variable gneisses and schist, quartzite, metaserpentinite, and mineral aggregates, plus mafic magmatic enclaves. With the exception of some leucocratic granites, the complex also displays a range of magmatic fabrics, including schlieren layering and banding and, diatexitic layering. Magmatic foliation is formed by alignment of biotite grains and/or surmicaceous enclaves. This outcrop provides a good introduction to the various types of enclaves and some of the magmatic fabrics characteristic of the intrusion.

Description

The outcrops here consist of biotite \pm garnet granite to granodiorite with hypidiomorphic granular to “pseudo” allotriomorphic granular texture and local zones with euhedral K-feldspar phenocrysts (Fig. 11A). Enclaves include migmatite, a variety of gneisses and schist, calc-silicate rocks, granite/granodiorite, mineral aggregates, massive quartz, and xenocrysts (Fig. 11B). The igneous and migmatitic enclaves are texturally similar to the host and are commonly rounded. Migmatitic enclaves reach several meters in diameter.

Magmatic foliation is defined by alignment of surmicaceous enclaves (biotite-rich mineral aggregates) (Figs. 11C & D). This fabric is part of a structural domain on the eastern side of the intrusion with N-NW strike and moderate dip. Layering is poorly exposed at this location, but some thin leucocratic bands are visible. These layers are typically only a few centimeters wide and commonly wrap around enclaves. In eastern Vega, the dips of layering and foliation are distinctly different (Figs. 11E & F).

Stop No. 1-2: Outcrops along the east side of Vikasjøen (Trollrevheian).

Location

Drive south from Floa and bear left at the first left turning after Vika. Park at UTM 32W 0632185, 7278864 then traverse southward along the shoreline exposures as far as UTM 32W 0632105, 7278795.

Introduction

This outcrop provides excellent exposure of a large xenolith, its preserved internal structure, and post-incorporation enclave deformation.

Description

This outcrop is composed of calc-silicate/marble xenolith surrounded by granodiorite similar to that observed at Stop 1-1. Large, in some cases kilometer-scale, xenoliths are sparsely distributed in the intrusion. These enclaves typically have long axes and subsolidus fabrics aligned subparallel to local magmatic layering. This xenolith has an approximate orientation of N58E and extends northward for one km.

The dominant fabric in the xenolith is formed by transposed layering; this fabric is referred to as S₂. Intrafolial rootless fold hinges and boudinage are also present. These structures are similar to ones mapped in host rocks along the northwest pluton contact (Stop 1-6), which have been correlated by Anderson et al. (2007) with the D₂ event described by Thorsnes and Løseth (1991). This transposed fabric was later folded into F₃ folds, which may also be seen at

this outcrop. The leucocratic rind that characterizes the contact between the xenolith and host plutonic rocks has also been folded (Figs. 12A & B).

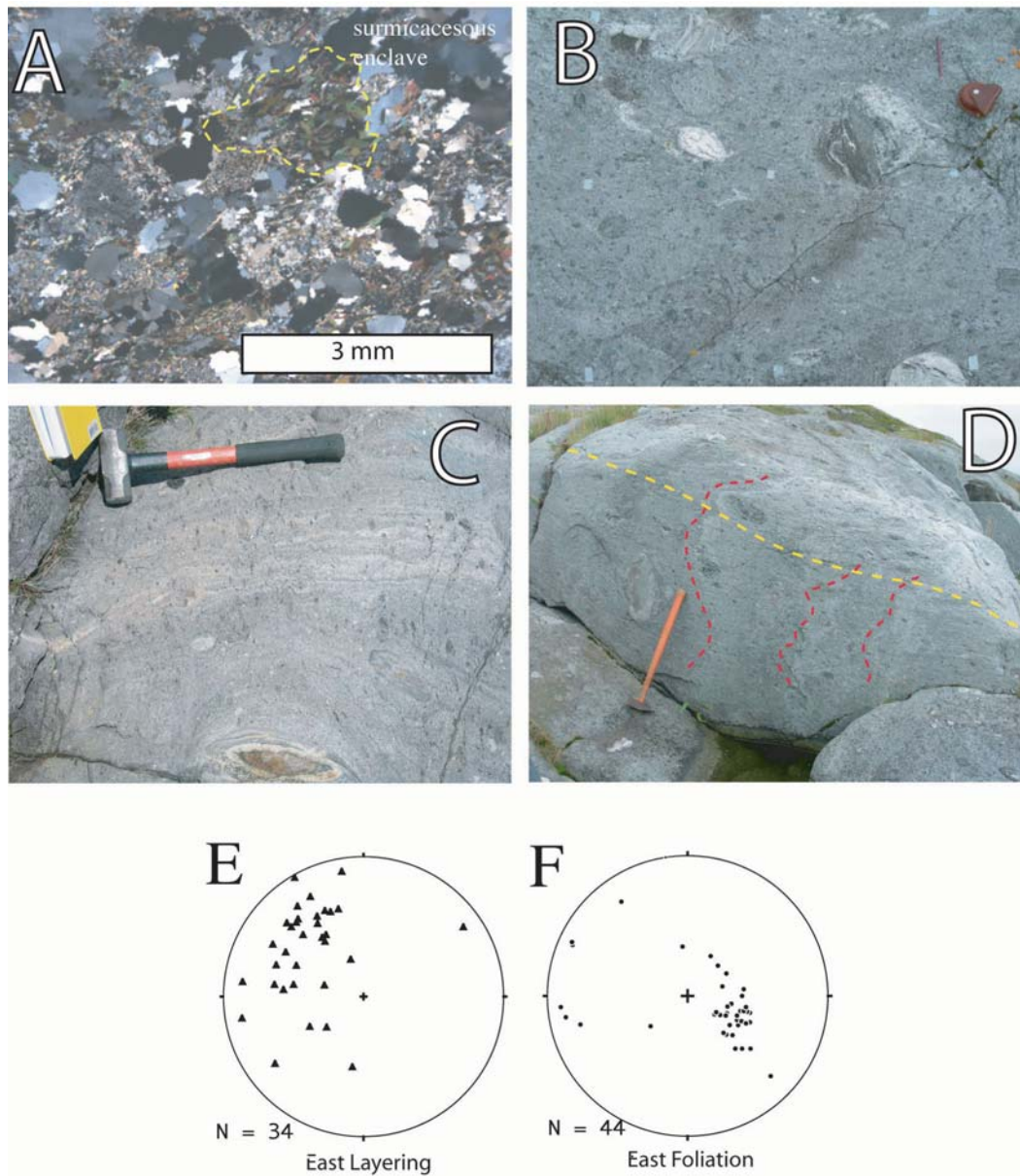


Figure 11. A) Crossed polar photomicrograph of granodiorite texture at Stop 1-1. The surmicaceous enclave is comprised of biotite, quartz, and feldspar. B) An assortment of gneissic, migmatitic, surmicaceous and other enclaves commonly observed on Vega. C) Leucocratic banding (parallel to hammer) exposed on eastern Vega, crosscut by a magmatic foliation defined by surmicaceous enclaves. D) Cross cutting foliation and layering where layering appears folded. E) Poles to magmatic layering from eastern Vega. F) Poles to magmatic foliation from eastern Vega.

A large quartzite xenolith exposed on the ridge to the northeast shows similar deformation (Vietti et al., 2005). The quartzite xenolith underwent boudinage and was split by injections of granodiorite. The deformation and back-intrusion of diverse, large xenoliths suggest that xenolith incorporation was temporally and spatially transgressive (Marko et al., 2005).

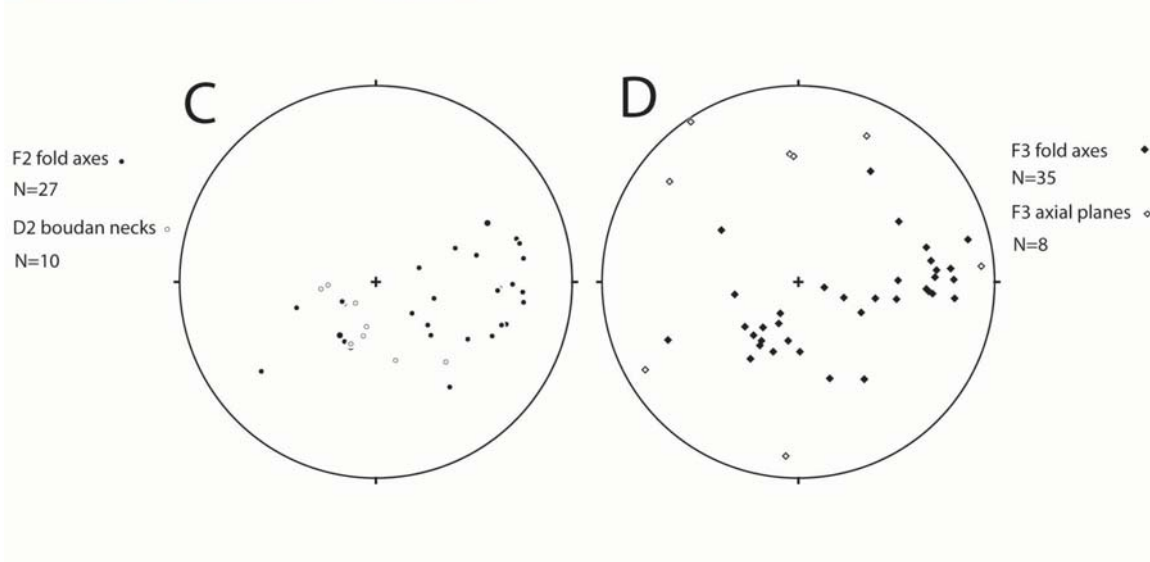
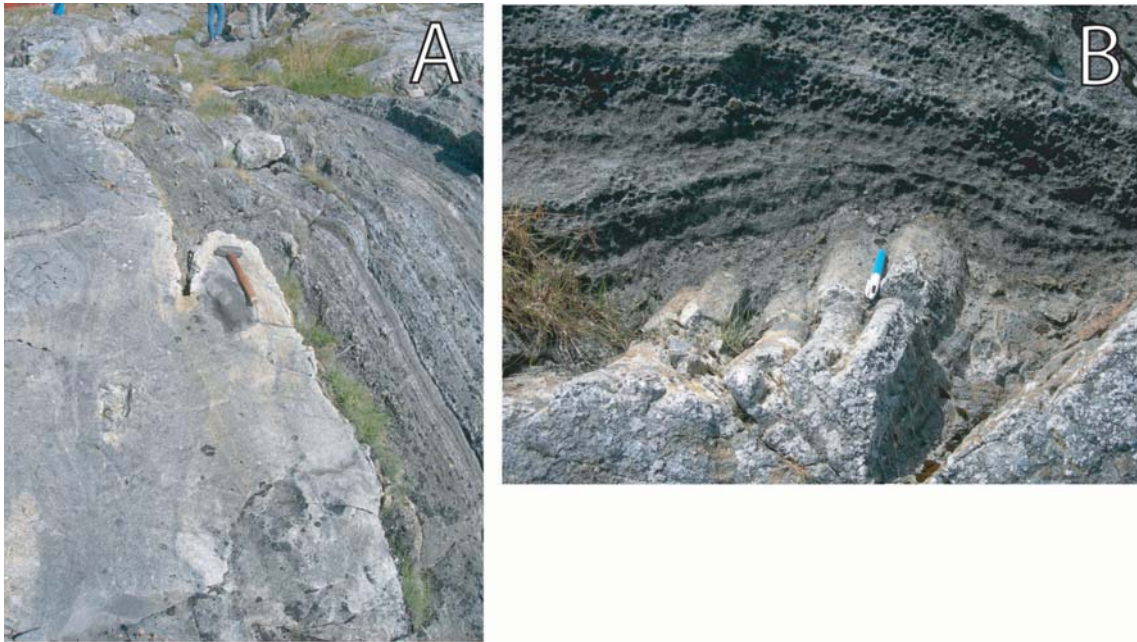


Figure 12. Contact relationship between the granitic host and a marble/calcsilicate enclave. A) The contact and leucocratic rind appear to be folded. B) Mullions in granite adjacent to the enclave. Lower hemisphere stereonets of C) F2 fold axes and boudin necks, and D) F3 fold axes and axial planes.

Stop No. 1-3: Levika area.

Location

From Vika, drive southwest through Eidem. Park on the south side of road near the football (soccer) goals at UTM 32W 0629816, 7279747. Traverse from this point southward along the rib of rock that extends seaward.

Introduction

This outcrop provides examples of magmatic fabrics and the enclave population on the southeastern side of Vega.

Description

The rock type at this location is garnet cordierite biotite granodiorite. Cordierite typically occurs as nodular aggregates. The magmatic fabric here is schlieren banding characterized by modal variations of biotite and K-feldspar (Fig. 13B). This fabric increases in intensity in outcrops to the west (Fig. 13A). However, individual layers are traceable for distances of no more than a few 10's of meters. The magmatic foliation observed at Stop 1-1 is not present.

Enclaves at this location include an assortment of schist, gneiss, and mineral aggregates. The proportion of fine- to medium-grained mafic enclaves at this location is larger than at Stop 1-1 and this higher abundance of such enclaves is observed at other outcrops in the southwestern part of the intrusion. Some of these mafic enclaves have cm-scale reaction rinds that exhibit grain coarsening or modal phase variations, interpreted to result from chemical reaction between the enclave and the host magma. Despite the evidence for physical incorporation of mafic material in this part of the pluton, the initial $^{87}\text{Sr}/^{86}\text{Sr}$ values from southern Vega are >0.730 .

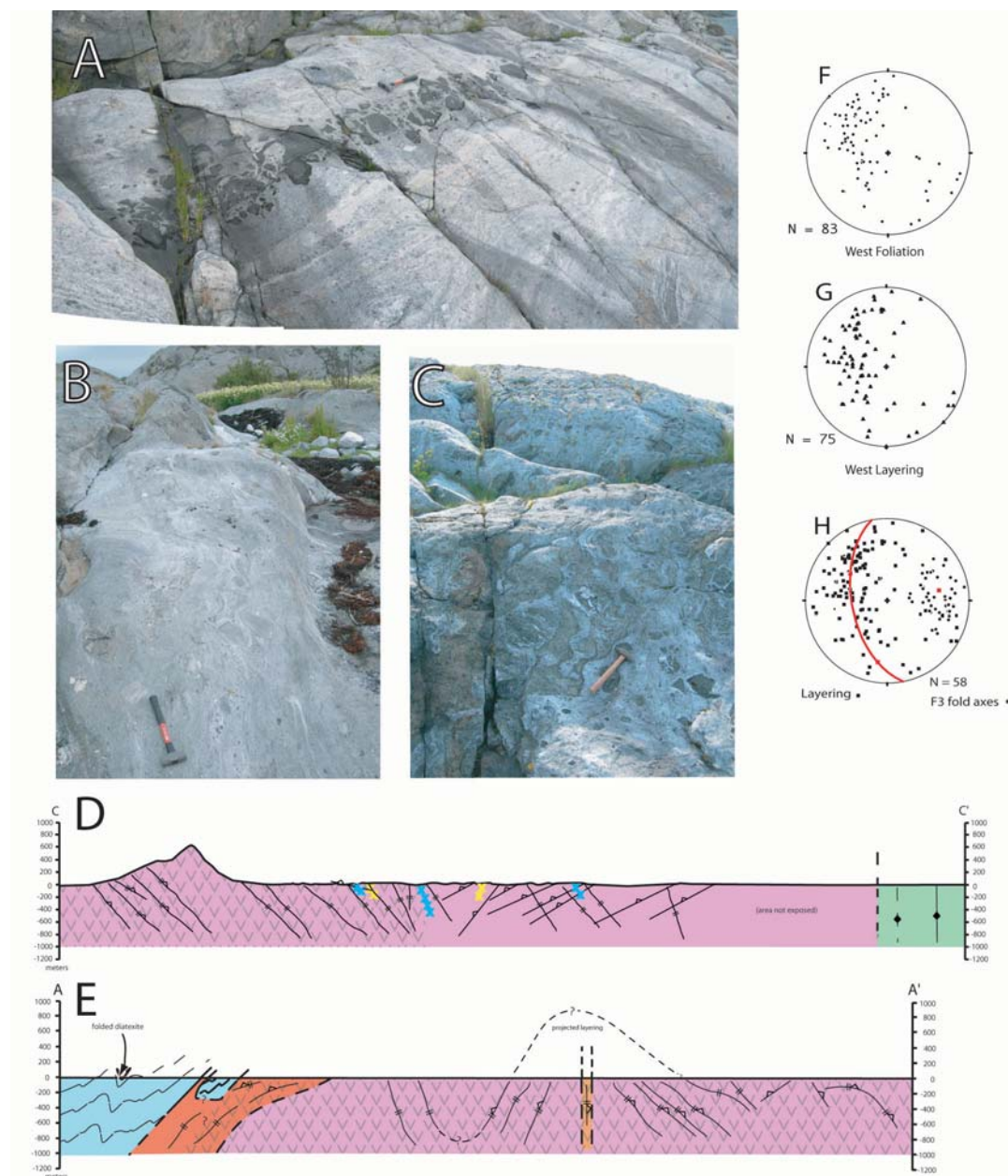


Figure 13 (preceding page). Structural observations from southern and western Vega. A) Well developed compositional banding similar to that observed at Stop 1-3. B) Anastomosing layering wrapped around a moderately well-sorted cluster of schist/gneiss enclaves. C) Migmatitic layering observed in a diatexitic enclave. D) Schematic cross section (C-C') through the southern part of Vega. Enclave locations are marked with an "X" (yellow = quartzite, blue = calcsilicate/marble). E) Schematic cross section (A-A') along the western side of Vega. Magmatic fabrics can be intermittently exposed but are pervasively observed across the intrusion. F) and G) Poles to magmatic fabrics on western Vega. Magmatic layering and foliation are typically subparallel to each other. H) Poles to magmatic layering on western Vega define a statistical girdle distributed about an axis with an orientation N80E 36NE. This axis has a similar orientation to F3 fold axes measured in host rocks along the northwestern contact.

Stop No. 1-4: Tangvika quay.

Location

Drive west from Gladstad through Valla and past the *skytobane* to the road that parallels the northwestern coast of the island. Look for a narrow road with a gate (near 7287900), turn right on this road and park at the end of the road (UTM 32W 0629230, 7287925). Traverse about 200 m to the southwest. Proceed over the small knob south of the quay and walk to approximately UTM 32W 0629097, 7287789.

Introduction

This stop provides good access to outcrops of dendritic and nodular quartz-cordierite aggregates.

Description

The rock type at this location is a cordierite \pm sillimanite \pm garnet biotite muscovite granite and granodiorite. The magmatic fabric consists of schlieren layering, which is subparallel to magmatic foliation formed by aligned biotite (Figs. 13F & G). The orientation of this fabric is variable, but south of this location the strike is consistent with variable dips (Fig. 13E).

The cordierite (now mostly retrogressed to pinite) displays two habits in this area. Both consist of aggregates of quartz + cordierite + biotite \pm garnet that have either a nodular or dendritic form (Figs. 14A, B, C). Cordierite grew over a pre-existing magmatic layering and fabric, and although it does not appear to be strained, some branches are aligned parallel to the magmatic fabric. Prismatic cordierite (Fig. 14D) is absent here; it is present only in the fine to medium grained granodiorite exposed in the center of the intrusion and on skerries to the west. Cordierite compositions are variable, with Mg/(Mg+Fe+Mn) values from 0.48 to 0.63.

Several lines of evidence support a magmatic origin for the cordierite: 1) The Na-in-cordierite thermometer (Mirwald, 1986) gives average temperatures of 675° and 700° \pm 30°C for cordierite-quartz aggregates and prismatic cordierite phenocrysts, respectively (Fig. 14F); 2) cordierite does not overprint what were probable sub-solidus diatexitic enclaves (Fig. 14C), and 3) cordierite is compositionally and texturally similar to cotectic and peritectic cordierites from the Velay granite and South Mountain and Musquodoboit Batholiths (Barbey et al., 1999; Erdmann, et al., 2004).

Crystallization of dendritic cordierite after development of the magmatic fabric suggests that some cordierite crystallized after emplacement of the magma. Similar cordierite-quartz aggregates are thought to nucleate by the reaction $2 \text{ Bt} + 6 \text{ Sil} + 9 \text{ Qtz} = 3 \text{ Crd} + 2 \text{ Kfs} + 2 \text{ V}$ (Barbey et al., 1999). Because garnet is associated with some cordierite-quartz aggregates, the reaction $2 \text{ Grt} + 4 \text{ Sil} + 5 \text{ Qtz} = 3 \text{ Crd}$ can be used to estimate equilibrium pressure, assuming sillimanite activity = 1. Such estimates indicate equilibrium conditions near 500 MPa. These aggregates were interpreted as the products of exhumation and possibly isobaric cooling by Barbey et al., (1999) and Siddoway et al., (2004) (Fig. 14F).

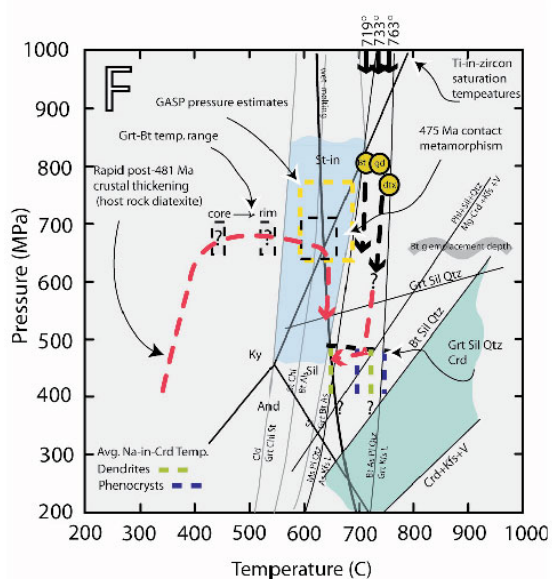
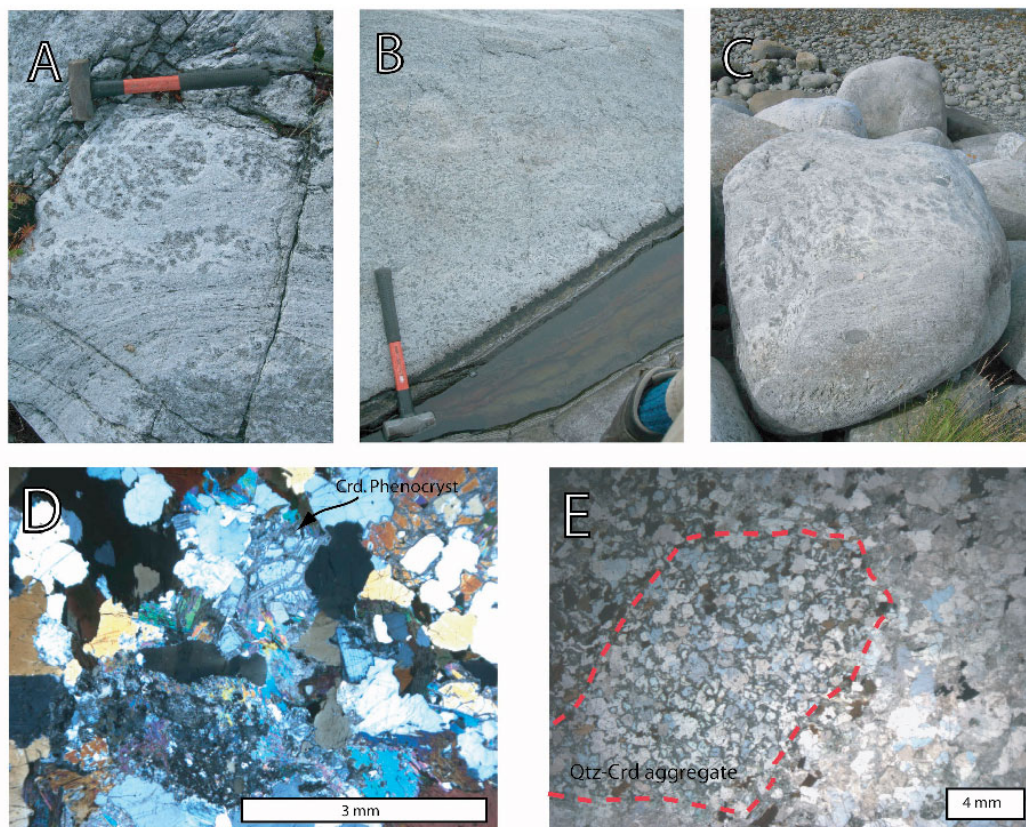


Figure 14. A) Dendritic cordierite overprinting the compositional layering and foliation. B) Nodular cordierite weakly aligned with magmatic fabrics. C) Cordierite growing around a diatexitic enclave. D) Image with crossed polars of cordierite phenocrysts in medium grained granodiorite. E) Qtz-Crd aggregate in granodiorite. F) Schematic P-T-t paths for Vega host rocks and magmas. Aluminosilicate and $\text{St} + \text{Chl} = \text{As} + \text{Bt}$ reactions (NaKFMASH after Pattison (2001). Cordierite-forming reactions $\text{Grt} + \text{Sil} + \text{Qtz} = \text{Crd}$, $\text{Bt} + \text{Sil} + \text{Qtz} = \text{Crd} + \text{Kfs} + \text{V}$ and water saturated melting curve (MASH and KFMASH) from Barbey et al., (1999). Other reactions after Spear (1993).

Stop No. 1-5: Sørneset coastline.

Location

From Tangvika, continue south until the road enters a gravel quarry. Parking is best at the northern end of the quarry.

Introduction

This brief stop provides participants an opportunity to see examples of nodular and dendritic cordierite.

Description

Boulders and cobbles along the shoreline provide the best-displayed and most striking examples of the range of cordierite habits seen in the pluton, including large dendrites.

Stop No. 1-6: Gullsvågsjøen area.

Location

Park where a narrow track leaves the road toward the right (UTM 32W 630000, 7288640), about 100 m east of the white house with a red roof. Follow the track northward toward the shore line and proceed past two boat houses along the shore. Cross to the peninsula to the north. The location of this crossing will be dependent on tide conditions.

Introduction

This locality highlights the structural aureole of the Vega pluton. The timing relations between pre- and syn-magmatic regional deformation and pluton emplacement is of particular interest.

Description

Figure 15 displays a geologic map of the area, showing major lithologic units and structural features. The main pluton–host rock contact is between cordierite-bearing granodiorite and calc-silicate rocks, marble, metasandstone, and pelitic gneiss and schist. The pluton contains deformed calc-silicate xenoliths and mafic magmatic enclaves. The aureole rocks are intruded by dikes and sills of leucogranite and by a composite intrusion of granodiorite and diatexite.

Within the aureole, three stages of deformation are recognized, two of which were pre-emplacment regional deformation (D1–2). The last (D3) stage was synchronous with pluton emplacement. D1 was an early, cryptic fabric-forming event; it was transposed by D2, which is defined by NW-trending, moderately plunging, tight to isoclinal folds and boudinage. D2 structures are cut by granitic dikes and are folded about E-W trending, upright, tight to open D3 folds. The axial planes of these D3 structures are sub-parallel to the pluton contact (Fig. 15). Boudinage of post-D2 granitic dikes also defines D3. Penetrative D3 structures become less pervasive >2 km away from the main pluton contact, but they have been observed outside of the aureole (Anderson et al., 2005).

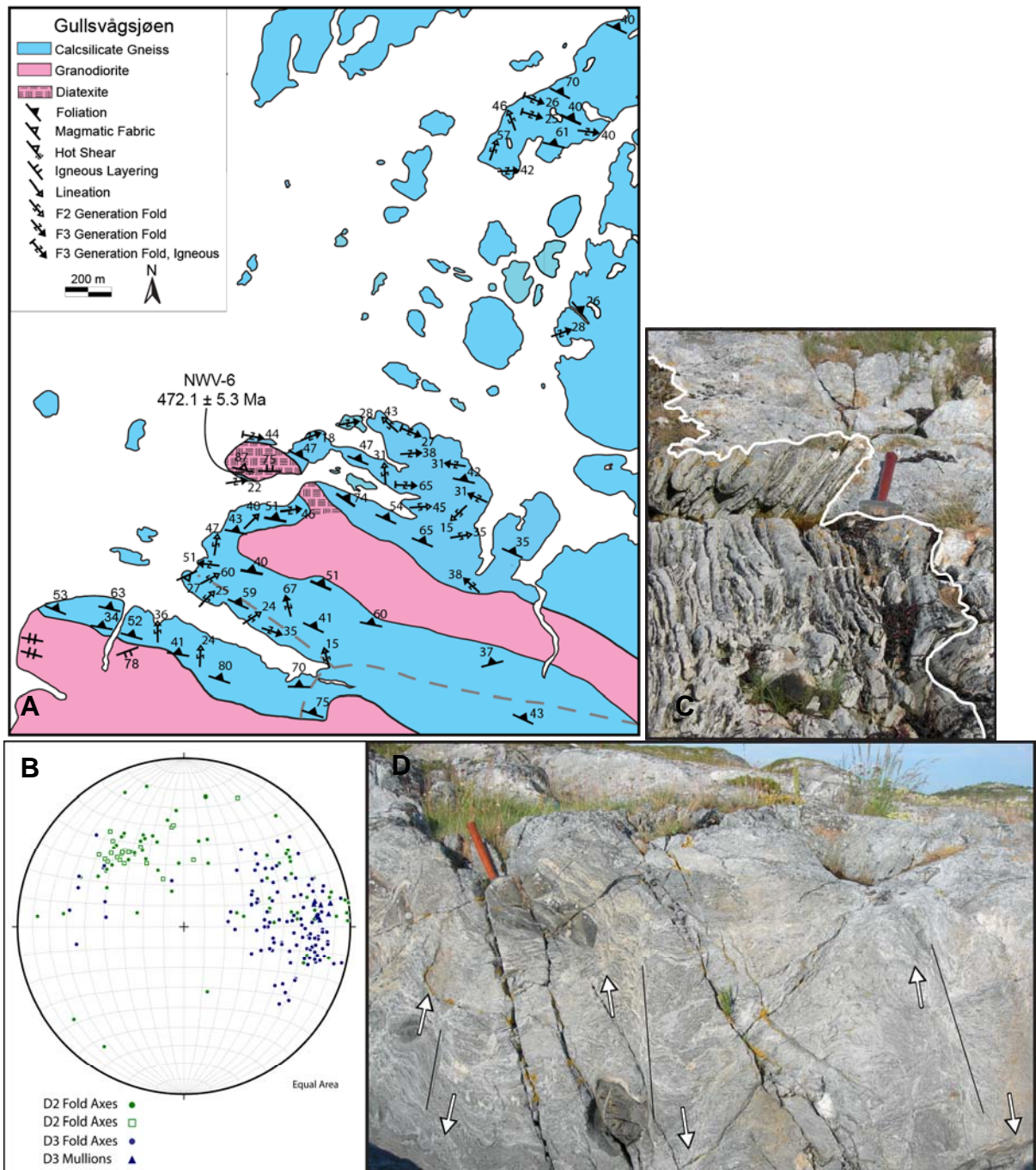


Figure 15: Gullsvågsjøen geology; A) Geologic map of the structural aureole of the Vega Pluton showing major units and structural features; B) Lower hemisphere stereonet of NW trending D2 and E-W trending D3 structural features, where D2 features plot within the D3 realm, D2 structures are interpreted to be involved in D3 deformation; C) Diatexite cutting folded host rocks; D) Diatexitic “hot shears” displaying dextral sense of shear which is consistent with D3 deformation, view to the NE.

The composite sheet of granodiorite and diatexite cuts folded and deformed host rocks (Fig. 15C). Internally, the contact between the diatexite and granodiorite is gradational over a few meters. The granodiorite is texturally and lithologically comparable to that of the Vega pluton. Folded and deformed metasedimentary xenoliths and mafic magmatic enclaves occur in the granodiorite and the diatexite; many of them exhibit shear sense similar to that of the D3

structures. The diatextite also exhibits syn-magmatic shear bands (32W 0630560, 7288687) and asymmetric, top to the east dextral folds, which are sub-parallel to F3 axial planes. These observations indicate that emplacement of the granodiorite–diatextite sheet was synchronous with that of pluton emplacement and regional (D3) deformation. Thus, the 472.1 ± 5.3 Ma (U-Pb, zircon) age of the dike constrains magmatism and D3 deformation to be late Early Ordovician (Barnes et al., 2007).

Day 2

Introduction. Nappes of the Helgeland Nappe Complex

The focus today is on the nappes that make up the Helgeland Nappe Complex. Five nappes have been mapped. From structurally highest to lowest, they are the Upper, Middle, Lower, Sauren-Torghatten, and Horta Nappes (see the Regional Geology section). Nappe depositional ages range from Neoproterozoic to Early Ordovician, as determined by U-Pb (zircon) ages of detrital zircons and chemostratigraphy of calcite marbles. Characteristic ages and lithologic features of the nappes are illustrated in Figures 2 and 3, which also show that the nappes are distinguished on the basis of their degree of metamorphism.

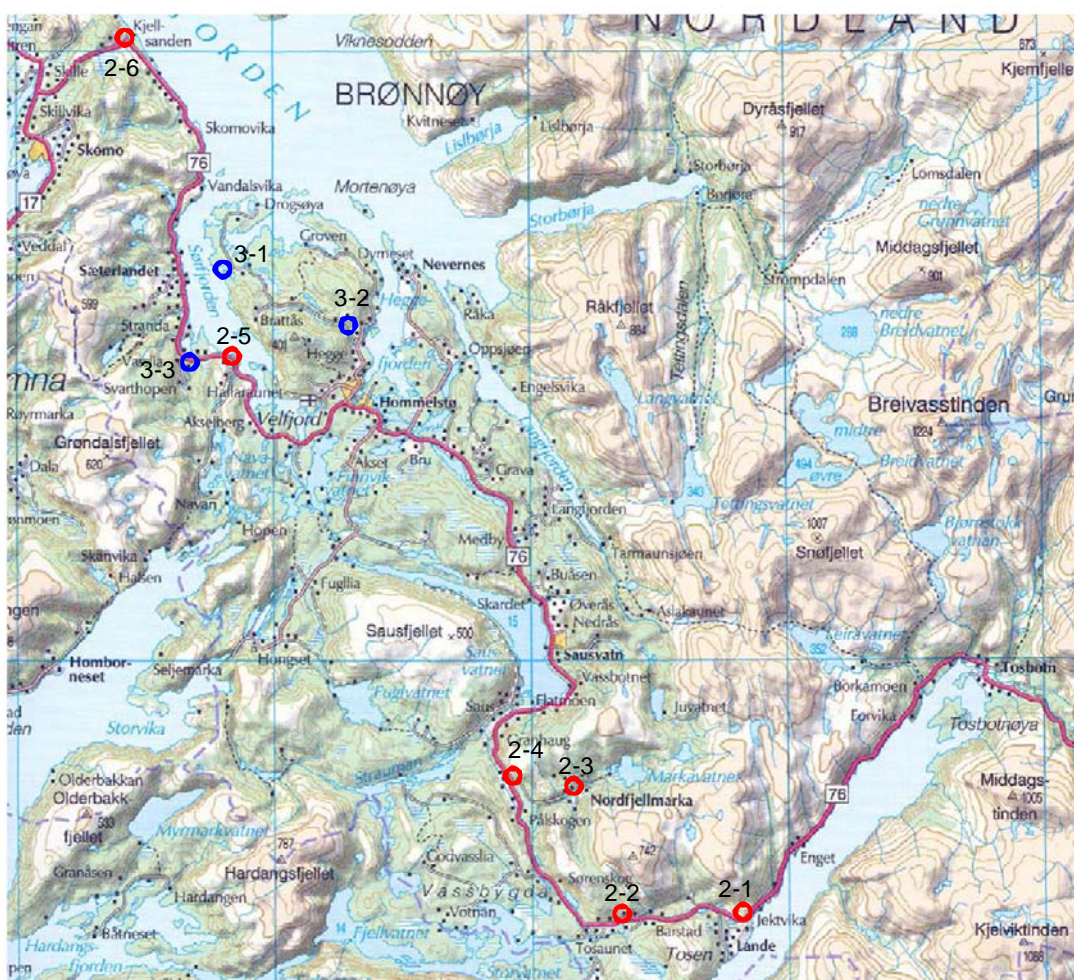


Figure 16. Road map for Day 2 and the first half of Day 3.

Stop No. 2-1: Route 76 road cuts near Lande.

Location

Park at the small turnout at UTM 33W, 0397370, 7239419 (Fig. 16). We will inspect the large road cuts to the east and west of this location.

Introduction

These road cuts provide a 3-D exposure of the migmatites and calc-silicate rocks of the Upper Nappe along with a range of intrusive rocks. Similar metamorphic and igneous rocks are exposed along the length of Tosenfjord toward Tosbotn. To the east, migmatitic rocks of the upper Nappe give way to a thick section of calc-silicate gneisses.

Description

Figure 17 is a composite photograph of the northern side of the main road cut showing principal rock units and their radiometric ages. The oldest rocks in this exposure are semi-pelitic migmatite and calc-silicate gneiss. Detrital zircons in migmatite suggest an age of deposition of Early Ordovician and the youngest zircons in the migmatite (480.8 ± 2.1 Ma) are interpreted to indicate the age of migmatization (Barnes et al., 2007). Stromatic (layered) migmatite is crosscut by diatexitic migmatite that lacks through-going internal structure and contains blocks of stromatic migmatite and calc-silicate gneiss. The diatexite consists of sillimanite, garnet, muscovite, biotite, plagioclase, and quartz; stromatic migmatites contain the same assemblage \pm cordierite. The T of partial melting was estimated using Ti-in-zircon thermometry on \sim 480 Ma zircons to be \sim 800°C and P was estimated using GASP thermobarometry to be 500–700 MPa.

A quartz dioritic intrusion just east of the main road cut yielded a U-Pb (zircon) age of 447.3 ± 2.8 Ma. Al-in-hornblende barometry (e.g., Anderson and Smith, 1995) combined with plagioclase-hornblende thermometry on this sample resulted in an estimated emplacement P of 330 ± 40 MPa at $T \sim 712 \pm 19^\circ\text{C}$. Two mafic intrusions, a net-veined monzonitic dike and a foliated, banded diorite, gave zircon ages of 436.7 ± 3.5 Ma and 436.9 ± 4.4 Ma, respectively.

Exposures of the Upper Nappe along Tosenfjord are characterized by a network of granitic and leucocratic tonalitic dikes. Two dated samples gave 431.9 ± 3.5 Ma and 424.7 ± 5.6 Ma (U-Pb, zircon). Several of these felsic dikes mingled with mafic magma. Particularly good examples are exposed on the southern face of the road cut.

As shown in Figure 6, Late Ordovician and Early Silurian plutonic rocks in the Tosenfjord area span a large compositional range and have characteristically high Sr contents. Rare earth element (REE) patterns (Fig. 17C, D) have steep negative slopes with weak negative Eu anomalies. Some of the granitic dikes have heavy REE contents below 10X chondrites, which suggests residual garnet in the source.

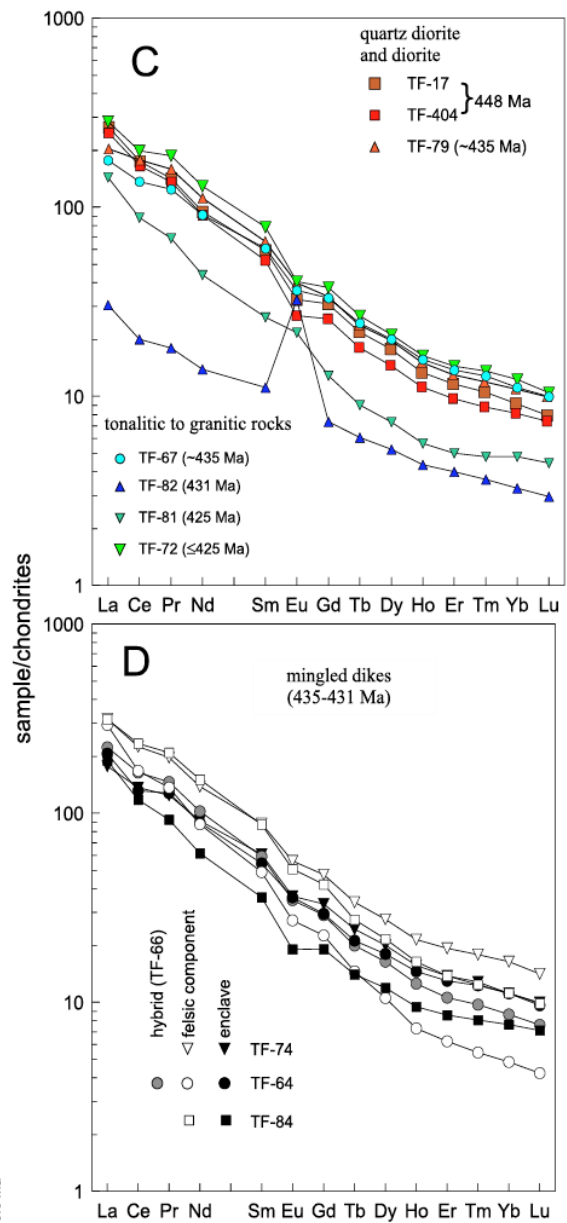
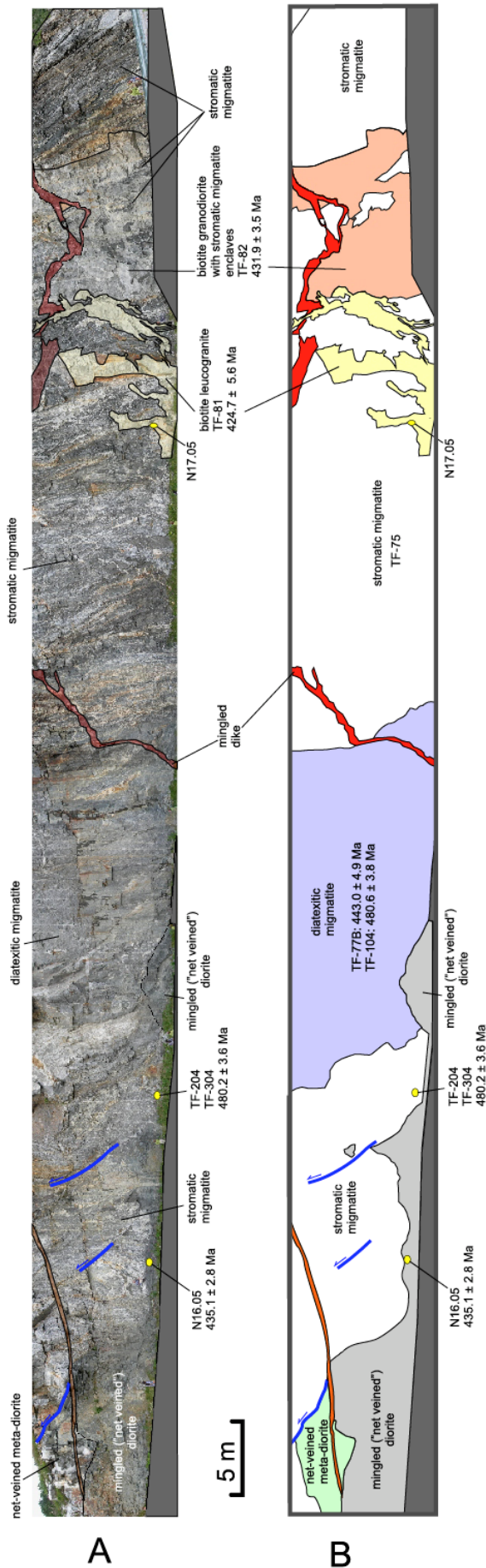


Figure 17. Composite photograph of the north face of the double road cut above Tosenfjord showing principal contacts and locations of dated samples. B. Sketch map of the composite photograph shown in A. C. Rare earth element patterns of mafic and felsic (tonalitic to granitic) dikes. Samples TF-17 and TF-404 are from the ca. 448 Ma intrusion exposed in the road cut to the east. D. Rare earth element patterns of mingled dikes showing the similarity in patterns of mafic and felsic end members.

Stop No. 2-2: Aunlia road cuts.

Location

This stop is in road cuts at Aunlia, UTM 33W 0392796, 7239406. These cuts were incomplete when visited in 2007, so specific parking locations were not known.

Introduction

These road cuts are in various semi-pelitic and calc-silicate schists of the Middle Nappe. They are cut by numerous leucocratic dikes similar to those seen at Stop 2-1. These dikes are, in turn, deformed.

Description

In contrast with the Upper Nappe, the Middle Nappe is characterized by amphibolite-facies assemblages and a lack of migmatites. Conglomerates are common in the Middle Nappe (see Stop 2-3), as are fine-grained semipelitic and calc-silicate schists. Rocks exposed here are of the latter type and are cut by numerous fine- to medium-grained granitic dikes similar to the <435 Ma dikes at Stop 2-1 (Fig. 18A). Dikes at this locality have not been dated, but a boudinaged granitic dike from the upper Markaevla drainage (~4.5 km north) yielded an age of 431.2 ± 3.6 Ma (Fig. 18B). A boudinaged gabbroic dike from the same an age of 442.2 ± 3.4 Ma (Fig. 18C).

Structures within the Aunlia road cuts are dominated by shallowly east-dipping foliations and recumbent tight to open folds. Sparse shallowly east-plunging lineations and sub-horizontal boudin hinge-lines are all consistent with near vertical shortening and east-directed extension. Based on the lack of observable crystal-plastic strain within the granitoid dikes, we interpret the deformation to be syn-magmatic. However, detailed structural and petrologic study of these rocks has not yet been undertaken.

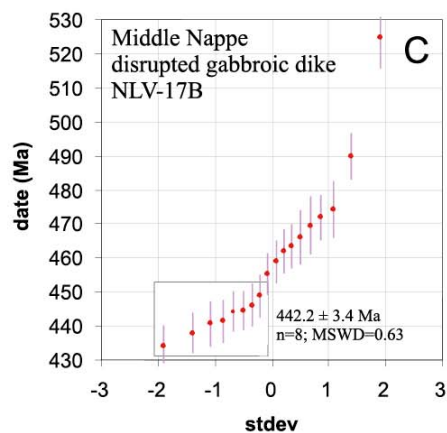
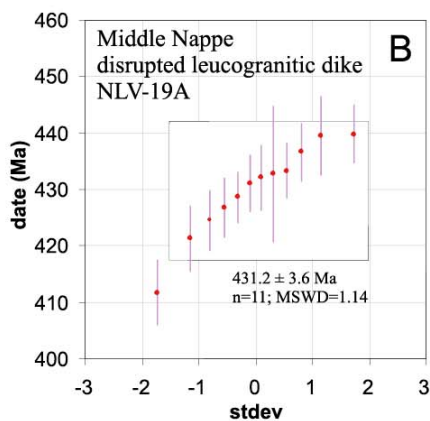


Figure 18. A. Road cut exposure of calc-silicate and semi-pelitic schist cut by leucogranitic dikes near Aunlia. B. U-Pb ages of zircon from a boudinaged granitic dike in the Middle Nappe (Barnes et al., 2007). C. U-Pb ages of zircon from a boudinaged gabbroic dike in the Middle Nappe (op.cit.).

Stop No. 2-3: Nordfjellmark road

Location

From Route 76, westbound, turn right (east) on the Nordfjellmark road. Follow this road 1.9 km to smooth exposures along the left (north) side of the road at UTM 33W 0391840, 7243300.

Introduction

This stop is at an excellent exposure of the Ånes conglomerate, a mafic, polymict conglomerate of the Middle Nappe.

Description

The Ånes conglomerate is an approximately 200 m thick conglomerate with a hornblende-rich matrix. The clast population is dominated by medium- to coarse-grained gabbros, fine-grained greenstones, with sparser trondhjemite and altered ultramafic clasts. Gabbro and greenstone clasts yield initial ϵ_{Nd} of +6.9 and +5.2 respectively, consistent with derivation from mafic rocks exposed lower in the section such as the Sørfjellet gabbro and Glommen amphibolite ($\epsilon_{Nd} = 7.3$ and 7.2).

Upsection to the east of this location are dismembered dikes of gabbro and granite. One of these, NLV-17B, yielded a U-Pb zircon age of 442 Ma (Fig. 18C), contemporary with intrusion of the Velfjord plutons (Day 3). This dike and a dismembered leucogranitic dike higher in the section (NLV-19A, 431 Ma; Fig. 18B) have initial ϵ_{Nd} of -0.9 and -0.8, respectively. These values indicate that the dike magmas had sources distinct from that supplying the source area of the Ånes conglomerate clasts.

Stop No. 2-4: Skogmoen

Location

Return to Route 76. Park at the intersection of the Nordfjellmark road and Route 76 and walk ~100m northward to outcrops at UTM 33W 0390438, 7243923.

Introduction

The contact between the lower and middle nappes was interpreted as a thrust contact by Thorsnes and Løseth (1991). However, the contact is moderately east-dipping and juxtaposes Lower Ordovician amphibolite-grade metasedimentary rocks of the Middle Nappe on Neoproterozoic granulite-grade migmatites of the Lower Nappe that form the high ridge to the west. This stop displays a rare glimpse of the structures that constrain the kinematic evolution of the shear zone.

Description

The shear zone that juxtaposes the Lower and Middle Nappes is subparallel to Highway 76 from Tosenfjord to Nevernes and may be greater than 1 km wide. Where exposed, the shear zone is defined by moderately east-dipping foliations, asymmetric folds with down-to-the-east vergence, and down-dip mineral lineations. At this stop, s-c structures in strongly-retrogressed schist are consistent with east-directed extension; s-planes dip gently east and are cut by moderately east-dipping c-planes. Deformed gabbros along the Nordfjellmark road (previous stop) a few hundred meters across strike are likely involved in the shearing and contain asymmetric amphibole porphyroclasts (after pyroxene) with down-to-the-east sense of shear.

To the north, exposures of the shear zone are covered. Xenoliths of Middle Nappe rocks, including serpentized peridotite, are present in the ca. 448 Ma Akset-Drevli and Hilstadfjellet plutons which crop out structurally beneath the projected trace of the shear zone (Figs. 2 & 19; Dumond et al., 2005), yet Middle Nappe rocks less than 100 m east of the Akset-Drevli pluton show no evidence of contact metamorphism. The northern trace of the shear zone is truncated by the 442 Ma. Andalshatten pluton (Day 3; Fig. 2; Anderson et al., 2007); therefore, the shear zone evidently records east-directed extension and exhumation between ca. 448 Ma emplacement of the Akset-Drevli pluton and ca. 442 Ma emplacement of the Andalshatten pluton (Yoshinobu et al., 2002). Exhumation is recorded in the migmatitic

aureoles of the Sausfjellet and Akset-Drevli plutons by a change of stable aluminosilicates from early kyanite to late cordierite (Barnes & Prestvik, 2000).

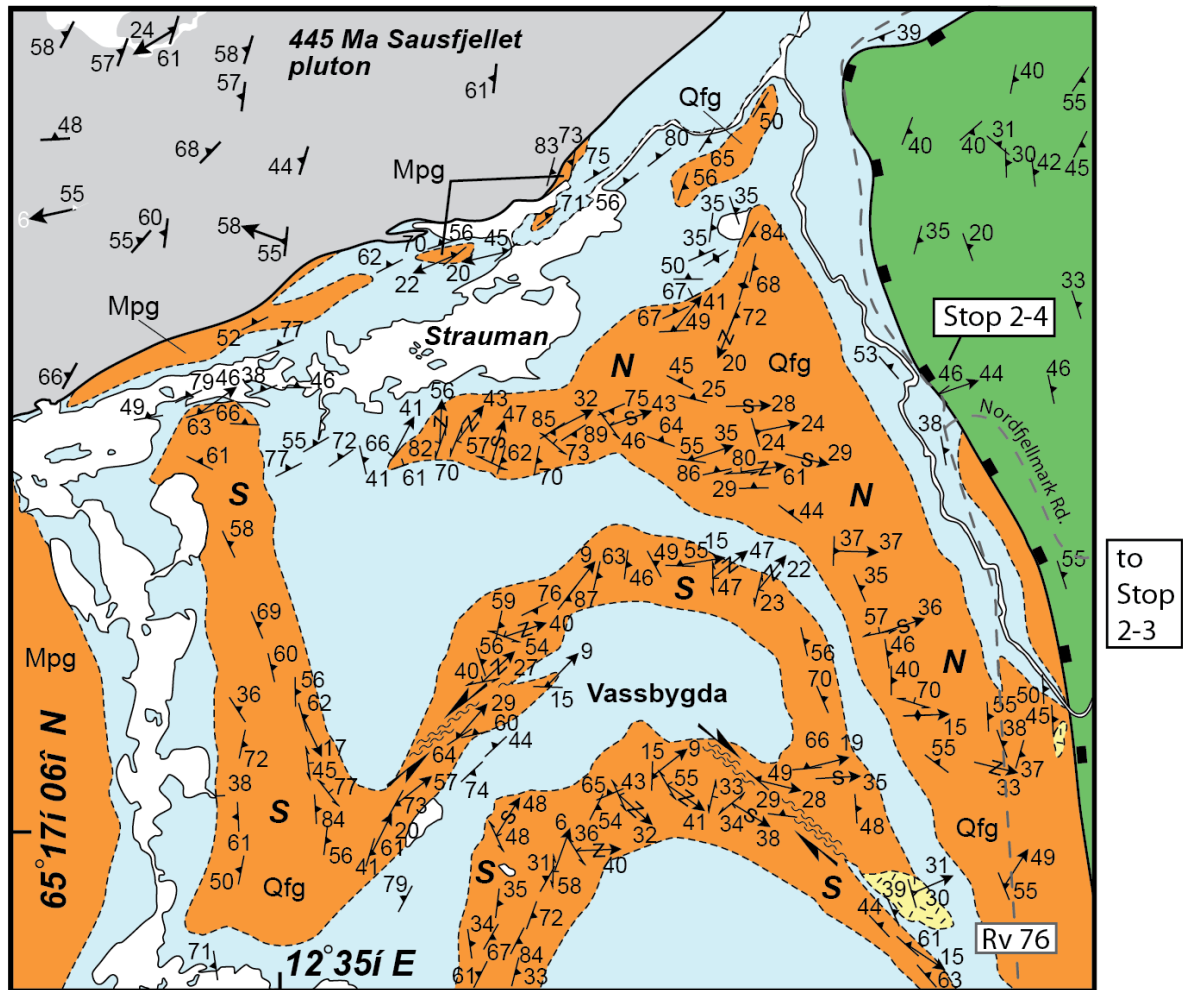


Figure 19. Geologic map from Dumond (2002) and Dumond et al. (2005) of the geology of the lower plate relations beneath the overlying Middle Nappe extensional shear zone (black bold line with rectangle ticks). Colors same as in Figs. 2, 3. Note rotation of preexisting lineations in the footwall into parallelism with the down-dip, east-northeast-plunging lineations at Stop 2-4.

Stop No. 2-5: Sjøvatnet.

Location

From Route 76, use the turnout at Sjøvatnet, west of large road cuts. UTM 33W 0382665 7257041.

Introduction

These road cuts provide excellent exposures of migmatitic metasandstone of the Lower Nappe.

Description

The Lower Nappe consists of marble, calc-silicate rocks, quartzofeldspathic migmatite, and semipelitic migmatite. This road cut shows an example of quartzofeldspathic migmatite of the Lower Nappe; these units are prominent ridge-formers. The gneiss is petrographically simple; it consists of biotite, plagioclase, K-feldspar, and quartz \pm muscovite \pm garnet.

The depositional age of the Lower Nappe has been determined as Neoproterozoic on the basis of chemostratigraphy of marbles (Trønnes, 1994; Trønnes & Sundvoll, 1995; Sandøy, 2003; Figure 5). Although migmatization was probably Ordovician in age, (Yoshinobu et al., 2002), no young zircons are present in this sample. This is consistent with the silica-rich nature of the leucosomes (to 79.1%): the high silica contents indicate quartz was residual after melting, which in turn suggests low-T migmatization and little or no zircon productivity.

Migmatization of pelitic and semipelitic rocks of the Lower Nappe was at relatively low-T, with melt + sillimanite + plagioclase \pm garnet as reaction products. Staurolite is commonly preserved as a reactant phase.

Ages of detrital zircons show distinct age maxima at \sim 1200, 1500, 1900, and 2800 Ma (Barnes et al., 2007; Fig. 4). The detrital zircons from the Lower Nappe at this locality and the Holm Peninsula (Fig. 4) are comparable to those from the Argyll and Southern Highlands Groups of the Dalradian Supergroup of Scotland (Cawood et al., 2007). The lack of Pan-African-aged zircons in these units was interpreted by Cawood et al. (2007) to indicate a depositional environment north of the Grenville front and adjacent to East Greenland.

Six samples of semipelitic migmatite from the Lower Nappe yielded ϵ_{Nd} values of -7.6 to -9.6, whereas a sample from the Sjøvatnet road cut yielded an ϵ_{Nd} of -14.7 (Barnes et al., 2002).

Stop No. 2-6: Gåslia.

Location

From the westbound lane of Route 76, turn right into ski area parking loop (Gåslia). Continue on the gravel road until it returns to the main highway. Park at this intersection, UTM 33W 0378908, 7266662.

Introduction

Road cuts on either side of the highway expose garnet mica schists of the Sauren-Torghatten Nappe. On clear days from this location, one has a clear view to the west of Torghatten.

Description

The common rock type here is garnet muscovite biotite feldspar quartz schist. Retrogression is common in these rocks, and one of the leaders (Barnes) thinks that sillimanite was part of the prograde assemblage, which would be consistent with middle amphibolite facies metamorphism. Elsewhere in the Sauren-Torghatten Nappe, garnet-staurolite-kyanite ± sillimanite assemblages have been reported (Heldal, 2001).

Detrital zircons from this locality range as old as ~2600 Ma. The bulk of concordant samples are in the 900–1500 Ma range and there are a small number of Ordovician zircons that yield an age of 480 ± 8 Ma (Fig. 4). Detrital zircons from a Sauren-Torghatten Nappe metasandstone collected in the aureole of the Andalshatten pluton (Day 3, Stop 5) yielded an date of 481.7 ± 2.8 Ma (Fig. 4; Barnes et al., 2007). These dates are interpreted to indicate deposition of the Sauren-Torghatten Nappe in Early Ordovician time.

Day 3

Introduction. Middle and Late Ordovician plutons of the Bindal Batholith

Today's focus will be on plutons of the Bindal Batholith emplaced between 465 and 440 Ma. Magma emplacement was in the middle crust (600 to 800 MPa) and, at least locally, was associated with syn-magmatic exhumation. Mafic magmas carried enough thermal energy to cause melting of their aureoles, which facilitated assimilation and local magma mixing. Some plutons in this age range were of batholithic scale and we will study the contact relations of one—the Andalshatten pluton—to observe processes of magma emplacement in middle crustal levels. The road map for the first three stops is Figure 16 from Day 2. The road map for the remainder of the stops is given after the description of Stop 3.

Stop No. 3-1: Shoreline between Lislvågen and Storvågen.

Location

Park in small turnouts along the road to Drogstøy at ~UTM 33W 0382728 7260102. After looking at exposures along the road, hike westward along the southern side of Lislvågen ~450 m to UTM 33W 0382320 7259903 where the contact is exposed along the shoreline.

Introduction

This stop provides an opportunity to see monzodioritic rocks of the 447 Ma Hillstadvjellet pluton and to inspect the contact of the pluton with its anatectic aureole.

Description

As the contact is approached in this area, massive monzodiorite of the pluton gives way to monzodiorite intruded by veins of garnet muscovite biotite granite (Fig. 20). This zone is succeeded by a homogeneous sillimanite staurolite garnet muscovite biotite diatexite. West of the diatexite, a range of migmatitic rocks crop out. These vary from stromatic to diatexitic and contain enclaves of calc-silicate rocks and medium- to fine-grained plutonic rocks. The medium to fine grained leucosomes are primarily leucogranite but some leucotonalite is present. Stingers of leucogranite are connected to larger pods of leucosome, which are elongate parallel to foliation and interfinger with the diatexite along foliation planes. Some

leucosomes are intimately folded with the host diatexite, but the same leucosomes contain folia and disrupted fragments of the host migmatite.

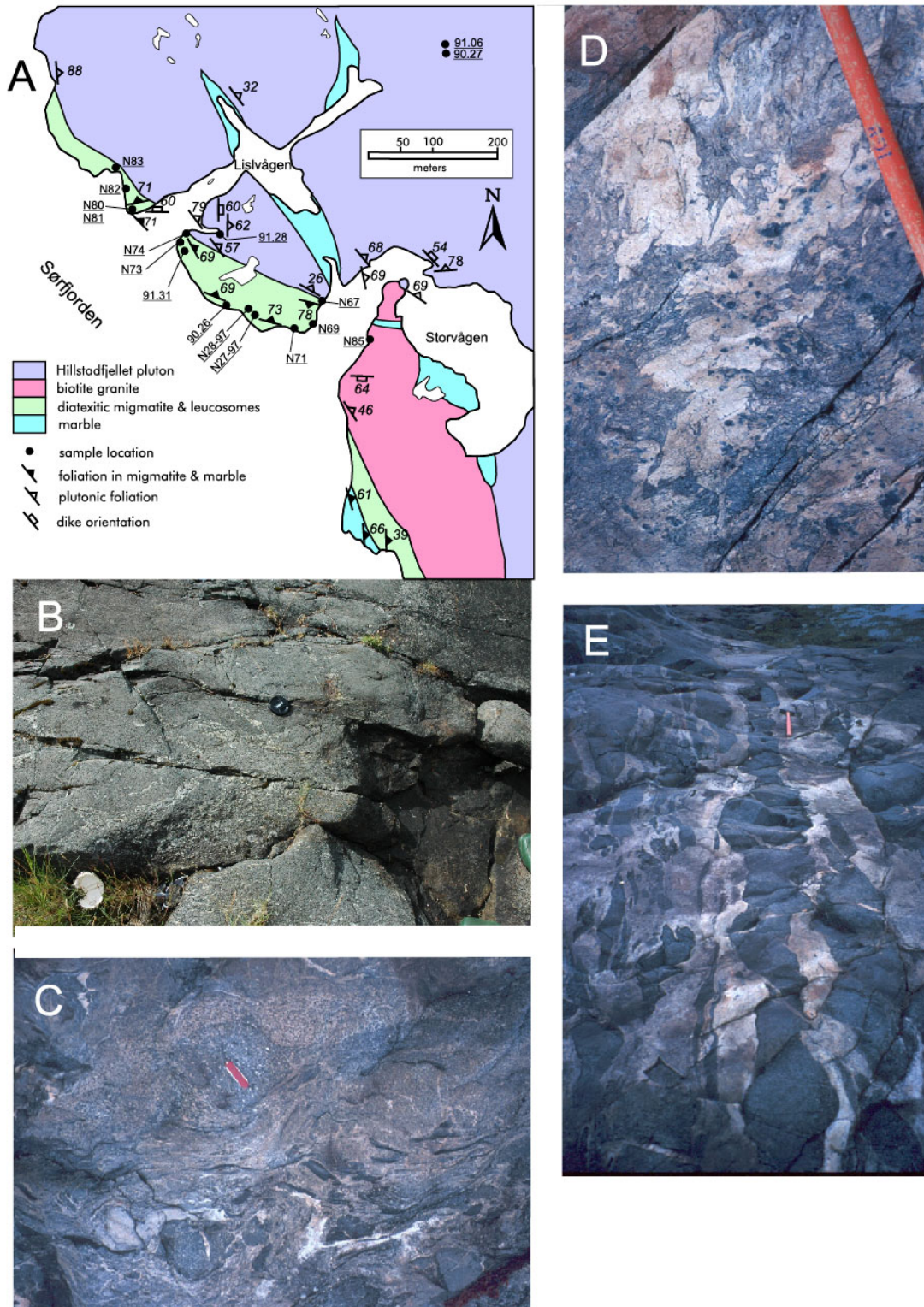


Figure 20. A. Geologic map of contact zone of the Hillstadjellet pluton along Sør fjord. B. Leucosomes from diatexitic migmatite back-veining monzodiorite; location N74. C. Medium-grained dioritic enclaves in contact migmatite. D. Leucosome segregation in contact migmatite. E. Boudinaged and disrupted fine-grained dioritic dikes, synmagmatic with host leucosomes; location N80.

The diatexites, leucosomes, and contact granite were intruded by fine- to coarse-grained dioritic dikes which are variably broken into angular to cusped, mafic enclaves. In this outcrop, mafic enclaves are common (Fig. 20) and in the exposures north of Lislvagen deformed, “syn-migmatitic dikes” crop out (Fig. 20). All of these features were interpreted by Barnes et al. (2002) to result from magma mingling and mixing as mafic magmas were emplaced into the still-molten migmatitic margins of the plutons. Barnes et al. (2002) suggested that such zones of hybridization may be analogous to deep-crustal zones of

hybridization associated with underplated magmas (see Stop 3-3). Such zones of hybridization characterize all of the mafic plutons in the Velfjord area

Local, late-stage, near-solidus deformation formed a strong foliation parallel to the intrusive contact. The intensity of the foliation is greater in the contact migmatites than in the pluton; the migmatites locally have S-C fabrics with down-to-the-east sense of shear.

Stop No. 3-2: Hundkjerka marble mine (optional)

Location

Return toward Hommelstø along the same route. Stop along the Drogstøy road at the overlook of the Hundkjerka mine, approximately 33W 0686300, 7257650.

Introduction

This optional stop is designed to provide an overview of marble deposits of the Helgeland Nappe Complex.

Description

Marble has been mined in small quantities in the Velfjord region for decades. It was originally used as monument stone, particularly the unusual blue marble found here and pink marble in Storbørja, but most of the marble is too coarse-grained and friable for such uses. In the mid-1990's, Brønnøy Kalk began large-scale mining of marble for industrial purposes, primarily as a whitener for computer paper and also for use in cement and gardening products. The Hundkjerka mine was the first of three mines opened by Brønnøy Kalk. The marble is part of a screen of metasedimentary rocks that strikes northwestward across the Hillstadjellet pluton. The screen apparently acted as a strain guide for syn- and post-emplacement deformation, because the marble contains blocks of silicate metasedimentary rocks as well as gabbroic and dioritic blocks. It is not uncommon for the latter blocks to be separated from the marble by rinds of syenite, which implies high-T, probably syn-magmatic interaction between the dioritic magma and the marble (see Barnes et al., 2003). The mine was abandoned when it was determined that prediction of the size and distribution of silicate blocks in the marble was impossible.

Chemostratigraphic dating of the marble screens in the Hillstadjellet pluton (Sandøy, 2003) shows these marbles to be Ordovician in age, whereas marbles of the Lower Nappe south and west of Hommelstø have Neoproterozoic isotopic signatures (Sandøy, 2003; Fig. 5). This raises an important question with regard to nappe nomenclature and tectonics: are marble screens within the Hillstadjellet pluton Ordovician parts of the Lower Nappe, or are they parts of the Middle Nappe stopped into the pluton? If the former, then the Lower Nappe preserves an unconformity similar to that seen in the Horta nappe. If the latter, then the Hillstadjellet pluton intruded the shear zone separating the Lower and Middle Nappes.

Stop No. 3-3: Svarthopen quarry.

Location

Continue west on Route 76 1.4 km to the entrance to the Svarthopen quarry at UTM 33W 0681450, 7257100. Park outside the entrance to the quarry and walk along the quarry haul road. The outcrops to be visited are near the quarry entrance; the best examples on the east side.

Introduction

Rocks exposed in the Svarthopen quarry provide an example of mingling and mixing of dioritic magmas with anatectic granitic magmas under middle crustal conditions.

Description

Beware of loose boulders!!! The Svarthopen pluton was thought by Barnes et al. (2002) to be coeval with the Velfjord plutons. However, U-Pb (zircon) dating (Barnes et al., 2007) indicated an age of 465.0 ± 1.5 Ma (Fig. 21A), significantly older than the Velfjord plutons but comparable to the Hortavær Intrusive Complex north of Leka (Fig. 2). The plutonic contact is exposed near the entrance to the quarry. In this area, numerous examples of magma mingling and mixing are exposed (Figs. 21B, C). The mafic end member was pyroxene hornblende \pm biotite quartz dioritic magma of the main part of the pluton and the felsic end members were granitic magmas with variable proportions of K-feldspar \pm garnet phenocrysts. Mixing produced a spectrum of hybrid compositions, as is shown by Nd and Sr isotopic data (Fig. 21D).

An unusual aspect of mixing at Svarthopen is the presence of garnet in some of the hybrid rocks (Fig. 21C). Specifically, garnet is present in hybrid samples of intermediate SiO_2 content and high Fe/Mg ratios. It appears that at the pressure of emplacement (c. 700 MPa), such hybrid compositions can stabilize magmatic garnet. The growth of garnet in Fe-rich, hybrid, *mid-crustal* magmas raises an interesting possibility for stability of magmatic garnet in the lower crust. In zones of magmatic underplating and crustal melting, Fe-rich hybrid magmas may crystallize garnet, which would then impose the typical “garnet signature” to the REE patterns of evolved granitic magmas.

Figure 21E is a schematic view of the types of interaction possible in the aureoles of hot, mid-crustal plutons such as the Svarthopen and Hillstadjellet (Stop 3-1). Barnes et al. (2002) viewed these interactions as small analogues of deep crustal underplating and intraplayering.

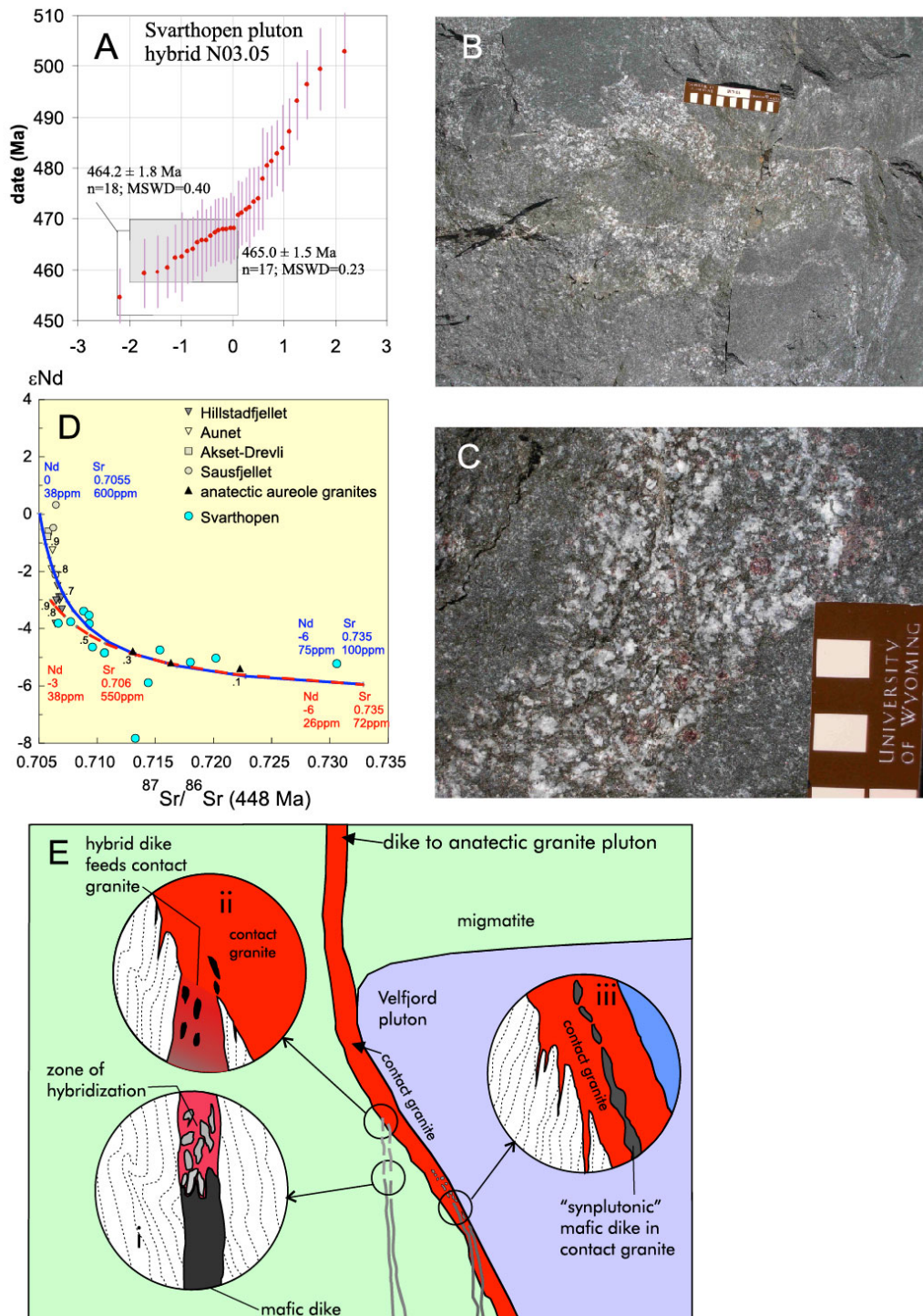


Figure 21. LA-ICPMS ages of zircons from a Svarthopen hybrid, with interpreted igneous age of 465 ± 1.5 Ma. B. Photograph of mixed zone, with mafic enclaves of variable color index. C. Close-up photograph of a felsic, garnet-rich vein in quartz dioritic host rock; Svarthopen quarry. D. Nd and Sr isotope variation for the Svarthopen pluton, Velfjord plutons, and associated contact granites (Barnes et al., 2002; Barnes et al., 2006; Frost & Barnes, unpublished data). The Svarthopen data are shown with two mixing curves, end members of which are coded according to the color of the curve. E. Schematic illustration of development and evolution of contact granites. Heat from the large dioritic plutons causes melting in the aureole. Reinjection of mafic magma results in hybridization (i), entrainment of mafic enclaves (ii), and syn-migmatitic dikes in leucosomes of the aureole (iii).

Stop No. 3-4: Andalsvågen ferry quay

Location

Take Route 76 to Route 17, then proceed north to the Horn–Andalsvågen ferry (Fig. 22). Take the ferry to Andalsvåg and park at the outcrops at the north end of the quay, UTM 379650, 7275400.



Figure 22. Road map for the second half of Day 3. We will depart for Stop 3-4 from the ferry quay at Horn.

Introduction

This stop will provide a brief introduction to the rocks and geology of the Andalsvågen pluton. Before crossing from Horn to Andalsvågen in clear weather glacially-sculpted exposures of the pluton may be seen across Velfjord forming the high ridge line to the east and north. Prominent peaks from south to north include Indrehatten, Hornstinden, and Stortinden. The Andalsvågen ferry quay and Stop 3-4 may be seen nestled in the U-shaped

valley due east of this stop. The prominent buttress on the western horizon of the Andalshatten pluton is underlain by a shallowly-east dipping, sub-planar contact between dark diorite and underlying grey granodiorite. Due north of the ferry quay at Horn is the flat-topped island of Hamnøya which is underlain by metasedimentary rocks of the Sauren-Torghatten Nappe in the southwest and granitic gneiss of unknown age.

Description

The Andalshatten pluton is one of the largest plutons within the Bindal Batholith. It intruded previously deformed metasedimentary and igneous rocks of the Upper, Middle, Lower, and Sauren-Torghatten nappes. The pluton was emplaced in the middle crust (~670 MPa; Yoshinobu et al, 2002) and was constructed incrementally by at least four distinct pulses of magma. The pulses include an eastern-most gneissic and schlieren-banded granodiorite, megacrystic granodiorite, diorite, and minor leucogranite. K-feldspar megacrystic granodiorite is volumetrically the most abundant rock type. The principal dioritic part of the pluton crops out east of Andalsvågen as the darker brown exposures.

Two pulses of the megacrystic granodiorite magma were dated using high precision chemical abrasion thermal ionization mass spectrometry (CA-TIMS) U-Pb dating of zircon. An eastern magmatic pulse yielded an age of 442.66 ± 0.18 Ma and a central-western pulse has an age of 442.86 ± 0.20 Ma (Anderson et al, 2007). The overlap in ages indicates that a significant volume of magma was emplaced over a geologically short period of time, roughly <500,000 years.

Xenoliths and screens are common throughout the pluton, as are mafic magmatic enclaves. The xenoliths and screens range in size from centimeter to kilometer-scale and their compositional variation mimics lithological variation in the host nappes (Fig. 23). The outcrops at this location are typical of megacrystic biotite granodiorite of the pluton. Hornblende is present in some samples and the accessory minerals are epidote, sphene, allanite, and zircon \pm tourmaline \pm muscovite. A north-northwest-trending magmatic fabric is common; it is defined by aligned centimeter-scale K-feldspar megacrysts.

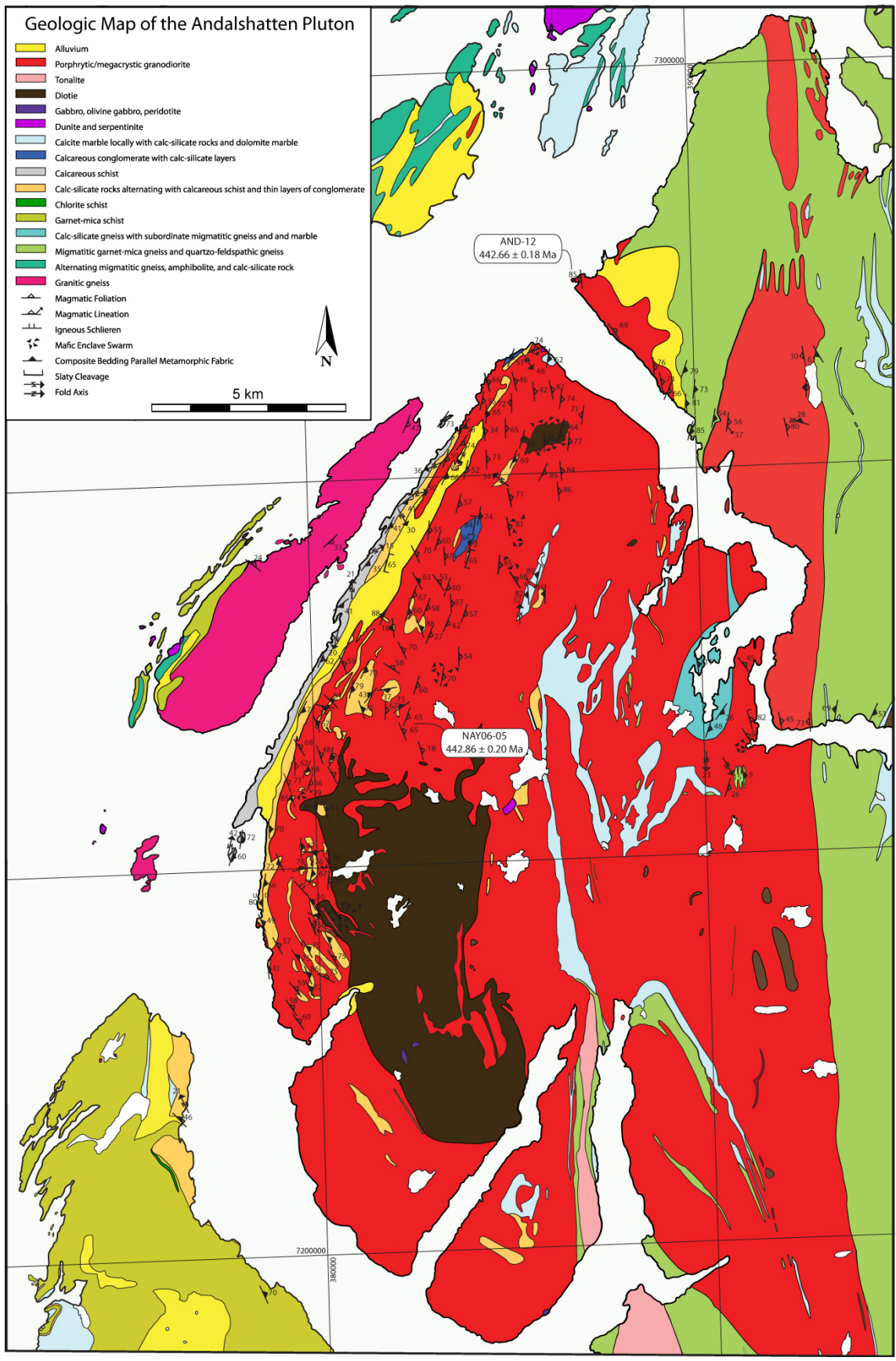


Figure 23. Geologic map of the Andalshatten pluton by Nordgulen et al. (1992) and H. Anderson and A. Yoshinobu 2006-2007 unpublished mapping.

Stop No. 3-5A: Vollvika East.

Location

Park in the turnout on the west (coast) side of Route 17 at UTM 33W 0378833, 7277706.

Introduction

This stop consists of an ~200 m-long traverse through the contact zone of the Andalshatten pluton with host rocks of the Sauren-Torghatten Nappe. Pre-emplacment structures associated with regional Early Ordovician contractional deformation and emplacement-related structures in a large metasedimentary pendant will be the focus of this stop.

Description

At the first stop along the traverse, steeply east-dipping contact of the megacrystic stage of the pluton with upright, isoclinally folded layered calc-silicate rocks. The granodiorite contains arcuate schlieren bands and within 2 meters of the host rock contact magmatic foliations are overprinted by a moderate crystal-plastic fabric. Twenty meters west of the contact, interlimb angles of folds increase and intrafolial folds and transposed bedding are observed. Although the rocks are strongly deformed, graded bedding and cross-stratification are preserved indicating that all folds are upright (Fig. 24). Detrital zircons from an arkose yield crystallization ages of ~481 Ma (Fig. 24; Barnes et al. 2007). Therefore, transposition of bedding and refolding must have occurred after 481 Ma and before emplacement of the Andalshatten pluton at 442 Ma. Continuing along the cliffs and past a small red structure a small peninsula is underlain by deformed, megacrystic granodiorite. Based on contact relations observed elsewhere, we interpret the granodiorite at this peninsula to be an apophyse of the main phase of the pluton projecting from the south and/or from below the level of exposure. A discussion of the timing and cause of structures seen along the traverse follows the description of Stop 3-5B.

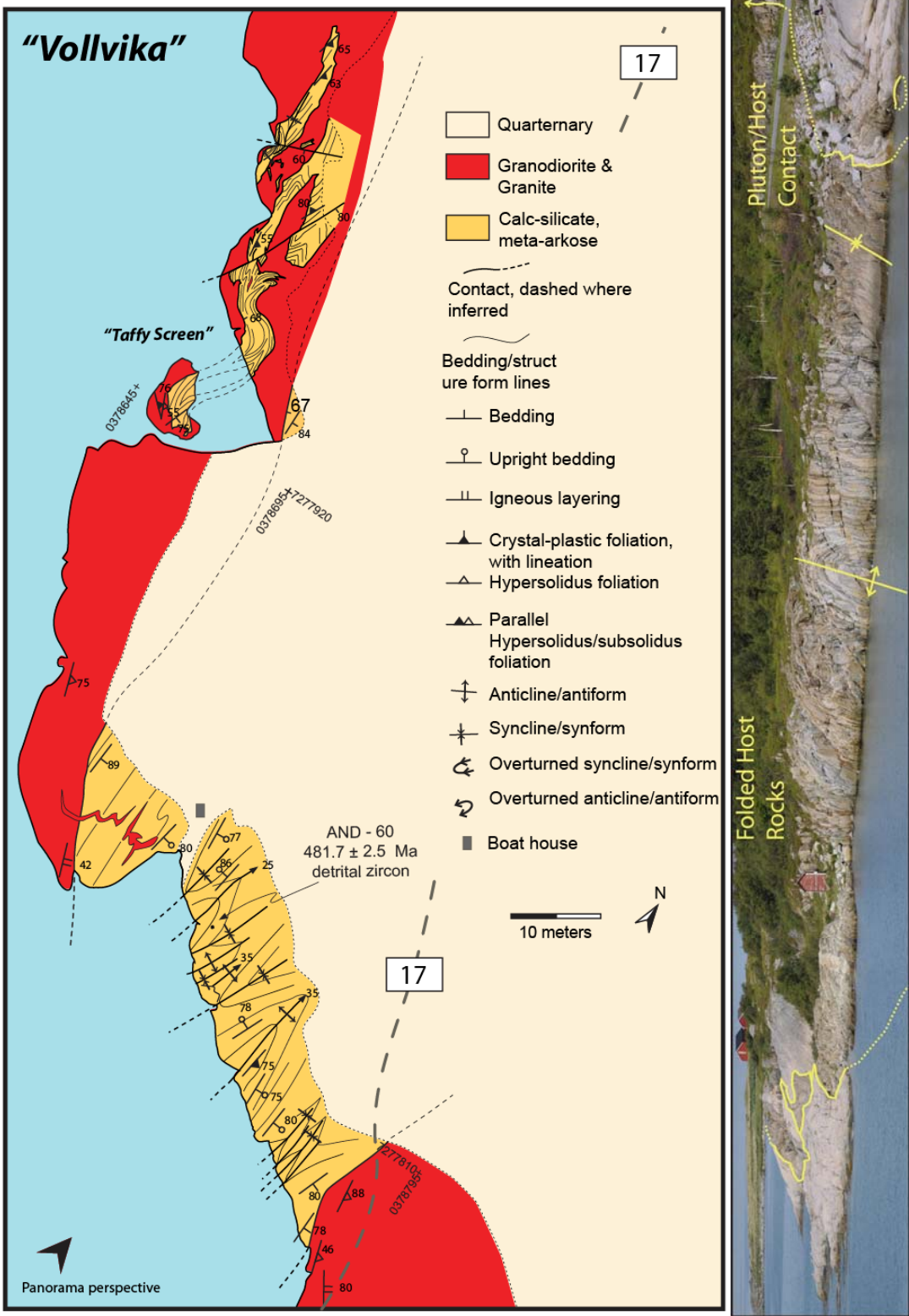


Figure 24: Geologic grid map of Vollvika coastline showing major units and structure and panoramic photo of Vollvika coastline.

Stop No. 3-5B: Vollvika West.

Location

This continues the traverse begun at Stop 3-5A.

Introduction

The western part of the traverse will focus on the outcrop-scale structural relations around deformed xenoliths within granodiorite sheets in the contact zone of the Andalshatten pluton. We will focus on the differences in observed strain in the xenoliths that are smaller than about 100 m across strike (see Fig. 24) as compared to the Vollvika screen (traverse at Stop 3-5A) and other screens preserved at higher elevations.

Description

One hundred meters north of the red structure observe the spectacularly exposed boudined xenolith in and above tide line. The boudin consists of layered calc-silicate metaclastic rocks that are tightly and isoclinally folded. Transposed bedding and occasional cross-stratification may be observed in the boudin. In the granodiorite a few meters away from this xenolith, magmatic fabrics are well preserved, but near the boudin hinge, crystal-plastic fabrics overprint the older fabrics. We interpret these patterns of deformation to indicate that the magma-xenolith package was of similar rheology during boudinage and that this deformation occurred above the solidus. Ten meters north of the boudined xenolith, dikes and sills of granite and granodiorite may be seen re-intruding the xenolith along bedding planes. A few undeformed m-thick mafic dikes with NE-trends cross-cut structures and lithologies here.

If time permits, continue north and observe sheets of granodiorite that intruded the calc-silicate host rocks. Note the tabular blocks of calc-silicate rocks that appear to have ‘spalled’ off of the larger xenoliths. Well-exposed vertically-plunging folds have geometries that are in stark contrast to fold axes mapped throughout the host rocks (Fig. 24; Anderson et al., 2007). We interpret these vertical folds as older, D2/D3 structures that were reactivated, tightened and rotated during emplacement of subsequent sheets of granodiorite at ca. 442 Ma (Anderson et al., 2007).

The structural behavior of the larger Vollvika screen (Stop 3-5A) and the smaller xenoliths such as the boudined xenolith at Stop 5B are distinct. The Vollvika screen and large, kilometric-scale screens preserved at higher elevations (Fig. 23) tend to preserve ‘regional patterns’ of structures and behave as intact, semi-rigid blocks within the Andalshatten pluton. Xenoliths smaller than ca. 100 m across strike tend to exhibit reactivation structures such as boudinage, refolding, and interlimb angle tightening that we interpret to be related to magma emplacement.

Folding and transposition observed at Stops 3-5A and 3-5B must have occurred after deposition of metasandstones containing ~481 Ma detrital zircons (Barnes et al., 2007) of the Sauren-Torghatten Nappe. The geometry and style of folding observed here is similar to that exposed along the NW coast of Vega (Stop 1-6), on the island of Ylvingen, and near Horn (Figs. 10, 23). At Vega, these folds are contemporaneous with host rock migmatization and emplacement of the Vega granodiorite at ~477 Ma (Anderson et al., 2005; Barnes et al., 2007). Therefore, we tentatively ascribe folding as seen in the rocks at Vollvika to regional D3 contractional deformation that was ongoing during (?) and/or after 481 Ma magmatism as represented by detrital zircons in the Sauren-Torghatten Nappe and ~477 Ma magmatism

associated with crustal melting and construction of the Vega pluton. It is not clear whether D2 structures are preserved in these rocks. Thus, the calc-silicate and metasandstone host rocks at Vollvika preserve a depositional, burial, and structural history that spans approximately 4 million years. During emplacement of the Andalshatten pluton at ca. 442 Ma, these structures were reactivated as displayed at Stop 3-5B.

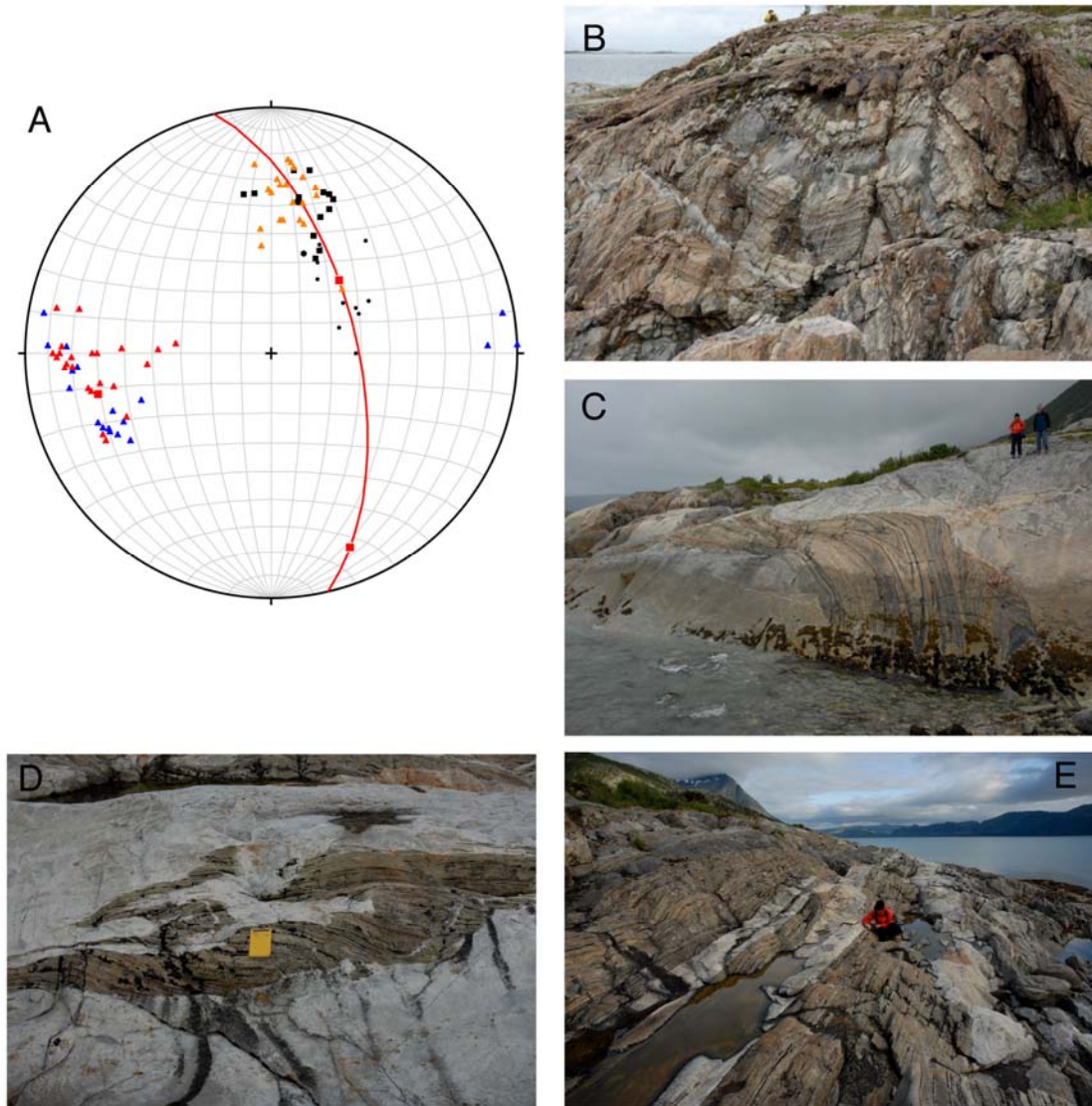


Figure 25. Structural relations at Vollvika. A) Poles to F3 axial planes (red, blue triangles) with an average girdle in red. Orange and black boxes reflect F3 fold axes. B) Transposed bedding in upright folds at Stop 3-5A. C) Large xenolith within granodiorite that underwent syn-magmatic boudinage at Stop 3-5B. D) Calc-silicate blocks 'spalled' off of host rocks during sheet intrusion. E) Sheets injected into calc-silicate host rocks further north of Vollvika.

Stop No. 3-6: Vistnesodden road cuts.

Location

Northbound on Route 17 at Forvik, turn right on the Vistnesodden Road. Follow this road ~2.5 km and park on the west side of the road near the gate. Walk back (south) to the road cut exposure at UTM 33W 0385154, 7292354.

Introduction

This stop provides an easily accessible example of contact relationships between the pluton and calc-silicate xenoliths.

Description

Metasedimentary xenoliths of interbedded stretched-pebble calcareous conglomerate, black phyllite, and calc-silicate rocks are completely enclosed by granodiorite and leucogranite. Skarn is locally developed in the calc-silicate rocks and is partly disrupted by quartz veins. In the center of some calc-silicate samples there are bright green spots with small (<1 mm) black crystals (chromite?). Such occurrences suggest a source of chromite from nearby ultramafic bodies.

The megacrystic granodiorite is generally protomylonitic with top-to-the-west S-C fabric (see south end of western road cut; Fig. 26). Sigma-porphyroclasts of K-feldspar overprint a hypersolidus K-feldspar foliation. A zone of protomylonite as much as 0.5 km wide characterizes the northwestern contact zone of the pluton. This is distinct from the Vollvika area, where protomylonitic fabrics are present within a few meters of screens and xenolith.

Zones of plutonic rock adjacent to the xenoliths at this stop are significantly more deformed, with a lineation defined by elongate hornblende and biotite. This fabric may have been the result of strain localization adjacent to xenoliths.



Figure 26: Dextral, 'top-to-the-west' S-C mylonites and sigma-porphyroclasts overprinting a hypersolidus foliation defined by potassium feldspar megacrysts and quartz aggregates. View to the southwest.

Stop No. 3-7: Forvik quarry

Location

Travel south on the Vistnesodden road. Turn left onto an unpaved road ~0.25 km from Route 17 road junction at Forvik. Park at the quarry, UTM 33W 0388323, 7290203

Introduction

The quarry is on land owned by Arnt Mathias Arntzen, proprietor of Handelsstedet Forvik, where we will have dinner. The quarry provides pristine exposures of protomylonitic Andalshatten megacrystic granodiorite and is an excellent location to collect a sample.

Description

The deformed megacrystic granodiorite has a strong S-C fabric and top-to-the-west sense of shear. K-feldspar megacrysts have recrystallized tails of quartz and feldspar. Tiled megacrysts show the same sense of shear. The pluton also contains centimeter-scale, highly elongate, mafic magmatic enclaves. Late, ultramylonitic aplitic dikes cut the granodiorite; these dikes have a strong lineation which is defined by biotite aggregates. A variety of veins cut the granodiorite; some contain large (cm-scale) possibly recrystallized biotite, hornblende and tourmaline crystals, others contain amazonite.

Day 4

Introduction. The Leka ophiolite and Skei Group

The focus of Day 4 is the Leka ophiolite and its cover sequence, the Skei Group (Fig. 27). The Leka ophiolite is the best-exposed Caledonian ophiolitic complex in Norway. It is particularly interesting because both the petrologic MOHO (the transition from tectonized mantle peridotite to layered cumulate ultramafic rocks) and the seismic MOHO (the transition from ultramafic to mafic rocks) are present. Although these boundaries will not be visited on this excursion, excellent examples of mantle tectonite, ultramafic cumulates, and mafic plutonic rocks will be seen.

The chemistry and mineralogy of the Leka ophiolite has traditionally been interpreted in terms of magmatic processes (e.g. Furnes et al., 1988; Pedersen & Furnes, 1991; Maaløe 2005). However, recent work focusing on serpentinization of the complex (Iyer et al., 2008a, b) and on extensive Ca-metasomatism (Austrheim & Prestvik, 2008) shows that orthopyroxene is unstable and that olivine and clinopyroxene are both compositionally sensitive to these processes. Most conspicuous is the formation of grossular-bearing rodingites and replacement of the primary minerals olivine, orthopyroxene and clinopyroxene by diopside. The serpentinization and rodingitization were most likely the results of ocean floor alteration and the Leka ophiolite thus represents a laboratory for obtaining information of ocean floor alteration complimentary to data derived from dredged and drilled samples from the ocean floor.

The Skei Group unconformably overlies the Leka ophiolite. It is primarily clastic and is characterized by thick conglomeratic sequences. Our focus will be on the age of the Skei Group and its relationship to other conglomeratic sequences in the HNC.

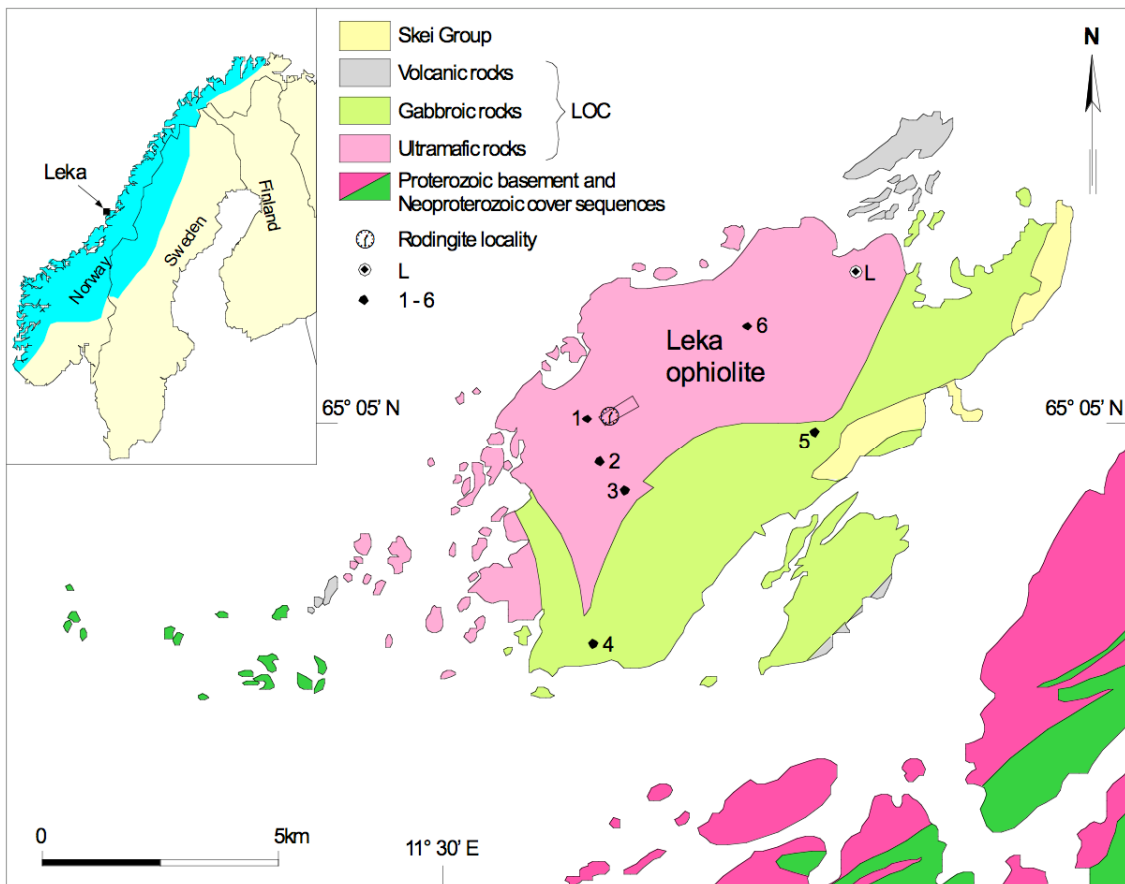
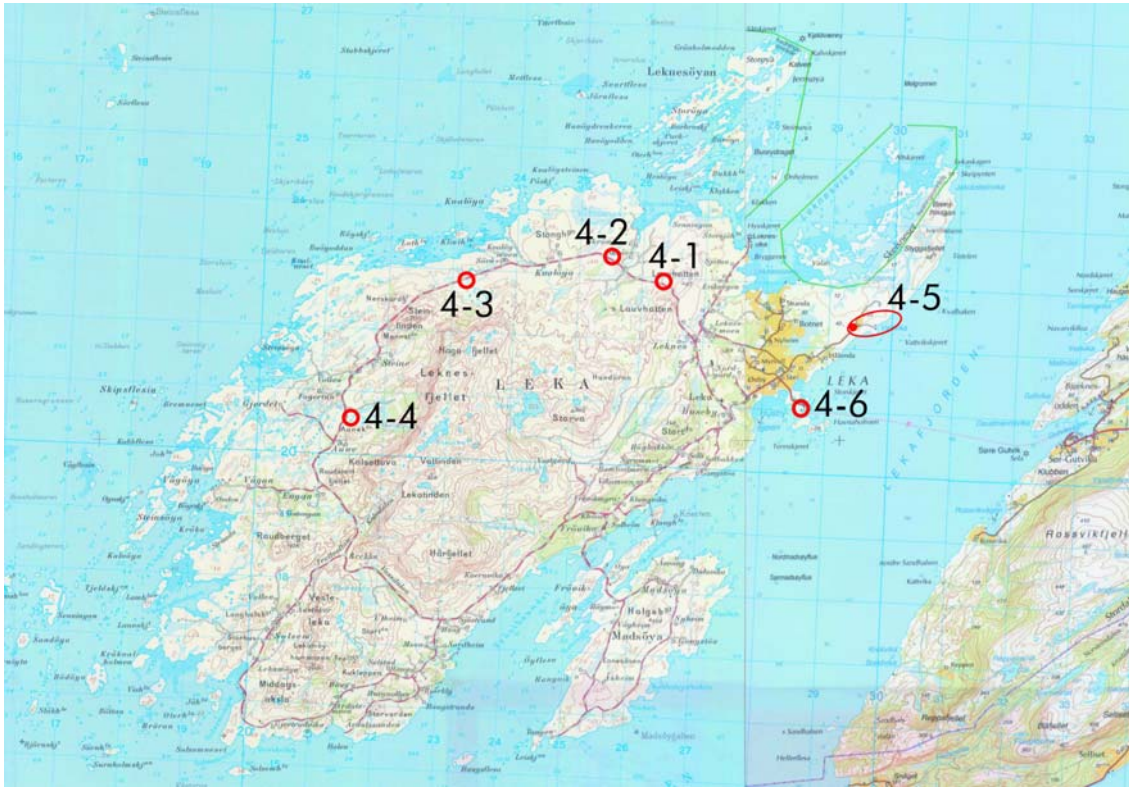


Figure 27. Road map of Leka with field trip stops and geologic map after Austrheim and Prestvik (2008).

Stop No. 4-1: Lauvhatten

Location

From the ferry quay drive to Husby and then turn right on the road to Leknes and Solsem. Drive ~2.5 km and park where telephone lines cross road, at UTM 32W 0626247 7222917.

Introduction

Serpentinized and Ca-metasomatized peridotite of the mantle section of the Leka ophiolite. This stop is located in the area where Maaløe (2005) described dunite bodies, websterite veins and orthopyroxenite dikes and where Austrheim and Prestvik (2008) reported replacement of olivine by diopside.

Description

The small road cut on the south side of the road shows the distinction between weathered and fresh surfaces of serpentinized ultramafic rock. On the north side of the road, walk to UTM 32W 0626267, 7222992. The peridotite here displays conspicuous small knobs on weathered surfaces, a structure deriving from the differential weathering between the main mass of the rock and the irregularly distributed clusters (sometimes developed as folia). The knobs represent serpentinized crystals of orthopyroxene and remnants of clinopyroxene, whereas the main rock mass (originally olivine) is a mixture of serpentine and remnants of olivine. Mineralogical and chemical features show that this rock type is more refractory than the *layered* ultramafic rocks of Leka, thus indicating that it represents depleted residual mantle material (tectonized harzburgite). This lithology is mixed with variously shaped and sized bodies of dunite (more yellow and smooth on weathered surface). These bodies increase in abundance towards the north (up section) and may represent even more refractory material than the harzburgite. Crosscutting dikes of dunite are also common in this area. They may represent accumulated olivine from magma channels. Also in this section are irregular, thin bands of pyroxenite (e.g. websterite).

The complex is cut by NE-trending shear zones (Fig. 28a) that can be followed for more than 100 m. The central part of the shear zones display a color more like the dunite. Locally breccia zones are developed (Fig. 28b) in which rounded to angular blocks of dunite are surrounded by dark websterite veins. Microtextures (Figs. 28c, d) reveal that the breccia is strongly Ca-metasomatized, with replacement of olivine and orthopyroxene by diopside. Note that the serpentine and chlorite around chromite are also replaced by diopside. We interpret these textural relationships as the result of multiple fluid pulses of varying composition during the serpentinization and rodingitization process.

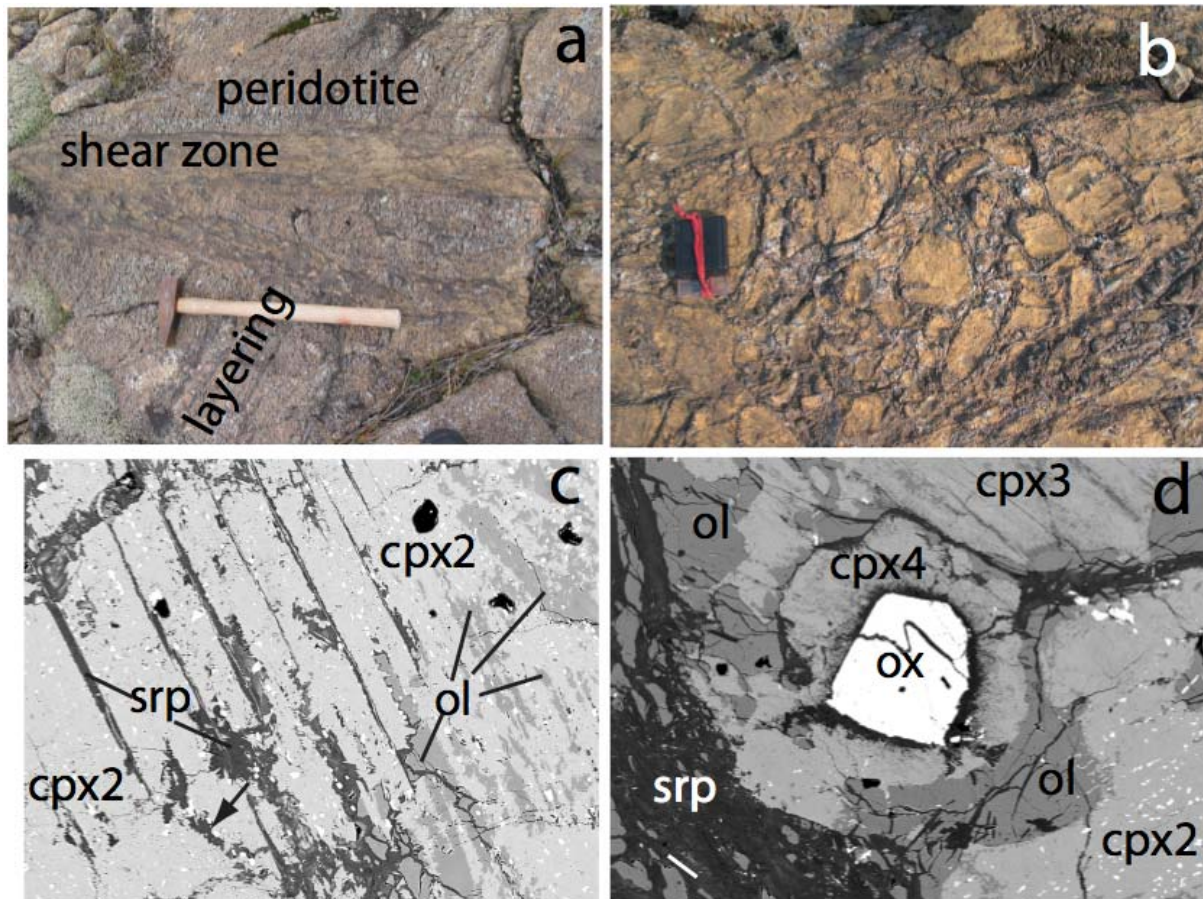


Figure 28. a) Shear zone transecting peridotite at a high angle to the layering. Note how the texture and the color of the shear zone appears more like dunite. b) Breccia with websterite veins (dark). c) Back-scatter electron (BSE) image from the websterite veins in the breccia shown in b). Serpentinized olivine (ol) is replaced by diopside (cpx2). d) BSE image from websterite vein in breccia shown in b). Chromite (ox) surrounded by diopside (cpx4). Cpx4 replaces chlorite, the dark inner rim about chromite. Cpx2 is characterized by oxide inclusions and forms by replacement of olivine. Cpx3 is formed by replacement of olivine. Srp = serpentine

Stop No. 4-2: Skråa block.

Location

Continue westward past the intersection to Skråen. Park where telephone lines cross the road at UTM 32W 0625500, 7223262.

Introduction

Layered ultramafic rocks of the Leka ophiolite.

Description

Walk NE across a large dunite layer to a small knob at UTM 32W 0625646, 7223272. This knob is underlain by thinly-layered clinopyroxenite, wehrlite, websterite, and minor dunite. Layers with grey weathering color are rich in clinopyroxene (wehrlite and clinopyroxenite), whereas the more or less reddish color of some layers represents primary orthopyroxene (now invariably serpentinized). Layering occurs on different scales in the Leka ophiolite, such as *large-scale layers* (several hundred meters thick), *macro-rhythmic units* (10–50 m), *small-scale rhythmic layers* (0.5–2 m), and very thin layering (cm scale). This location is within the

so-called Skråa block (Furnes et al., 1988) of the layered sequence of the Leka ophiolite (i.e. above the petrological MOHO). The dunite and the thinly layered sequence may each represent a macro-rhythmic unit of this block.

Stop No. 4-3: South of Kvaløya farms

Location

Continue westward ~2.5 km. Park at the turnout on the right side of the road, opposite a very small road-side quarry, at UTM 32W 0623114, 7222829. From the eastern side of the small quarry, walk ~200 m on a bearing of ~S20E to UTM 32W 0623162, 7222647.

Introduction

Chromite layers in dunite of the layered ultramafic section of the Leka ophiolite.

Description

Chromite layers in dunite. Some of the macro-rhythmic units are characterized by dunite with thin (0.5–5cm) layers of chromite. A few chromite layers are as much as 15cm thick. This stop is within a dunite-chromite unit that can be traced for more than 3 km. Wherever chromite is found, it is associated with dunite. Based on evidence from many layers, the crystallization sequence is olivine – chromite – clinopyroxene – orthopyroxene, followed by plagioclase in the gabbroic section.

Stop No. 4-4: North of Aunekollen

Location

Continue south-westward ~3.3 km. Park where the road makes a turn to the right at UTM 32W 0621403, 7220566. It is best to park on the left-hand side of the road. Walk ~150 m in a S60E direction, to UTM 32W 0621510, 7220519.

Introduction

Rodingite in the layered ultramafic and gabbroic section of the Leka ophiolite.

Description

This outcrop is within the Steine Layered Series of the Steinstind block (Furnes et al., 1988), near the first appearance of gabbroic layers (i.e., plagioclase stable). Within a sequence of predominantly dunite, wehrlite and websterite, 1–3 m sequences of layered gabbro occur (Fig. 29). The gabbro is thinly layered and varies from melagabbro, via leucogabbro to anorthosite. The complex is cut by sets of steep fractures or shear zones that make a high angle with the layering (Fig. 29). Some layers of anorthosite (5–15 cm thick) have been rodingitized around such fracture zones with the development of three distinct metasomatic zones along the plagioclase layer. A central grossular dominated zone (Fig. 30a) extends for up to 2 m along strike and gives way to a clinozoisite-dominated zone which is followed outward by a LILE-enriched zone characterized by phlogopite.

The variation of CaO, Al₂O₃, K₂O, and Na₂O are shown in Figures 31a and 31b. Assuming constant volume, the rodingite formed from the anorthosite by addition of 20g CaO per 100g of rock. This locality is one of several 100-meter-long zones where garnet veining has been found. The rock types that alternate with the plagioclase layers display textures indicating a

number of Ca-releasing reactions ($\text{Cpx} \rightarrow \text{Chl}$, $\text{Cpx} \rightarrow \text{Srp}$, $\text{Cpx} \rightarrow \text{Amph}$) and Ca-consuming reactions ($\text{Opx} \rightarrow \text{Cpx2}$, $\text{Ol} \rightarrow \text{Cpx2}$, $\text{Cpx1} \rightarrow \text{Cpx2}$). Chloritization and serpentinization (Fig. 30b) of clinopyroxene were the main Ca-source for the rodingitization process.

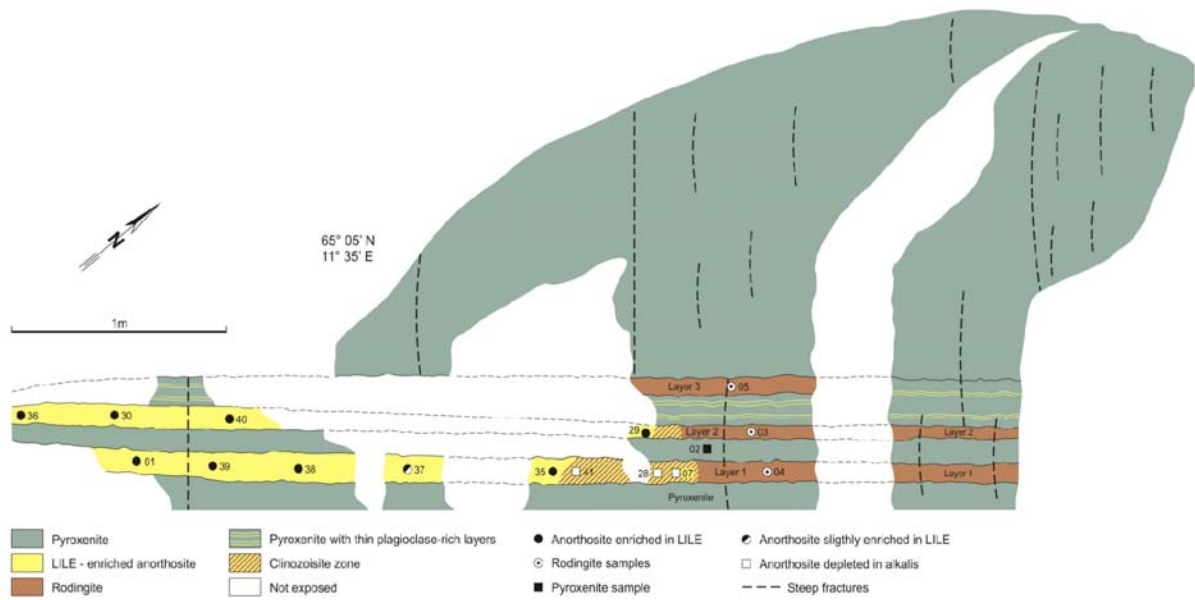


Figure 29. Outcrop map of the Aunekollen area rodingite locality.

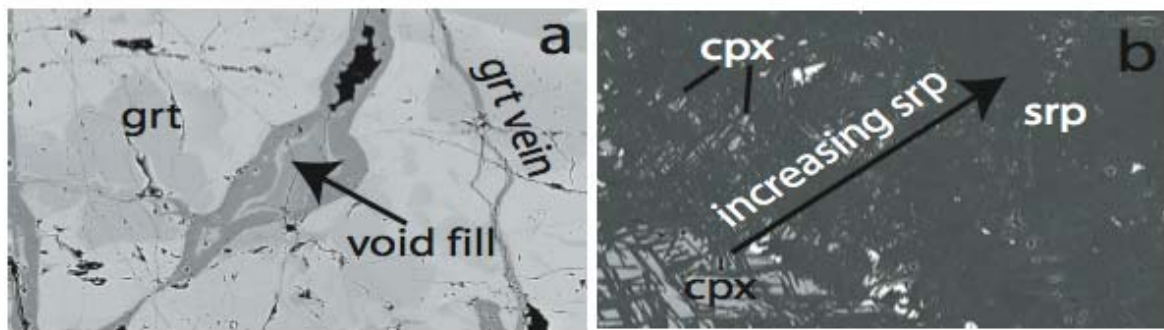


Figure 30. Backscatter images of (a) grossular-dominated rodingite zone and (b) serpentinized clinopyroxene.

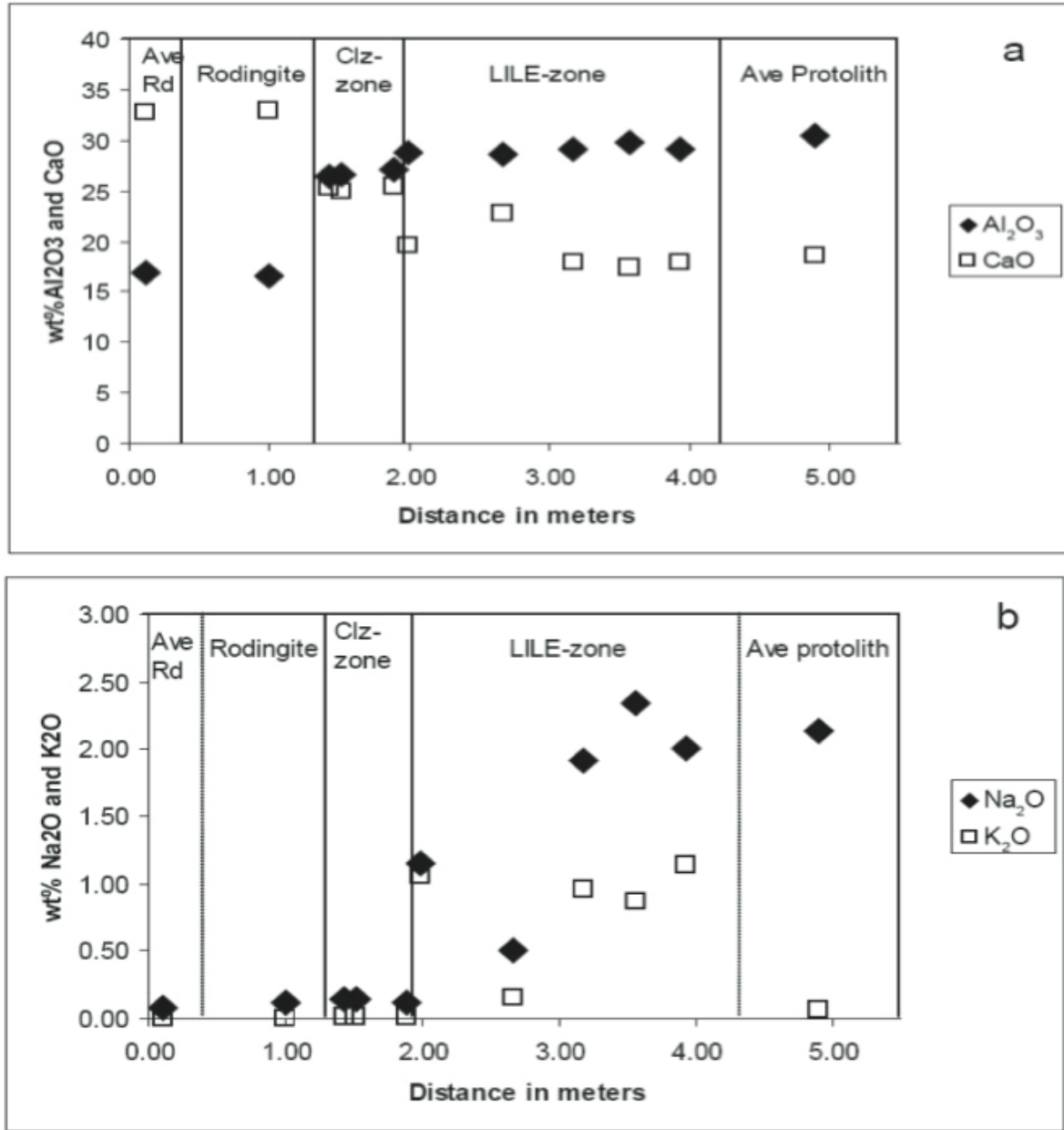


Figure 31. Geochemical variation from rodingitized to non-rodingitized rocks. a). Al₂O₃ and CaO contents. b) Na₂O and K₂O contents.

Stop No. 4-5: Leka geology trail in Våttvika–Stortjørna area.

Location

From Husby, drive northeast to the trailhead parking at UTM 32W 0629526, 7222393. Follow the Leka geology trail, which is marked with white arrows.

Introduction

The Leka geology trail provides access to outcrops of dated quartz keratophyre and exposures of the Skei Group, the cover sequence of the Leka ophiolite.

Description

The trail initially follows a narrow road toward the sea, but leaves this road ~200m from the parking area. The first stop is at UTM 32W 0629777, 7222304, where quartz keratophyre crops out. This rock was dated at 497 Ma by Dunning & Pedersen (1988). This age is considered to be the age of the Leka ophiolite.

The second stop is at UTM 32W 0629866, 7222472, where the contact of metavolcanic/quartz keratophyre with conglomerates of the Skei Group is exposed. The Skei Group is divided by a thin marble into the Skeineset and Havna Formations. The lowermost Skeineset Formation is composed of polymict conglomerate and is well exposed at this location. Clasts are dominantly mafic, but clasts of quartz keratophyre, metasandstone, carbonate and trondhjemite are also present. Sedimentary features including graded bedding, trough cross beds and scour and fill structures are preserved locally.

The majority of the clasts collected from this conglomerate yield initial ϵ_{Nd} of +7, consistent with derivation from oceanic basement, such as that represented by the Leka ophiolite (Fig. 32; McArthur et al., 2006). Two meta-igneous cobbles have less radiogenic ϵ_{Nd} of 0 and +4. Either these cobbles have a different source than the local basement, such as an arc with less extreme depleted mantle compositions, or these cobbles have been affected by CO₂-metasomatism. Two large (~70 cm diameter) metasandstone clasts were collected from the Skeineset polymict conglomerate exposed on Havneholmen. These have much more negative ϵ_{Nd} of -11 and -12. The detrital zircon population in one of these clasts resembles sources in the Lower Nappe (Fig. 32 and Fig. 4), suggesting that Leka was proximal to the Lower Nappe when the Skeineset Formation was deposited.

The third stop is at UTM 32W 0629953, 7222535, where black phyllite is overlain by pale metasandstone. These units form the uppermost part of the Havna Formation, which overlies the Skeineset Formation. The initial ϵ_{Nd} of -14 for the black schist indicates a Proterozoic continental source for this sediment. Similarly negative ϵ_{Nd} have been documented for fine-grained metasedimentary samples stratigraphically high in the Middle Nappe (Frost et al. 2006).

From this locality, follow the trail westward up the hill, where it meets the tourist trail near a burial mound at UTM 32W 0629770 7222620. Return to the parking area.

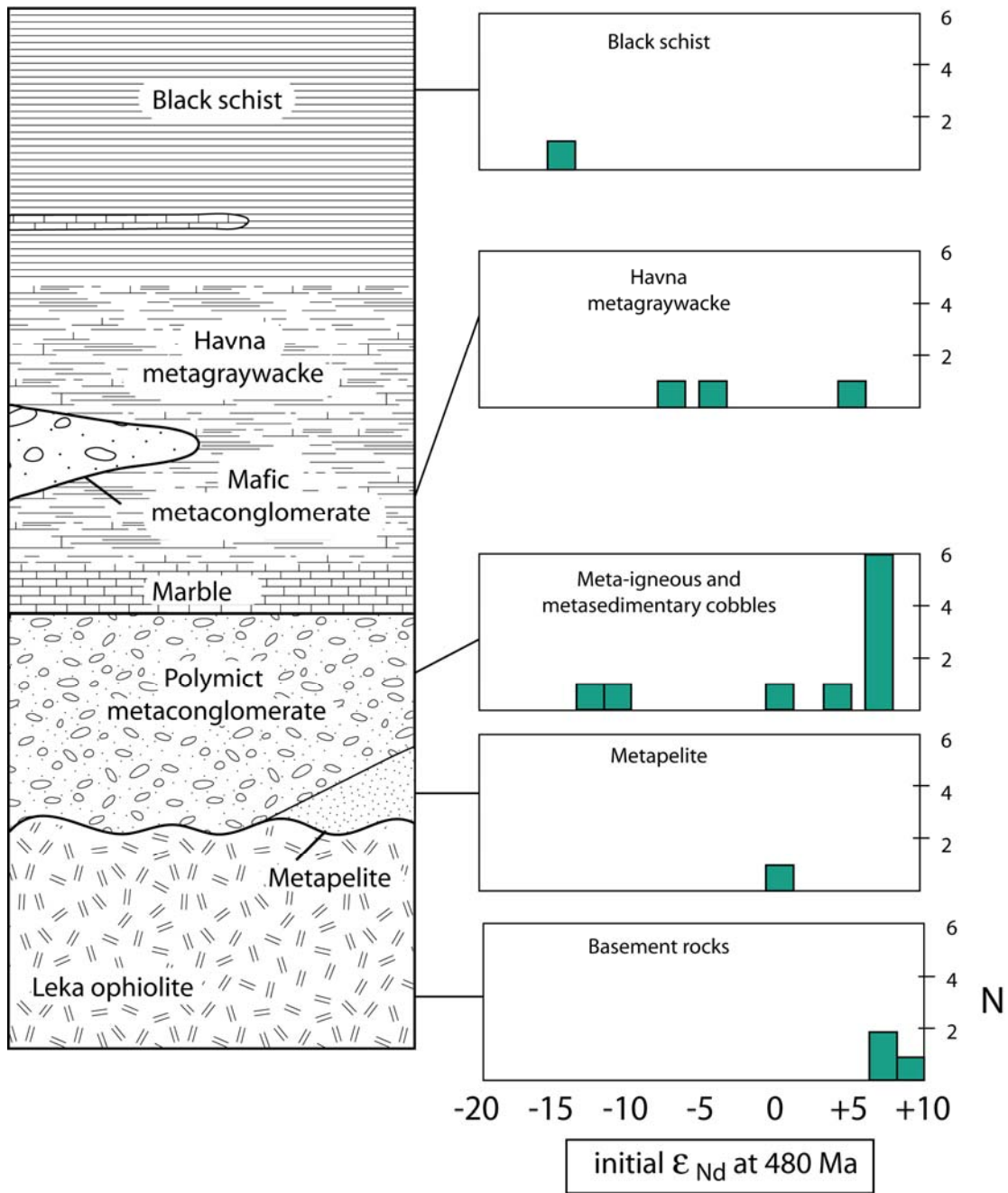


Figure 32. Schematic diagram of stratigraphy at Leka and histograms showing Nd isotopic results. Initial ϵ_{Nd} values increase up-section. Stratigraphy after Sturt et al. (1985).

Stop No. 4-6: Quarry at the Skei ferry terminus.

Location

The quarry is immediately west of the ferry terminal at UTM 32W 0628582, 7221005.

Introduction

The quarry exposes greywacke that exhibits graded bedding from sandy greywacke to finer mudstone. Needles of amphibole cross-cut the bedding and are more abundant in the fine-grained horizons.

Description

A thin marble unit well exposed at Leka Camping marks the base of the Havna Formation. The greywacke exposed in this quarry stratigraphically overlies this marble, and composes the middle member of the Havna Formation. It has been interpreted as a shallow marine turbidite deposit (Sturt et al., 1985). A large Havna greywacke sample composed of multiple graded beds yielded an initial ϵ_{Nd} of -3.2. A sandstone horizon yielded ϵ_{Nd} of +5.5 and mudstone horizon yielded ϵ_{Nd} of -5.7, indicating sedimentary unmixing of a composite source. The U-Pb ages of zircon recovered from this greywacke (Fig. 33) are exclusively Ordovician, and suggest a cryptic arc source composed of both depleted mantle and more evolved components. The date of deposition of the Havna Formation is constrained by the date of the youngest detrital zircon, 471 ± 8 Ma (Fig. 33).

In summary, the Skei Group records deposition of high- to low-energy sedimentary rocks upon the Leka ophiolite basement. Many of the clasts in the basal conglomerates appear to be locally derived, but the presence of metasandstone clasts requires the presence of a proximal continental source, possibly the Lower Nappe. Fine-grained rocks higher in the section appear to incorporate a greater proportion of continental detritus than do the metapelites in the basal formation. The Ordovician detrital zircon ages of the Havna greywacke suggest that deposition occurred very close in time to metamorphism related to nappe stacking.

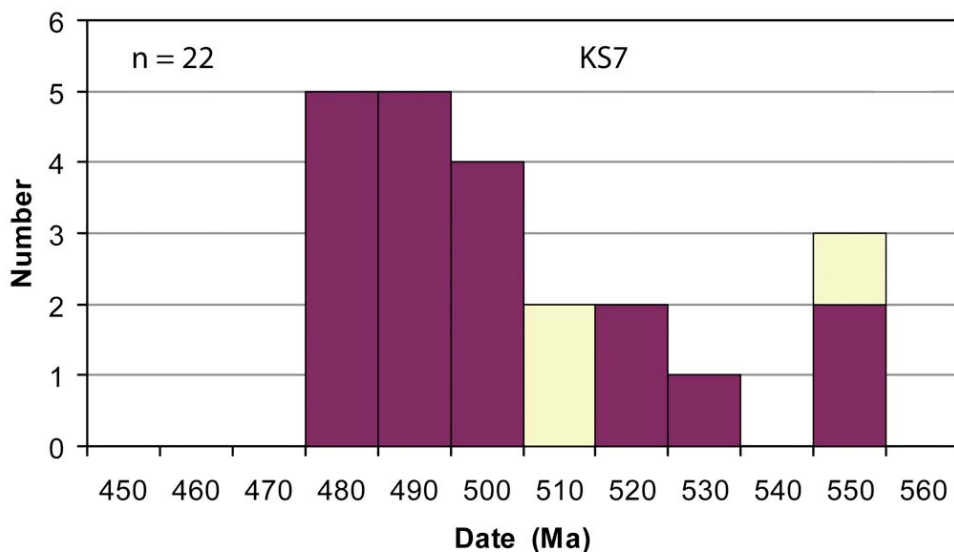


Figure 33. Histogram plot showing U-Pb zircon age data from the Leka Havna metagraywacke (KS7). Dark colored bars indicate concordant ages and light colored bars indicate discordant ages as defined by a 5% discordancy filter.

Day 5

Introduction. Middle Nappe structures and Scandian extension in the Helgeland Nappe Complex.

Today we will look again at tectonic relations in the HNC nappes. In particular, we will consider the timing of internal imbrication in the Middle Nappe. In addition we will look at evidence for Scandian extension of the HNC along a regional shear zone, the Kollstraumen detachment.

Major extensional detachments that modified the Caledonian nappe stack were first recognized in western Norway (e.g. Hossack 1984, Norton 1986). In central Norway, similar structures were described from the Høybakken detachment zone west of Trondheim (Séranne 1992), and on a more regional basis in north-central Norway by Braathen et al. (2000). Subsequent to these studies, a number of major extensional detachments and shear zones have been identified onshore in northern Central Norway (Fig. 34), and linked to geophysical evidence for the continuation offshore; for details, see Eide et al. (2002), Larsen et al. (2002), Nordgulen et al. (2002), Osmundsen et al. (2002, 2003, 2005), Olesen et al. (2002), and Skilbrei et al. (2002).

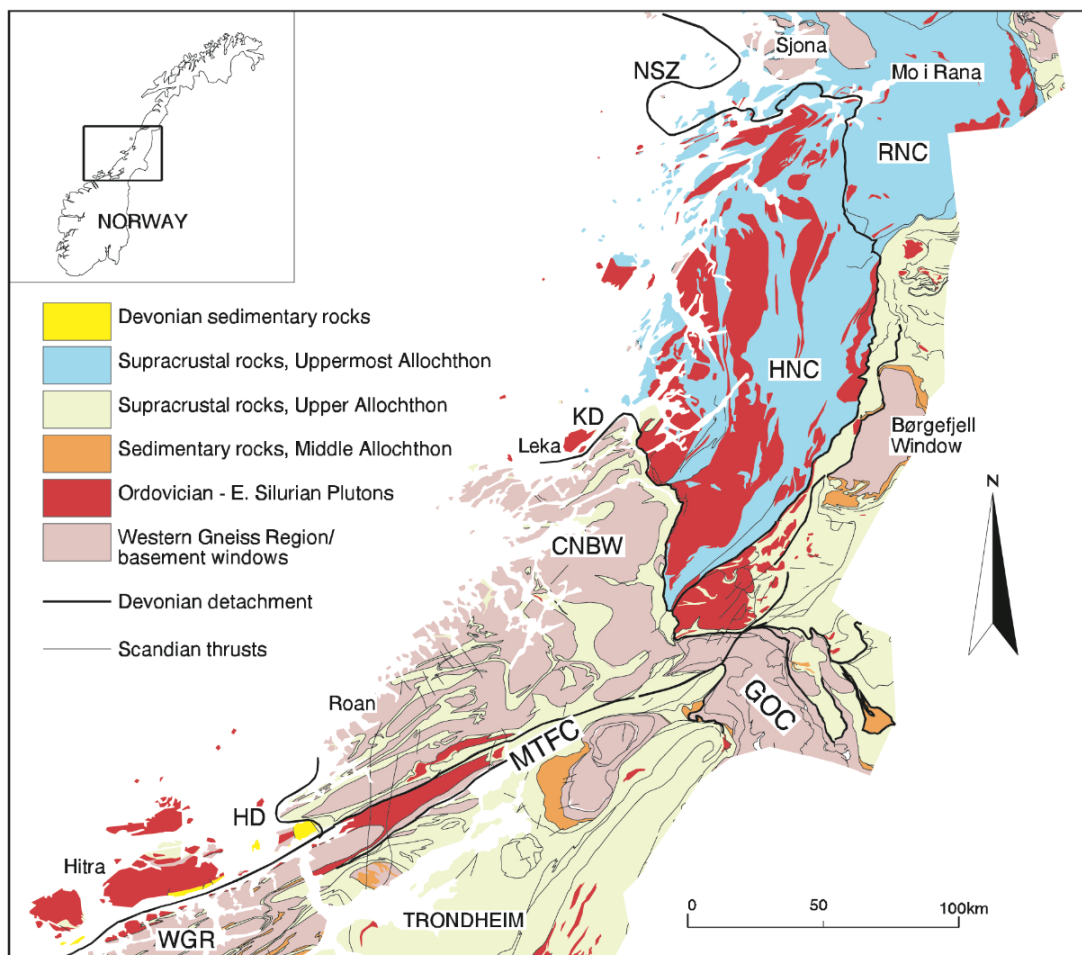


Figure 34. Tectonic map of the Helgeland Nappe Complex (HNC), and Central Norwegian Basement Window (CNBW). KD = Kollstraumen detachment; WGR = western gneiss region; GOC = Grong-Olden Culmination; NSZ = Nesna shear zone; RNC = Rödingsfjället Nappe Complex; MTFC = Møre-Trøndelag Fault Complex.

Stop No. 5-1: Road cuts along Simlestraumen

Location

From Route 17 park in the turnout on the fjord-side of the road at UTM 33W 0362963, 7218334.

Introduction

This stop provides an opportunity to see a section of strongly deformed rocks along the Kollstraumen detachment zone that separates the HNC from the subjacent Central Norwegian Basement Window (CNBW).

Description

Structurally below the Kollstraumen detachment zone, Palaeoproterozoic orthogneisses and overlying supracrustal rocks of the Skjøtingen Nappe (local name equivalent to the Seve Nappe of the Upper Allochthon) form the northern CNBW. During the Scandian event, these rocks were metamorphosed at medium to high grade and acquired a penetrative ductile fabric folded by roughly orogen-parallel, NE-SW-oriented, upright regional folds. Approaching the Kollstraumen detachment zone, the regional NE-SE foliation changes in attitude, and becomes approximately parallel with the strike of the detachment (Fig. 35). Large sheets of orthogneiss that are present as concordant mega-lenses in supracrustal rocks may represent cut-off antiforms, now occurring as folded sheets separated from the subjacent basement (see section in Fig. 36). The geometries are either related to Scandian contraction or, alternatively, but less likely, to the Early Devonian extensional event.

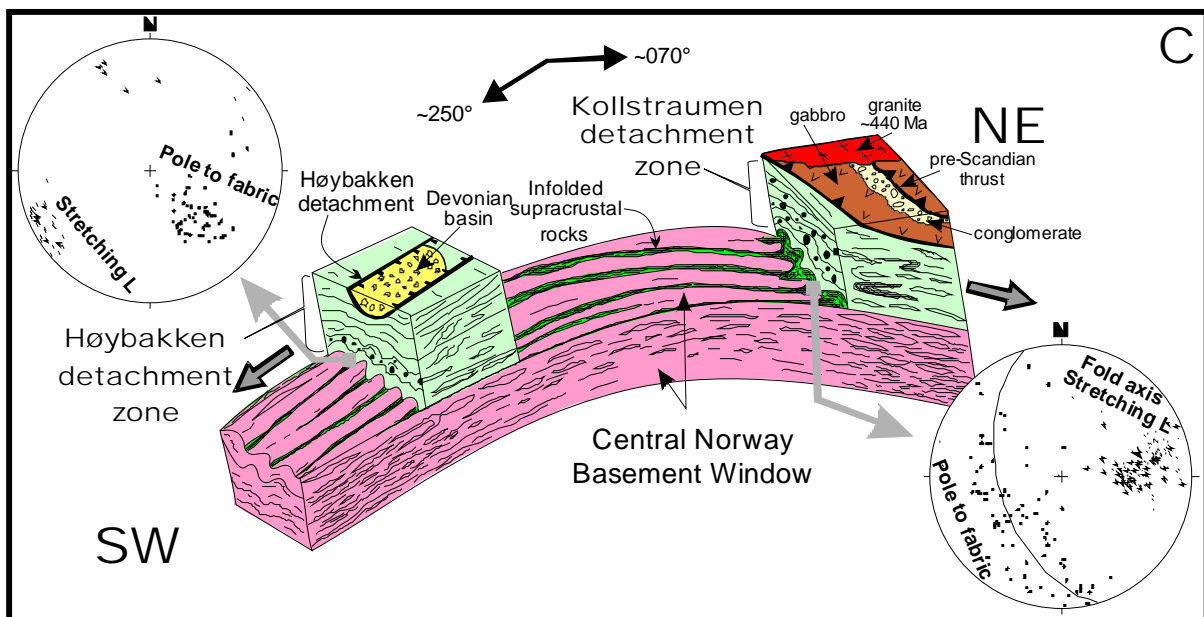


Figure 35. Diagram showing the geometry of the Høybakken and Kollstraumen detachments zones (adapted from Braathen et al. 2000). The stereoplots (lower hemisphere, equal area) show poles to mylonitic foliation, fold axes (asterisks) and stretching lineations (triangles). The Høybakken (HD) and Kollstraumen detachments (KD; Braathen et al. 2000; Nordgulen et al. 2002) separate the Uppermost Allochthon rocks from the subjacent Central Norway basement window (CNBW). The HD exhibits top-WSW sense of shear, whereas the shear sense on the KD is to the ENE; i.e. the opposite of the HD. The CNBW formed in response to Devonian orogen-parallel extension along the detachment zones.

The road cuts on the southwest side of the road expose a contact between granitic gneiss mapped as part of the CNBW (Mesoproterozoic) and schist, calc-silicate rocks and marble. It is commonly difficult to separate structures that can confidently be assigned to Devonian extensional shear from those that may be related to Scandian or even older events. However, the presence in the contact zone of a strongly deformed pegmatite dated at 401 ± 3 Ma (Schouenborg 1988) shows that the shear deformation post-dates the Scandian thrusting. Along the road cut, kinematic indicators are common within SL- and LS-tectonised rocks, and rare in the L-tectonites. Examples of ductile shear fabrics, shear-related folds, and winged porphyroclasts support top-ENE shear along the Kollstraumen detachment zone during the Devonian event (cf stereoplot in Fig. 35).

Stop No. 5-2: Quarry and road cuts north of Sandvikfjellet

Location

From Route 17, take Route 801 toward Terråk and drive 3.1 km. Drive past the small quarry on the right (south) side of the road; the safest parking is on the left (north) side of the road. Walk back to the quarry and road cuts to the west.

Introduction

This stop provides an opportunity to study metagabbroic rocks and the contact with overlying deformed calcareous conglomerates of the HNC.

Description

The section along Sørfjorden (Fig. 36) takes us back to issues of nappe construction and pre-Scandian internal imbrication of nappe units. The regional map of this area, and the WSW-ENE section along Sørfjorden, shows that there is a repetition of SE-dipping units composed of slices of metagabbro overlain by metasedimentary rocks (Fig. 36). Evidence from further south (Kolbotnet, Fig. 36), shows that the structurally lowermost metagabbro was thrust over calc-silicate rocks and marbles that belong to the CNBW. Other rock units include orthogneiss and grey, fine-grained mylonites and ultramylonites of partly uncertain origin. Across Sørfjorden to the north, the majestic Heilhornet pluton (ca. 438 Ma; Barnes et al. 2007) cuts sharply across the contacts between the different rock units of the imbricate zone (Fig. 37). Hence, the imbricate zone represents a pre-Scandian repetition of nappe units.

At this stop, a medium-grained metagabbro is disconformably overlain by a calcareous conglomerate that fines upwards into meta-sandstones with layers of grit and conglomerate. The conglomerate clasts are predominantly carbonate rocks but sparse greenstone, metagabbro, jasper, and fine-grained quartz-rich rocks are present. The matrix is carbonate-rich. Competent clasts have equidimensional shapes in contrast to highly flattened and elongate incompetent clast with the shape of prolate ellipsoids ($x > y \gg z$). A decrease in strain is present from highly sheared metagabbro and conglomerates at the contact to less deformed conglomerates cut by sheared mafic sheets away from the contact.

The metasediments have been interpreted to represent a fluvial to shallow-marine braided stream and fan-delta deposit. Similar meta-gabbros are also present to the north and east of the Heilhornet Pluton, where they are associated with ultramafic rocks and locally pillow lava. This rock association is interpreted to be a dismembered ophiolite and are correlated with occurrences of ophiolite fragments in the wider Helgeland region (e.g. the Leka Ophiolite Complex).

Two biotite-bearing silicate clasts yielded initial ϵ_{Nd} of -3.3, a value similar to those of clasts from conglomerates stratigraphically high elsewhere in the Middle Nappe. Sandstone, siltstone and pebble conglomerate immediately upsection of this outcrop, by contrast, have initial ϵ_{Nd} of -14 to -15, suggesting an isotopically evolved source was shedding detritus at this time.

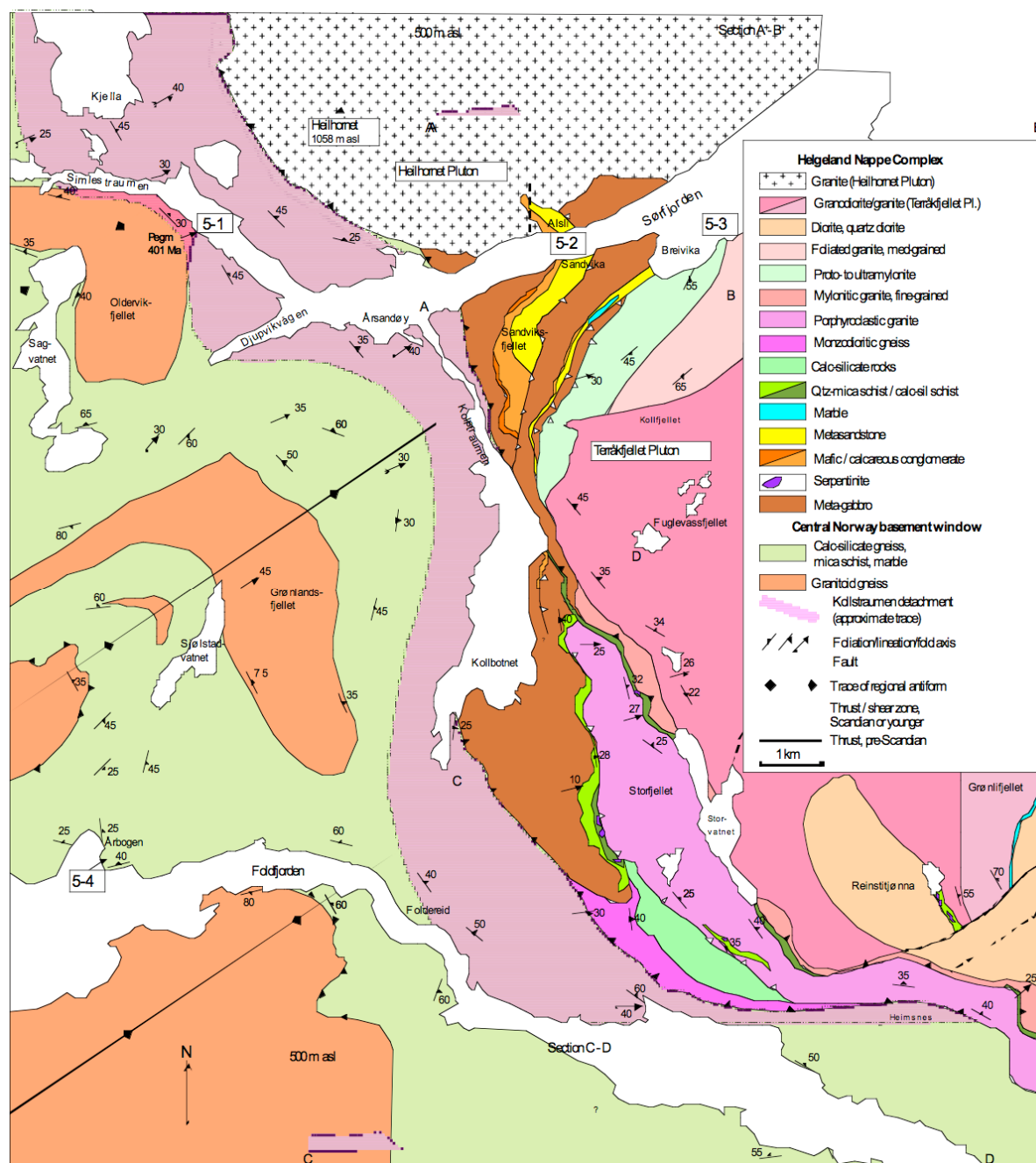


Figure 36. Geological map of the northeastern part of the CNBW and the southwest part of the HNC. At Stop 5-1 (Simlestraumen) a strongly sheared and folded pegmatite dated at 401 ± 3 Ma (Schouenborg 1988) occurs within the Kollstraumen detachment. The approximate trace of highly strained rocks along the Kollstraumen detachment zone is schematically indicated below the base of the HNC. Note how the NE-SW-oriented strike of the foliation in the CNBW changes progressively towards the detachment zone. Sections A-B and C-D illustrate the main features of an imbricated zone forming a major duplex at the base of the HNC (see Stop 5-2 and 5-3). Early Silurian dykes occur in the southeast limb of a regional synform, at Årbogen, north of Foldfjorden (Stop 5-4). Figure adapted from Nordgulen et al. (2002).

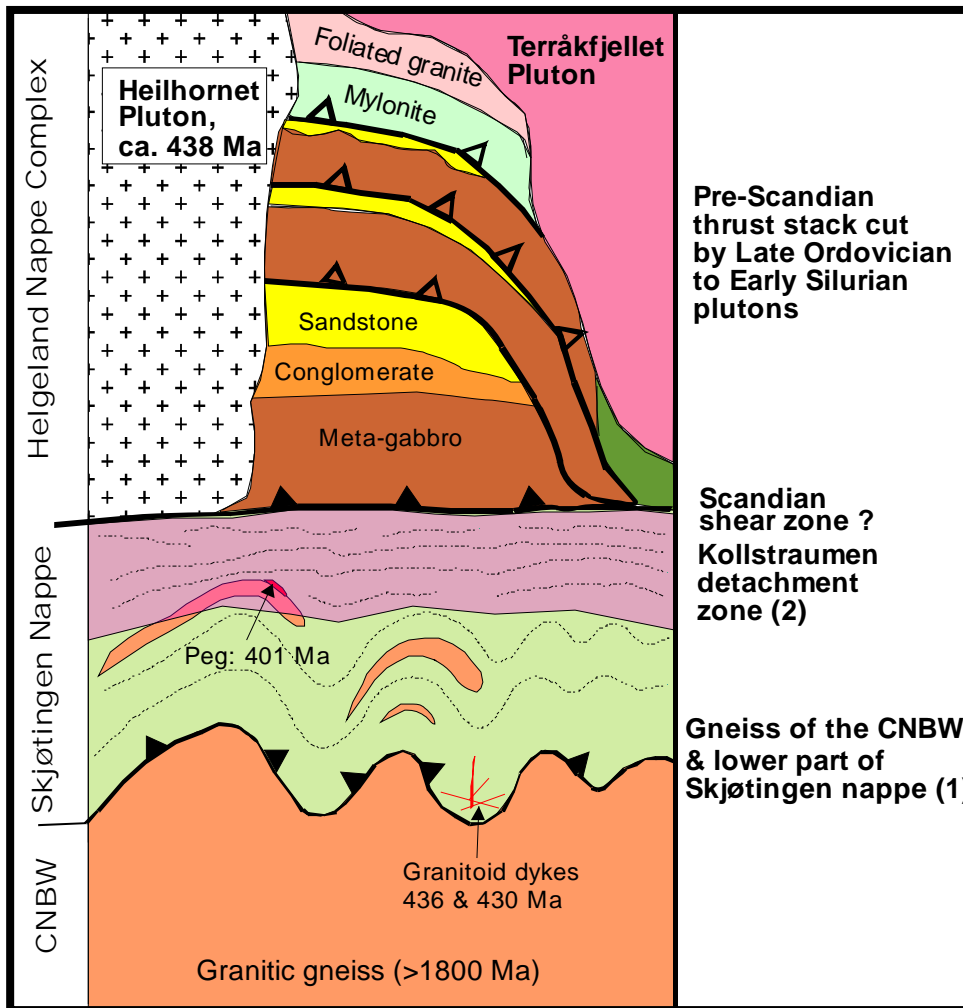


Figure 37. Schematic section that outlines the main lithologies, tectonostratigraphic units and structural relationships across the Kollstraumen detachment zone (see map and legend in Fig. 36). From base to top, the section has been subdivided into three parts: 1) the upper Proterozoic gneisses of the CNBW and the overlying supracrustal rocks of the Skjøtingen Nappe (Upper Allochthon); 2) the Kollstraumen detachment zone; and 3) the basal part of the HNC. See also the box diagram illustrating the structural relationships across the entire CNBW shown in Figure 35. Figure adapted from Nordgulen et al. (2002).

Stop No. 5-3: Road cuts near Saltbunesodden, NE of Breivika (optional)

Location

Drive 2.6 km eastward toward Terråk. Pass the settlement at Breivika and park along the right (east) side of the road; UTM 0371060, 7217440.

Introduction

Mylonitic monzodiorite is exposed along the road towards the NE.

Description

Grey mylonites with variable strain intensity (protomylonites to local ultramylonites) are present structurally above the imbricate zone along Sørfjorden. The mylonites were probably derived from a monzodioritic precursor. The planar fabric dips ca. 60 degrees to the southeast. Concordant sheets (<5 cm wide) of highly deformed mafic to intermediate composition are present.

Along strike to the southwest, the mylonitic rocks are cut by medium-grained granodiorite of the Terråkfjell pluton (Fig. 36). This pluton is undated; however, the rocks are geochemically similar to the Kråkfjellet pluton and considered to be Late Ordovician or possibly earliest Silurian in age. The mylonites are therefore pre-Scandian and probably related to the internal imbrication of nappe units of the HNC.

Stop No 5-4: Åbogen

Location

From the junction on Route 17 ca. 1.5 km northwest of Foldereid, take Route 770 toward Kolvereid and Vikna and drive 5 km to Åbogen. Turn around and retrace the route (south) for ca. 300 m and park along the right (west) side of the road. UTM 33W 0361300, 7207950.

Introduction

Along the road cut at this locality there are good examples of folding and boudinage of Early Silurian dikes cutting calc-silicate gneisses of the Skjøtingen Nappe.

Description

A number of different granitoid dykes cut the NE-dipping (30–40 degrees) amphibolite-facies foliation in the calc-silicate gneisses on the southeast limb of a regional synform (Fig. 36). Some ductile deformation has affected the dykes, and depending on their initial orientation, the dykes have been folded and boudinaged. The field relations show that the dykes have been subjected to sub-horizontal flattening and locally a NE-trending, shallow-plunging lineation occurs along their margins.

Based on cross-cutting relationships, the following sequence of intrusion has been established (Fig. 38).

1. Grey, medium- to fine-grained biotite tonalite (436 ± 2 Ma; zircon); the rock is metaluminous with high Na_2O and relatively high Sr contents. Two generations of titanite are present: brown titanite has an age of 418 ± 2 Ma, whereas a pale-brown generation formed at or after 402 ± 3 Ma.

2. Weakly peraluminous, medium-grained biotite+muscovite±garnet granite, partly pegmatitic (not dated).
3. Weakly peraluminous, medium-grained biotite+muscovite±garnet granite locally grading into fine-grained granite, aplite, and pegmatite (430 ± 4 Ma). Monazite is very abundant and yields an age of 401 ± 1 Ma.

U-Pb dates on dykes of tonalite and granite that intruded supracrustal rocks of the Skjøtingen Nappe have yielded ages of 436 Ma and 430 Ma, respectively. Combining geochronological and structural data, we infer that the granite dykes may overlap in time with earliest Scandian contractional deformation. Later deformation of the dykes may have occurred during continued Scandian contraction as well as extension parallel to the regional fold axis. Titanite and monazite U-Pb dates from the dykes (c. 401-402 Ma) coincide in time with numerous pegmatites in central Norway and are interpreted to date metamorphism during latest Scandian exhumation of the Central Norway Basement Window.

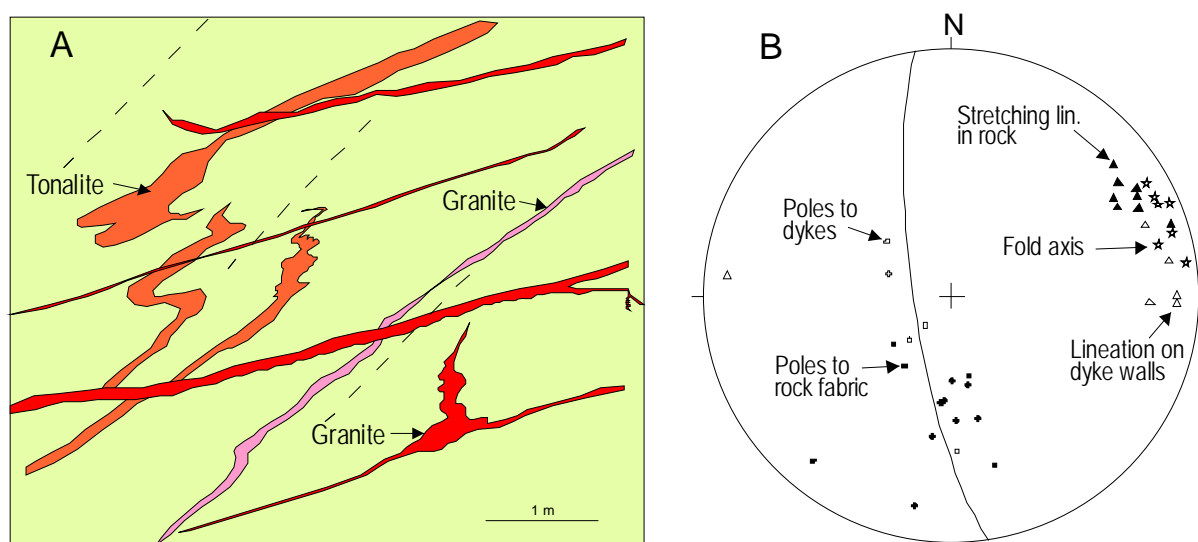


Figure 38. A. Sketch of cross-cutting relationships described for stop 5-4. B. Stereogram of structural data for stop 5-4.

Discussion

Sediment provenance and paleogeographic considerations.

Detrital zircon populations in Neoproterozoic Lower Nappe metasediments are similar to the Argyll and Southern Highlands Groups of the Dalradian Supergroup of Scotland (Barnes et al., 2007). This similarity suggests that the Lower Nappe sediments had a provenance similar to that of the Dalradian. Such zircons may have been derived from either Laurentia or Baltica. In the case of the Dalradian Supergroup, Cawood et al. (2003, 2007) suggested that the sediment source was the Laurentian craton (East Greenland) and that the depositional basin lay north of the topographic expression of the Grenville/Sveconorwegian orogen, thereby blocking detritus from the Pan-African orogen. A similar origin for the Lower Nappe metasedimentary rocks is consistent with the consensus that the HNC is peri-Laurentian.

These detrital zircon data along with previous studies relating the HNC to Laurentia (e.g., Yoshinobu et al., 2002; Roberts et al., 2007) prompted Barnes et al. (2007) to suggest that the Lower Nappe and the Neoproterozoic part of the Horta nappe were rift fragments from the

Laurentian margin. In this interpretation, the ophiolitic basement rocks of intercalated nappes (Fig. 3) are part of the oceanic crust that separated rift fragments from each other or from Laurentia. This model is similar to those developed for Early Ordovician ophiolites in the Caledonian–Appalachian orogen (e.g. Cawood et al., 1995; van Staal et al., 1998; Waldron and van Staal, 2001; Hatcher et al., 2004; Hibbard et al., 2007). In these models, the microcontinents serve as the basement for Cambro-Ordovician arcs.

Aside from the stratigraphically lower, Neoproterozoic part of the Horta nappe, for which no detrital zircon data are available, the remaining dated metasedimentary units in the HNC are all Early Ordovician. However, a metasandstone sample from the Sauren-Torghatten Nappe and cobbles from the Skei Group and Sauren-Torghatten Nappe contain detrital zircon populations essentially identical to those from the Lower Nappe (Fig. 4). Although it is possible that the detritus in these Early Ordovician basins had the same source as Lower Nappe sediments, the abundance of conglomerates and coarse sandstones in the Sauren-Torghatten and Skei Group metasedimentary sections suggests significant local topographic relief and/or short transport distance from the sediment source (e.g., Heldal, 2001; McArthur, 2007). We therefore suggest that a more likely source of these sediments was the Lower Nappe itself.

The origins of the Cambro-Ordovician detrital zircons (485–520 Ma) in all of the Lower Ordovician Nappes are enigmatic. Volcanic activity may have accompanied circa 480 Ma crustal melting in the Lower and Upper Nappes, but this activity cannot explain zircons with earliest Ordovician and Cambrian ages. Regionally, the 470–500 Ma time period was characterized by numerous suprasubduction zone ophiolites and primitive arcs, including the Leka ophiolite and many others in the Upper Allochthon (summary in Slagstad, 2003). However, an origin of abundant zircons from primitive suprasubduction zone magmas is problematic because of the limited zircon productivity in such systems. Taconian arc magmatism in Newfoundland included both mafic and felsic components (e.g., van Staal et al., 1998; Slagstad, 2003; Hibbard et al., 2007), and it is possible that similar arcs existed closer to the Early Ordovician basins of the HNC. If so, no vestige of such arcs has been identified in the Norwegian Caledonides or in East Greenland.

In the HNC, Lower Ordovician clastic and carbonate sediments were deposited on Neoproterozoic sedimentary “basement” rocks and on Cambrian ophiolitic basement rocks. As noted above, an arc source is probable for some of these sediments. However, McArthur (2007) showed that the ϵ_{Nd} values of fine-grained metasedimentary rocks of the Sauren-Torghatten Nappe decrease upward. This decrease indicates increasing importance of Proterozoic sediment provenance during Early Ordovician time. Whether this change in provenance is related to a decrease in Early Ordovician arc component, and increase in sediment contribution from the Lower Nappe, or increasing proximity to the Laurentian margin is unclear.

Timing of nappe imbrication and metamorphism.

Nappes of the Helgeland Nappe Complex were imbricated after migmatization of the Lower and Upper Nappes (~480 Ma; Yoshinobu et al., 2002; Barnes et al., 2007) and before emplacement of crosscutting plutons. The oldest truly crosscutting plutons are the ~447 Ma Akset-Drevli pluton and the 442 Ma Andalshatten pluton (Yoshinobu et al., 2002). However, the 478 Ma S-type Botnafjellet pluton (Barnes et al., 2007) intruded rocks interpreted to be part of the Lower Nappe (i.e., Neoproterozoic) yet the pluton contains inherited Cambrian and

Early Ordovician zircons. These observations indicate that imbrication had occurred by 478 Ma and are consistent with cooling ages of 475 ± 3 Ma (U-Pb, titanite) from the Middle Nappe (Barnes et al., 2007) and 474 ± 5 Ma (K-Ar, amphibole) from the Upper Nappe (James et al., 1993). In this interpretation, post-imbrication regional metamorphism and anatexis of the Horta Nappe produced the parental magmas to the S-type Vega and Botnafjellet plutons, with upward emplacement of the latter into the Lower Nappe.

Evidently, metamorphic activity in the HNC began with high-grade metamorphism of the Lower and Upper Nappes and was followed by imbrication of all nappes by approximately 478 Ma. Migmatization of the Horta Nappe and consequent S-type granitic magmatism followed, along with amphibolite-facies metamorphism of the structurally higher nappes. This sequence and timing of events is consistent with the regional metamorphic assemblages in the nappes: kyanite zone in the Sauren-Torghatten Nappe (Heldal, 2001) and sillimanite zone in the Lower, Middle, and Upper Nappes, with metamorphic cordierite common only in the Upper Nappe (Yoshinobu et al., 2002; Reid, 2004).

The cause of nappe amalgamation is currently speculative. Meyer et al. (2003) interpreted docking of the Uppermost and Upper Allochthons to be before the 456–458 Ma emplacement of the Nesna Batholith. It is thus possible that docking of the Uppermost and Upper Allochthons was responsible for collapse and amalgamation of the Helgeland Nappe Complex.

Bindal Batholith magmatism

478–470 Ma

The earliest magmatism of the Bindal Batholith involved emplacement of voluminous peraluminous to strongly peraluminous felsic magmas. In many orogenic belts, crustal melting to form peraluminous magmas is ascribed to conductive heating of the thickened crust followed by exhumation and decompression partial melting. However, in the HNC, initial Bindal magmatic activity post-dated amalgamation of the HNC nappes by no more than 3–5 m.y. This short time between crustal imbrication and crust-dominated magmatism was probably not sufficient for crustal heating to solidus conditions. Instead, the association of mafic enclaves, disrupted mafic dikes, and sparse hornblende-rich mafic intrusions associated with 478–470 Ma plutons suggests that crustal melting was caused by deep-seated intrusion of hydrous (?) mafic magmas.

465 Ma

Following nappe amalgamation, volumetrically minor mafic magmatism occurred, as exemplified by the Hortavær igneous complex and the Svarthopen pluton at ~465 Ma. On the basis of major and trace element variations, one can argue that these two plutonic systems had similar basaltic parental magmas (Figs. 6 & 7). However, their petrologic evolution was by distinctly different mechanisms: the Hortavær magmas by assimilation-fractional crystallization (Barnes et al., 2005b) and the Svarthopen magmas by mixing with crustal melts. The mafic rocks in both systems have trace element characteristics of a supra-subduction zone origin.

450–440 Ma

Beginning at about 450 Ma, Bindal magmatism became more voluminous and widespread (Fig. 2). Most plutons in this age range are metaluminous and calc-alkalic to alkali-calcic (Figs. 6 & 7), and a significant number are mafic (gabbro-diorite-monzodiorite). However, few primitive compositions are present, with parental magmas of well-studied plutons typically andesitic. Trace element patterns indicate a suprasubduction zone setting and Sr and Nd isotopic compositions suggest significant interaction with crustal rocks, which is consistent with the andesitic parental compositions.

439–424 Ma

The oldest pluton in this time frame is the ca. 438 Ma Heilhornet pluton (Fig. 2); plutonism continued until ~424 Ma. This time interval was characterized by mafic, intermediate, and felsic magmas. The few detailed geochemical studies suggest a suprasubduction zone origin of the mafic magmas. With the exception of the Heilhornet pluton, this group of rocks is characterized by higher Sr contents than most older Bindal plutons. Moreover, some young granitic rocks (e.g., Tosenfjord granitic dikes) contain low abundances of heavy REE (Fig. 17) and high Sr/Y ratios indicative of an origin by partial melting of lower crust with garnet in the residue.

Not only are 439–424 Ma plutons widespread in the HNC, they are also common in the Beiar and Rödingsfjället Nappe Complexes (Tørudbakken & Brattli, 1985; R. Larsen, pers. comm.). Moreover, crustal melting and plutonism in this age range is characteristic of the Caledonides of northeast Greenland (e.g., Kalsbeek et al., 2001; Andresen et al., 2007). In contrast to the HNC, older magmatism in the Rödingsfjället Nappe Complex and northeast Greenland Caledonides was sparse or absent.

Evidently, the Ordovician magmatic and tectonic activity that characterizes the crustal evolution of the HNC did not affect exposed part so of the East Greenland Caledonides. This isolation of both tectonism and magmatism fits nicely with the concepts outlined above: that the HNC originated as a series of rift fragments (so-called “strip continents”?) with intervening ocean basins separating individual rift fragments from each other and from Laurentia. If so, then the voluminous Lower Ordovician clastic deposits of the HNC require either an intra-Iapetan landmass large enough to supply the sediments (and one with significant topography) or close enough proximity to Laurentia to permit progradation of clastic wedges onto and over the various HNC basement terranes. The distinctive magmatic history of the HNC during Ordovician time suggests that the HNC was distal from Laurentia during Early Ordovician time, and only made a close approach during the Llandovery (early Silurian), when granitic magmas invaded much of the Uppermost Allochthon and Laurentia. One of the outstanding questions regarding magmatism during Scandian time is the relationship between granitic magmatism (source rocks and heat source), tectonic position in the growing stack of allochthons, and breadth of the early Silurian magmatic event.

Acknowledgements

Funding for research presented on this field trip was provided by the Norwegian Geological Survey, the U.S. National Science Foundation through grants EAR-0439750 (Barnes, Yoshinobu, and Frost), EAR-9814280 (Barnes), the Texas Tech University Research Enhancement Fund (Yoshinobu), the Geological Society of America (Marko and Anderson), and the Department of Geosciences, Texas Tech University. We gratefully acknowledge Melanie Barnes for her assistance in the field and lab and Jostein Hiller for superb navigating and sailing and his support of geological research at the Leka Steinsenter. We acknowledge the fine thesis work of current and former students Heather Anderson, Greg Dumond, Yuija Li, Wayne Marko, Lindy McCulloch, Jeff Oalman, Kristin Reid (Texas Tech), and Laura Vietti and Kelsey McArthur (University of Wyoming).

References

- Andersen, T.B. & Jamtveit, B., 1990: Uplift of deep crust during orogenic extensional collapse: a model based on field studies in the Sogn-Sunnfjord area of Western Norway. *Tectonics* 9, 1097-1111.
- Andersen, T.B. & Jansen, Ø.J. 1987: The Sunnhordland Batholith, western Norway: Regional setting and internal structure, with emphasis on the granitoid plutons. *Norsk Geologisk Tidsskrift* 67, 159-183.
- Anderson, H., Yoshinobu, A., & Barnes, C.G., 2005: Deformation, migmatization, and intrusive diatexites along the contact of the ~470 Ma Vega pluton, Helgeland Nappe Complex, north-central Norway. *Eos Transactions of the American Geophysical Union* 86, Fall Meeting Supplement, Abstract V13E-0597.
- Anderson H.S., Yoshinobu, A.S., & Chamberlain, K., 2007: Xenolith incorporation in plutons: Implication to stoping assimilation, and incremental pluton construction, Andalshatten Pluton, Norwegian Caledonides. *Geological Society of America Abstracts with Programs* 39, 225.
- Andresen, A., Rehnström, E.F., & Holte, M., 2007: Evidence for simultaneous contraction and extension at different crustal levels during the Caledonian orogeny in NE Greenland. *Journal of the Geological Society, London* 164, 869-880.
- Austrheim, H. & Prestvik, T. 2008: Rodingitization and hydration of the oceanic lithosphere as developed in the Leka Ophiolite, north-central Norway. *Lithos* (in press).
- Barbey, P., Marignac, C., Montel, J.M., Maraudiere, J., Gasquit D. Jabbori, J., 1999, Cordierite growth textures and the conditions of genesis and emplacement of the crustal granitic magmas; the Velay Granite Complex (Massif Central, France), *Journal of Petrology*, v. 40, no. 9, p. 1425-1441.
- Barnes, C. G., & Prestvik, T., 2000: Conditions of pluton emplacement and anatexis in the Caledonian Bindal Batholith, north-central Norway. *Norsk Geologisk Tidsskrift* 80, 259-274.
- Barnes, C., Yoshinobu, A., Prestvik, T., Nordgulen, Ø., Karlsson, H., & Sundvoll, B., 2002: Mafic magma intraplating: anatexis and hybridization in arc crust, Bindal Batholith, Norway. *Journal of Petrology* 43, 2171-2190.
- Barnes, C. G., Prestvik, T., Barnes, M. A. W., Anthony, E. Y., & Allen, C. M., 2003: Geology of a magma transfer zone: the Hortavær Igneous Complex, north-central Norway. *Norwegian Journal of Geology* 83, 187-208.
- Barnes, C.G., Dumond, G., Yoshinobu, A. S., & Prestvik, T., 2004: Assimilation and crystal accumulation in a mid-crustal magma chamber: The Sausfjellet pluton, north-central Norway. *Lithos* 75, 389-412.
- Barnes, C.G., Frost, C.D., & Nordgulen, Ø., 2005a: Mid-crustal magma mixing and forced garnet stability in a Caledonian pluton, north-central Norway. *Eos Transactions of the American Geophysical Union* 86, Fall Meeting Supplement, Abstract V13E-0594.
- Barnes, C. G., Prestvik, T., Sundvoll, B., & Surratt, D., 2005b: Pervasive assimilation of carbonate and silicate rocks in the Hortavær igneous complex, north-central Norway. *Lithos* 80, 179-199.
- Barnes, C.G., Frost, C.D., & Nordgulen, Ø., 2006: Mid-crustal magma mixing and forced garnet stability in Late Ordovician plutons, Norwegian Caledonides. *Bulletin of the Geological Society of Finland*, Special Issue 1, 14.
- Barnes, C.G., Frost, C.D., Yoshinobu, A.S., McArthur, K., Barnes, M.A. Allen, C.M., Nordgulen, Ø. & Prestvik, T., 2007: Timing of sedimentation, metamorphism, and plutonism in the Helgeland Nappe Complex, north-central Norwegian Caledonides. *Geosphere* 3, 683-703.

- Bingen, B., Nordgulen, Ø., & Solli, A., 2002: U–Pb geochronology of Paleozoic events in the Mid Scandinavian Caledonides. In Eide, E.A. (coord.): *BATLAS—Mid Norway plate reconstruction atlas with global and Atlantic perspectives*, 66–67. Geological Survey of Norway, Trondheim.
- Birkeland, A., Nordgulen, O., Cumming, G. L., & Bjorlykke, A., 1993: Pb–Nd–Sr isotopic constraints on the origin of the Caledonian Bindal Batholith, central Norway. *Lithos* 29, 257–271.
- Braathen, A., Nordgulen, Ø., Osmundsen, P.-T., Andersen, T.B., Solli, A. & Roberts, D. 2000: Devonian, orogen-parallel, opposed extension in the Central Norwegian Caledonides. *Geology* 28, 615–618.
- Braathen, A., Osmundsen, P.T., Nordgulen, Ø., Roberts, D. & Meyer, G.B. 2002: Orogen-parallel extension of the Caledonides in northern Central Norway: an overview. *Norwegian Journal of Geology* 82, 225–241.
- Cawood, P.A., van Gool, J.A.M., & Dunning, G.R., 1995: Collisional tectonics along the Laurentian margin of the Newfoundland Appalachians. In Hibbard, J.P., van Staal, C.R., & Cawood, P.A., eds., *Current Perspectives in the Appalachian-Caledonian Orogen: Geological Association of Canada Special Paper* 41, 283–301.
- Cawood, P.A., Nemchin, A. A., Smith, M., & Loewy, S., 2003: Source of the Dalradian Supergroup constrained by U–Pb dating of detrital zircon and implications for the East Laurentian margin. *Journal of the Geological Society, London* 160, 231–246.
- Cawood, P.A., Nemchin, A.A., & Strachan, R., 2007: Provenance record of Laurentian passive-margin strata in the northern Caledonides: Implications for paleodrainage and paleogeography. *Geological Society of America Bulletin* 119, 993–1003.
- Corfu, F., Torsvik, T.H., Andersen, T.B., Ashwal, L.D., Ramsay, D.M. & Roberts, R.J. 2006: Early Silurian mafic-ultramafic and granitic plutonism in contemporaneous flysch, Magerøy, northern Norway: U–Pb ages and regional significance. *Journal of the Geological Society, London*, 163, 291–301, doi: 10.1144/0016-764905-014.
- Dunning, G.R., & Pedersen, R.B., 1988: U/Pb ages of ophiolites and arc-related plutons of the Norwegian Caledonides: implications for the development of Iapetus. *Contributions to Mineralogy and Petrology* 98, 13–23.
- Dumond, G., Yoshinobu, A. S., & Barnes, C. G., 2005: Midcrustal emplacement of the Sausfjellet pluton, central Norway: Ductile flow, stoping, and in situ assimilation. *Geological Society of America Bulletin* 117, 383–395.
- Eide, E.A., Haabesland, N.E., Osmundsen, P.T., Andersen, T.B., Roberts, D. & Kendrick, M.A. 2005: Modern techniques and Old Red problems – determining the age of continental sedimentary deposits with ⁴⁰Ar/³⁹Ar provenance analysis in west-central Norway. *Norwegian Journal of Geology* 85, 133–149.
- Eide, E.A., Osmundsen, P.T., Meyer, G.B., Kendrick, M.A. & Corfu, F. 2002: The Nesna Shear Zone, north-central Norway: an ⁴⁰Ar/³⁹Ar record of Early Devonian–Early Carboniferous ductile extension and unroofing. *Norwegian Journal of Geology* 82, 317–339.
- Erdmann, S., Clarke, D.B., MacDondald, M.A., 2004, Origin of chemically zoned and unzoned cordierites from the South Mountain and Musquodoboit Batholiths, Nova Scotia, Transactions of the Royal Society of Edinburgh: Earth Sciences, vol. 95, pp. 99–110.
- Fossen, H. 1992. The role of extensional tectonics in the Caledonides of southern Norway. *Journal of Structural Geology* 14, 1033–1046.
- Fossen, H. & Dunlap, W.J. 1998. Timing and kinematics of Caledonian thrusting and extensional collapse, southern Norway: evidence from ⁴⁰Ar/³⁹Ar thermochronology. *Journal of Structural Geology* 20, 765–781.
- Frost, B. R., Barnes, C. G., Collins, W. J., Arculus, R. J., Ellis, D. J., & Frost, C. D., 2001: A geochemical classification for granitic rocks. *Journal of Petrology* 42, 2033–2048.
- Frost, C., Vietti, L., McArthur, K., Barnes, C., Nordgulen, O, & Meredith, M., 2006: Sediment provenance in the Helgeland Nappe Complex (HNC), Norwegian Caledonides: Nd isotopic data and implications for Ordovician tectonic evolution. *Geological Society of America Abstracts with Programs*, 38, 419.
- Furnes, H., Pedersen, R.B., & Stillman, C.J. 1988: The Leka Ophiolite Complex, central Norwegian Caledonides: field characteristics and geotectonic significance. *Journal of the Geological Society of London* 145, 401–412.
- Gee, D.G. 1975: A tectonic model for the central part of the Scandinavian Caledonides. *American Journal of Science* 275A, 468–515.
- Gee, D.G., & Sturt, B.A., (eds.), 1985: *The Caledonide Orogen—Scandinavia and Related Areas*. New York, Wiley, 1266 p.
- Greiling, R.O., & Garfunkel, Z., 2007: An Early Ordovician (Finnmarkian?) foreland basin and related lithospheric flexure in the Scandinavian Caledonides. *American Journal of Science* 307, 527–553.
- Grenne, T., Ihlen, P., & Vokes, F., 1999: Scandinavian Caledonide metallogeny in a plate tectonic perspective. *Mineralium Deposita* 34, 422–471.

- Gustavson, M. 1969: The Caledonian mountain chain of the southern Troms and Ofoten areas. Part II. Caledonian rocks of igneous origin. *Norges geologiske undersøkelse* 261, 110 p.
- Gustavson, M., 1975, VEGA, berggrunnsgeologisk kart H.18, M. 1:100 000, Norges geologiske undersøkelse.
- Gustavson, M., 1977, Berggrunnsgeologisk kart Flovær H17, målestokk 1:100.000, Norges geologiske undersøkelse.
- Gustavson, M., and Prestvik, T., 1979, The igneous complex of Hortavær, Nord-Trøndelag, central Norway: *Norges geologiske undersøkelse Bulletin*, v. 348, p. 73–92.
- Hacker, B.R., Andersen, T.B., Root, D.B., Mehl, L., Mattinson, J.M. & Wooden, J.L. 2003: Exhumation of high-pressure rocks beneath the Solund Basin, Western Gneiss Region of Norway. *Journal of Metamorphic Geology* 21, 613–629, doi: 10.1046/j.1525-1314.2003.00468.x.
- Hacker, B.R. & Gans, P.B., 2005: Continental collisions and the creation of ultrahigh-pressure terranes: Petrology and thermochronology of nappes in the central Scandinavian Caledonides. *Geological Society of America Bulletin* 117, 117–134, doi: 10.1130/B25549.1.
- Halverson, G.P., Dudás, F.Ö., Maloof, A.C., & Bowring, S.A., 2007: Evolution of the $^{87}\text{Sr}/^{86}\text{Sr}$ composition of Neoproterozoic seawater. *Palaeogeography, Palaeoclimatology, Palaeoecology* 256, 103–129.
- Hansen, J., Skjerlie, K.P. Pedersen, R.-B. & de la Rosa, J. 2002: Crustal melting in the lower parts of island arcs: an example from the Bremanger Granitoid Complex, west Norwegian Caledonides. *Contributions to Mineralogy and Petrology* 143, 316-335.
- Hatcher, R.D., Jr., Bream, B.R., Miller, C.F., Eckert, J.O., Jr., Fullagar, P.D., & Carrigan, C.W., 2004: Paleozoic structure of internal basement massifs, southern Appalachian Blue Ridge, incorporating new geochronologic, Nd and Sr isotopic, and geochemical data. In Tollo, R.P., Corriveau, L., McLelland, J., & Bartholomew, M.J., (eds.), *Proterozoic Tectonic Evolution of the Grenville Orogen in North America, Geological Society of America Memoir* 197, 525–547, Boulder.
- Heldal, T., 2001: Ordovician stratigraphy in the western Helgeland Nappe Complex in the Brønnøysund area, north-central Norway. *Norges geologiske undersøkelse Bulletin* 438, 47–61.
- Hibbard, J.P., van Staal, C.R., & Rankin, D.W., 2007: A comparative analysis of pre-Silurian crustal building blocks of the northern and the southern Appalachian orogen. *American Journal of Science* 307, 23–45.
- Hossack, J.R., 1984: The geometry of listric normal faults in the Devonian basins of Sunnfjord, W. Norway. *Journal of the Geological Society, London* 141, 629-637.
- Iyer, K., Austrheim, H. John, T. & Jamtveit, B. 2008a: Serpentinization of the oceanic lithosphere and some geochemical consequences. Constraints from the Leka Ophiolite complex, Norway. *Chemical Geology* (in press).
- Iyer, K. Jamtveit, B. Mathisen, J., Malthe-Sørensen, A. & Feder, J. 2008b: Reaction assisted hierarchical fracturing during serpentinization. *Earth and Planetary Science Letters* (in press).
- James, D.W., Mitchell, J.G., Ineson, P.R., & Nordgulen, Ø., 1993: Geology and K/Ar chronology of the Målvika scheelite skarns, central Norwegian Caledonides. *Norges geologiske undersøkelse Bulletin* 424, 65–74.
- Kalsbeek, F., Jepsen, H. F., & Nutman, A. P., 2001: From source migmatites to plutons: tracking the origin of ca. 435 Ma S-type granites in the East Greenland Caledonian orogen. *Lithos* 57, 1–21.
- Kirkland, C.L., Daly, J.S., Eide, E.A. & Whitehouse, M.J. 2006: The structure and timing of lateral escape during the Scandian Orogeny: A combined strain and geochronological investigation in Finnmark, Arctic Norwegian Caledonides. *Tectonophysics* 425 (1-4), 159-189.
- Kirkland, C.L., Daly, J.S. & Whitehouse, M.J. 2005: Early Silurian magmatism and the Scandian evolution of the Kalak Nappe Complex, Finnmark, Arctic Norway: *Journal of the Geological Society, London*, 162, 985–1003.
- Larsen, Ø., Skår, Ø., & Pedersen, R.-B., 2002: U-Pb zircon and titanite geochronological constraints on the late/post-Caledonian evolution of the Scandinavian Caledonides in north-central Norway. *Norsk Geologisk Tidsskrift* 82, 1-13.
- Maaløe, S. 2005: The dunite bodies, websterite and orthopyroxeneite dikes of the Leka ophiolite complex, Norway. *Mineralogy and Petrology* 85, 163–204.
- Marko, W., Barnes, M., Vietti, L., McCulloch, L., Anderson, H., Barnes, C., & Yoshinobu, A., 2005: Xenolith incorporation, distribution, and dissemination in a mid-crustal granodiorite, Vega pluton, central Norway. *Eos Transactions American Geophysical Union* 86, Fall Meeting Supplement, Abstract V13E-0596.
- Marko, W., Yoshinobu, A., & Barnes, C., 2006: Multiple pre-Scandian tectonothermal events preserved in the central Norwegian Caledonides. *Geological Society of America Abstracts with Programs* 38, 418.
- McArthur, K.L., 2007, Tectonic construction and sediment provenance of a far-travelled nappe, west-central Norway. Unpublished M.S. thesis. University of Wyoming, Laramie.

- McArthur, K., Frost, C., Barnes, C., & Prestvik, T., 2006: Nd and Sr isotopic data on conglomerate clasts in the Sauren-Torghatten Nappe, north-central Norway: a record of oceanic provenance. *Geological Society of America Abstracts with Programs* 38, 419.
- Melezhik, V., Gorokhov, I., Fallick, A., & Gjelle, S., 2001: Strontium and carbon isotope geochemistry applied to dating of carbonate sedimentation: an example from high-grade rocks of the Norwegian Caledonides. *Precambrian Research* 108, 267–292.
- Melezhik, V. A., Roberts, D., Fallick, A. E., Gorokhov, I. M., & Kusnetzov, A. B., 2005: Geochemical preservation potential of high-grade calcite marble versus dolomite marble: implication for isotope chemostratigraphy. *Chemical Geology* 216, 203–224.
- Meyer, G. B., Grenne, T., & Pedersen, R. B., 2003: Age and tectonic setting of the Nesåa Batholith: implications for Ordovician arc development in the Caledonides of central Norway. *Geological Magazine* 140, 573–594.
- Mirwald, P.W., 1986, Is cordierite a geothermometers?, *Fortschritte der Mineralogie*, v. 64., p. 119.
- Nissen, A. L., Roberts, D., & Gromet, L. P., 2006: U-Pb zircon ages of a tonalite and a granodiorite dyke from the southeastern part of the Bindal Batholith, central Norwegian Caledonides. *Norges geologiske undersøkelse Bulletin* 446, 5–9.
- Nordgulen, Ø., 1993, A summary of the petrography and geochemistry of the Bindal Batholith: Geological Survey of Norway, Report, v. 92.111.
- Nordgulen, Ø., & Schouenborg, B., 1990: The Caledonian Heilhornet pluton, north-central Norway: geological setting, radiometric age and implications for the Scandinavian Caledonides. *Journal of the Geological Society, London* 147, 439–450.
- Nordgulen, Ø., & Sundvoll, B., 1992: Strontium isotope composition of the Bindal Batholith, Central Norwegian Caledonides. *Norges geologiske undersøkelse Bulletin* 423, 19–39.
- Nordgulen, Ø., Thorsnes, T., & Husmo, T., 1989: TERRÅK 1825 III, 1:50000, foreløpig berggrunnskart, Norges geologiske undersøkelse.
- Nordgulen Ø., Fjeldheim, T., Ihlen, P.M., Nissen, A.L., & Solli, A., 1992: VEVELSTAD foreløpig berggrunnskart 1826-3, 1:50,000, Norges geologiske undersøkelse.
- Nordgulen, Ø., Bickford, M. E., Nissen, A. L., & Wortman, G. L., 1993: U-Pb zircon ages from the Bindal Batholith, and the tectonic history of the Helgeland Nappe Complex, Scandinavian Caledonides. *Journal of the Geological Society, London* 150, 771–783.
- Nordgulen, Ø., Solli, A. & Sundvoll, B. 1995: Caledonian granitoids in the Frøya–Froan area. *Norges geologiske undersøkelse, Bulletin* 427, 48–51.
- Nordgulen, Ø., Braathen, A., Corfu, F., Osmundsen, P. T., & Husmo, T., 2002: Polyphase kinematics and geochronology of the late-Caledonian Kollstraumen detachment, north-central Norway. *Norwegian Journal of Geology* 82, 299–316.
- Nordgulen, Ø., Lindstøm, M., Solli, A., Barnes, C.G., Sundvoll, B. & Karlsson, H.R. 2001: The Caledonian Smøla-Hitra Batholith, Central Norway. *GSA Northeast Section, Abstract with Programs* 33 (1), A32.
- Norton, M.G. 1986: Late Caledonian extension in western Norway: a response to extreme crustal thickening. *Tectonics* 5, 195–204.
- Ogg, J. G., 2004: Status of divisions of the International Geologic Time Scale. *Lethaia* 37, 183–199.
- Olesen, O., Lundin, E., Nordgulen, Ø., Osmundsen, P. T., Skilbrei, J. R., Smethurst, M. A., Solli, A., Bugge, T., & Fichler, C., 2002: Bridging the gap between the onshore and offshore geology in Nordland, northern Norway. *Norwegian Journal of Geology* 82, 243–262.
- Osmundsen, P.T. & Andersen, T.B. 2001: The Devonian basins of western Norway: products of large-scale sinistral transtension? *Tectonophysics* 332, 51–68.
- Osmundsen, P.T., Andersen, T.B., Markussen, S., & Svendby, A.K., 1998: Tectonics and sedimentation in the hanging wall of a regional extensional detachment: the Devonian Kvamshesten basin, W. Norway. *Basin Research* 10, 213–234.
- Osmundsen, P. T., Sommaruga, A., Skilbrei, J. R., & Olesen, O., 2002: Deep structure of the Mid Norway rifted margin. *Norwegian Journal of Geology* 82, 205–224.
- Osmundsen, P.T., Braathen, A., Nordgulen, Ø., Roberts, D., Meyer, G.B. & Eide, E. 2003: The Devonian Nesna shear zone and adjacent gneiss-cored culminations, North-Central Norwegian Caledonides. *Journal of the Geological Society, London* 160, 137–150.
- Osmundsen, P.T., Braathen, A., & Sommaruga, A., et al. 2005: Metamorphic core complexes and gneiss-cored culminations along the Mid-Norwegian margin: an overview and some current ideas. *In: Wandås, B., Eide, E.A., & Gradstein, F. (eds.) Onshore–Offshore Relationships on the Mid-Norwegian Margin. Norwegian Petroleum Society, Special Publications* 12, 29–31.
- Osmundsen, P. T., Eide, E. A., Haabesland, N. E., Roberts, D., Andersen, T. B., Kendrick, M., Bingen, B., Braathen, A., & Redfield, T. F., 2006: Kinematics of the Høybakken detachment zone and the Møre-Trondelag Fault Complex, central Norway. *Journal of the Geological Society, London* 163, 303–318.

- Pattison, D., 2001, Instability of Al₂SiO₅ “triple-point” assemblages in muscovite+biotite+quartz-bearing metapelites, with implications, *American Mineralogist*, vol. 86. pp. 1414-1422.
- Pedersen, R.B., & Furnes, H., 1991: Geology, magmatic affinity and geotectonic environment of some Caledonian ophiolites in Norway. *Journal of Geodynamics* 13, 183–203.
- Pedersen, R.-B. & Dunning, G.R. 1992: Evolution of arc crust and relations between contrasting sources: U-Pb (age), Nd and Sr isotopic systematics of the ophiolitic terrain of SW Norway. *Contributions to Mineralogy and Petrology* 128, 1-15.
- Prestvik, T., 1972: Alpine-type mafic and ultramafic rocks of Leka, Nord-Trøndelag. *Norges Geologiske Undersøkelse* 273, 23–34.
- Prestvik, T., 1980: The Caledonian ophiolite complex of Leka, north central Norway. In Panayiotou, A. (ed.): *Proceedings international ophiolite symposium Cyprus 1979*, 555–566. Cyprus Geological Survey Department.
- Reid, K., 2004: Magmatic processes in the Tosenfjord region, north-central Norway: Implications for the evolution of the Helgeland Nappe Complex. Unpublished MS thesis, Texas Tech University, Lubbock, 111 pp.
- Roberts, D., 2003, The Scandinavian Caledonides: Event chronology, palaeogeographic settings and likely modern analogues. *Tectonophysics* 365, 283–299, doi: 10.1016/S0040-1951(03)00026-X.
- Roberts, D., & Gee, D.G., 1985, An introduction to the structure of the Scandinavian Caledonides, in Gee, D.G. & Sturt, B.A. (eds) *The Caledonide Orogen—Scandinavia and Related Areas*: Chichester, John Wiley and Sons, p. 55–68.
- Roberts, D., Melezhik, V. & Heldal, T., 2002: Carbonate formations and early NW-directed thrusting in the highest allochthons of the Norwegian Caledonides: evidence of a Laurentian ancestry. *Journal of the Geological Society, London* 159, 117–120.
- Roberts, D., Nordgulen, Ø. & Melezhik, V., 2007: The Uppermost Allochthon in the Scandinavian Caledonides: From a Laurentian ancestry through Taconian orogeny to Scandian crustal growth on Baltica. In Hatcher, R. D., Jr., Carlson, M. P., McBride, J. H. & Martínez Catalán, J. R. (eds.): *4-D Framework of Continental Crust: Geological Society of America Memoir* 200, 357–377. Geological Society of America, Boulder.
- Sandøy, R., 2003: Geological variations in marble deposits. The geometry, internal structure and geochemical variations of the industrial mineral marble deposits in the Velfjord area. Doktor ingeniørvhandling 2003:30, Norges teknisk-naturvitenskapelige universitet, 534 pp.
- Schouenborg, B. 1988: U/Pb-zircon datings of Caledonian cover rocks and cover-basement contacts, northern Vestranden, central Norway. *Norsk Geologisk Tidsskrift* 68, 75-87.
- Séranne, M. & Séguret, M. 1987: The Devonian basins of western Norway: tectonics and kinematics of an extending crust. In: Coward, M.P., Dewey, J.F. & Hancock, P.L. (eds) *Continental Extensional Tectonics*. Geological Society, London, *Special Publications* 28, 537–548.
- Séranne, M., 1992: Late Palaeozoic kinematics of the Møre-Trøndelag Fault Zone and adjacent areas, Central Norway. *Norsk Geologisk Tidsskrift* 72, 141-158.
- Siddoway, C.S., Richard S.M., Fanning C.M. Luyendyk, B.P., 2004: Origin and emplacement of a middle Cretaceous gneiss dome, Fosdik Mountains, West Antarctica, in Whitney, D.L., Teyssier, C., Siddoway, C.S., eds., Geological Society of America, Special Paper 380, p. 267-294.
- Skilbrei, J. R., Olesen, O., Osmundsen, P. T., Kihle, O., Aaro, S., & Fjellanger, E., 2002: A study of basement structures and onshore-offshore correlations in Central Norway. *Norwegian Journal of Geology* 82, 263-279.
- Skjerlie, K.P. 1992: Petrogenesis and significance of late Caledonian granitoid magmatism in western Norway. *Contributions to Mineralogy and Petrology* 110, 473-487.
- Skjerlie, K.P., Pedersen R.-B., Wennberg O.P. & De la Rosa J. 2000: Volatile phase fluxed anatexis of metasediments during late Caledonian ophiolite obduction: evidence from the Sogneskollen Granitic Complex, west Norway. *Journal of the Geological Society, London*, 157, 1199-1213.
- Slagstad, T., 2003: Geochemistry of trondhjemites and mafic rocks in the Bymarka ophiolite fragment, Trondheim, Norway: Petrogenesis and tectonic implications. *Norwegian Journal of Geology* 83, 167–185.
- Spear, F.S., 1993, *Metamorphic Phase Equilibria and Pressure-Temperature-Time Paths*, Mineralogical Society of America, Monograph, BookCrafters, Inc., Chelsea, Michigan, pp.798
- Steltenpohl, M.G., Andresen, A., Lindstrøm, M., Gromet, P., and Steltenpohl, L.W., 2003: The role of felsic and mafic igneous rocks in deciphering the evolution of thrust-stacked terranes: An example from the north Norwegian Caledonides: *American Journal of Science* 303, 149–185, doi: 10.2475/ajs.303.2.149.
- Stephens, M.B., & Gee, D.G., 1989, Terranes and polyphase accretionary history in the Scandinavian Caledonides, in Dallmeyer, R.D. (ed) *Terranes in the Circum-Atlantic Paleozoic Orogens*. Geological Society of America *Special Paper* 230, 17–30.

- Stephens, M.B., Gustavson, M., Ramberg, I.B., & Zachrisson, E., 1985: The Caledonides of central-north Scandinavia--a tectonostratigraphic overview. *In* Gee, D. G., & Sturt, B. A. (eds.): *The Caledonide Orogen—Scandinavia and Related Areas*, 135–162. Wiley, New York.
- Sturt, B.A., Andersen, T.B., & Furnes, H., 1985: The Skei Group, Leka. An unconformable clastic sequence overlying the Leka Ophiolite. *In*: Gee, D.G. & Sturt, B.A. (eds.) *The Caledonide Orogen—Scandinavia and Related Areas*. Wiley, New York, 395–405.
- Terry, M.P. & Robinson, P. 2004: Geometry of eclogitefacies structural features: Implications for production and exhumation of UHP and HP rocks, Western Gneiss Region, Norway. *Tectonics* 23, TC2001, doi: 10.1029/2002TC001401.
- Thorsnes, T., & Løseth, H., 1991: Tectonostratigraphy in the Velfjord-Tosen region, southwestern part of the Helgeland Nappe Complex, Central Norwegian Caledonides. *Norges geologiske undersøkelse Bulletin* 421, 1–18.
- Trønnes, R. G., 1994: Marmorforekomster i Midt-Norge: Geologi, isotopgeokjemi og industrimineralpotensiale, Rapport. Norges Geologiske Undersøkelse, 21 pp.
- Trønnes, R.G., & Sundvoll, B., 1995: Isotopic composition, deposition ages and environments of Central Norwegian Caledonian marbles. *Norges geologiske undersøkelse Bulletin* 427, 44–47.
- Tucker, R. D., Robinson, P., Solli, A., Gee, D. G., Thorsnes, T., Krogh, T. E., Nordgulen, Ø., & Bickford, M. E., 2004: Thrusting and extension in the Scandian hinterland, Norway: new U-Pb ages and tectonostratigraphic evidence. *American Journal of Science* 304, 477–532.
- Tørudbakken, B.O., & Brattli, B., 1985: Ages of metamorphic and deformational events in the Beiarn Nappe Complex, Nordland, Norway. *Norges geologiske undersøkelse Bulletin* 399, 27–39.
- van Staal, C., J. Dewey, Niocaill, C.M., & McKerrow, W.S., 1998: The Cambrian–Silurian tectonic evolution of the northern Appalachians and British Caledonides: history of a complex, west and southwest Pacific-type segment of Iapetus. *In*: Blundell, D., & Scott, A., (eds.), *Lyell: the past is the key to the present: Geological Society, London, Special Publication* 143, 199–242.
- Vietti, L.A., McCulloch, L., Marko, W.T., Barnes, M.A., Frost, C.D., & Nordgulen, Ø., 2005: Disaggregation of quartzite enclaves in the S-type Vega pluton, north-central Norway. *Eos Transactions American Geophysical Union*. 86, Fall Meeting Supplement, Abstract V13E-0595.
- Waldron, J.W.F., & van Staal, C.R., 2001: Taconian orogeny and the accretion of the Dashwoods block: A peri-Laurentian microcontinent in the Iapetus Ocean. *Geology* 29, 811–814.
- White, A. J. R., & Chappell, B. W., 1977: Ultrametamorphism and granitoid genesis. *Tectonophysics* 43, 7–22.
- Yoshinobu, A. S., Barnes, C. G., Nordgulen, Ø., Prestvik, T., Fanning, M., & Pedersen, R. B., 2002: Ordovician magmatism, deformation, and exhumation in the Caledonides of central Norway: An orphan of the Taconic orogeny? *Geology* 30, 883–886.
- Yoshinobu, A., Reid, K., Barnes, C., & Allen, C.M., 2005: Crustal melting in the Helgeland Nappe Complex, central Norway. *Eos Transactions American Geophysical Union* 86, Fall Meeting Supplement Abstract V13E-0598.